DEVELOPMENT OF MATHEMATICAL MODELS FOR PREDICTING THE CAPACITY OF WASTE-BASED SUSTAINABLE GREEN STRUCTURAL ELEMENTS FOR NEW-GENERATION RAPID CONSTRUCTION TECHNIQUES

YENİ NESİL HIZLI İNŞAAT TEKNİKLERİ İÇİN ATIK BAZLI SÜRDÜRÜLEBİLİR YEŞİL YAPI ELEMANLARININ KAPASİTESİNİ TAHMİN ETMEYE YÖNELİK MATEMATİKSEL MODELLERİN GELİŞTİRİLMESİ

ÖZNUR KOCAER KUL

ASSOC. PROF. ALPER ALDEMİR

Supervisor

Submitted to

Graduate School of Science and Engineering of Hacettepe University

as a Partial Fulfillment to the Requirements

for be Award of the Degree of Doctor of Philosophy

in Civil Engineering

2024

To my beloved spouse…

ABSTRACT

DEVELOPMENT OF MATHEMATICAL MODELS FOR PREDICTING THE CAPACITY OF WASTE-BASED SUSTAINABLE GREEN STRUCTURAL ELEMENTS FOR NEW-GENERATION RAPID CONSTRUCTION TECHNIQUES

ÖZNUR KOCAER KUL

Doctor of Philosophy, Department of Civil Engineering
Supervisor: Assoc. Prof. Alper ALDEMİR
June 2024, 108 pages

The escalation of natural disasters globally is evidenced by a significant increase in frequency and severity over recent years. Earthquakes worldwide, spanning 20 years from 1998 to 2017, resulted in approximately 750,000 fatalities and impacted over 125 million people. Turkey is located in a critical seismic belt with over 500 active faults; 92% of the population resides close to active faults. Unfortunately, due to this critical location, the 7.8 magnitude earthquake in Kahramanmaraş, Turkey, in 2023 caused significant damage to thousands of buildings and spurred urgent demolition and reconstruction efforts by government authorities. These catastrophes leave millions displaced, lacking necessities, and suffering significant economic setbacks. Alongside disasters, political instability in many regions further exacerbates housing challenges, necessitating rapid, safe, and sustainable urbanization efforts to accommodate the growing population. To overcome these challenges, it is necessary to develop structural systems that are adaptable, cost-effective, and can be quickly transported to desired locations. Circular economy principles, essential for waste reduction, extend beyond material usage to encompass production practices. Sustainable construction necessitates reducing environmental impacts across the building's lifecycle and value chain, aligning with circular economy principles. At this point, Design for Manufacture and Assembly (DfMA) and Design for Deconstruction (DfD)

play a crucial role in simplifying processes to minimize disadvantages while maximizing the benefits of modular construction.

Addressing these challenges motivates the present thesis, which focuses on designing a building system that integrates circular economy principles, maximizes waste recycling, and allows for the reuse of elements. It includes an in-depth analysis of Construction and Demolition Waste (CDW) based geopolymers to develop mathematical models for predicting the capacity of building elements. By encompassing a broad parameter range, the study seeks to develop a new stress-strain model applicable to various types of geopolymers, facilitating sustainable construction practices. To this end, a stress-strain model was initially developed on compressive behavior, followed by the formulation of geopolymer's flexural behavior based on experimental findings. In estimating the ultimate moment capacities, the proposed stress-strain model was validated by 36 bending tests from the literature, demonstrating minor deviations and enhanced accuracy compared to ACI318. A soft database of 50 beam specimens with varying mechanical properties and reinforcement patterns was also established, generating numerical models for all possible parameter combinations to determine load capacities. The performance of the proposed method, stress-strain models from the literature and the ACI318 procedure were investigated and provided promising results with an absolute mean percentage error of 5.13% regardless of the failure mode.

Continuing the mathematical modeling of geopolymer concrete, a comprehensive material model was developed to predict the flexural capacities of geopolymer columns, inspired by Kent and Park's confinement model. The proposed stress-strain model, validated with 41 test results, accurately estimated moment capacity. Comparison with moment-curvature curves from six recent experiments confirmed the model's accuracy for performance-based design calculations. Additionally, comparisons with four international codes (ACI318, BS8110-97, TS500, and AASHTO) revealed significant deviations in flexural capacity calculations; however, highlighting the proposed model's strong correlation with the experimental data, ensuring accurate predictions for geopolymer columns.

Keywords: Design for Manufacturing and Assembly, Design for Deconstruction, Construction and Demolition Wastes, Demountable Structural Systems, Circular Economy

ÖZET

YENİ NESİL HIZLI İNŞAAT TEKNİKLERİ İÇİN ATIK BAZLI SÜRDÜRÜLEBİLİR YEŞİL YAPI ELEMANLARININ KAPASİTESİNİ TAHMİN ETMEYE YÖNELİK MATEMATİKSEL MODELLERİN GELİŞTİRİLMESİ

ÖZNUR KOCAER KUL

Son yıllarda doğal afetler küresel ölçekte ciddi bir sıklık ve şiddetle artış göstermektedir. 1998'den 2017'ye 20 içinde gerçekleşen depremler, yaklaşık 750.000 ölüme neden oldu, 125 milyonu aşkın insanı etkiledi. Türkiye, 500'den fazla aktif fay hattı bulunan kritik bir deprem kuşağındadır ve nüfusun %92'si, aktif fay hatlarına yakın konumlanmış kentsel alanlarda yaşamaktadır. Ne yazık ki, 2023'te Türkiye'nin Kahramanmaraş kentinde meydana gelen 7.8 büyüklüğündeki deprem, binlerce binaya ciddi zarar vermiş, hükümet yetkililerini acil yıkım ve yeniden inşa çabalarına zorlamıştır. Bu felaketler milyonlarca insanı yerinden etmiş, temel ihtiyaçlarını karşılayamaz hale getirmiş ve ciddi ekonomik problemlere sebep olmuştur. Doğal afetlerin yanı sıra, birçok bölgede siyasi istikrarsızlıklar barınma sorunlarını kötüleştirmekte; hızlı, güvenli ve sürdürülebilir kentleşme çabalarını zorunlu kılmaktadır. Bu zorlukların üstesinden gelmek için, istenilen konumlara hızlı bir şekilde taşınabilen, uygun maliyetli ve adapte edilebilir yapı sistemleri geliştirmek gerekmektedir. Atık azaltımı için esas olan döngüsel ekonomi prensipleri, malzeme kullanımının ötesinde üretim uygulamalarını da kapsamaktadır. Sürdürülebilir yapı, bina yaşam döngüsü boyunca ve değer zincirinin tamamında çevresel etkileri azaltmalı, döngüsel ekonomi prensipleriyle uyumlu olmalıdır. Tasarım ve İmalat için Dizayn (DfMA) ve Dekonstrüksiyon için Dizayn (DfD) yaklaşımları, modüler yapı sistemlerinin faydalarını maksimize etmekte ve dezavantajları minimuma indirmekte önemli bir rol oynamaktadır.

Bu zorlukların üstesinden gelmek, döngüsel ekonomi prensiplerine entegre, atık geri dönüşümünü üst noktalara taşıyan ve yapısal elemanların yeniden kullanımına izin veren bir yapı sistemi tasarlamaya odaklanan mevcut tezin temel motivasyonunu oluşturmaktadır. Bina yapısal elemanlarının kapasitelerini tahmin etmek için matematiksel modeller geliştirmek için İnşaat ve Yıkıntı Atıkları (İYA) temelli jeopolimerlere derinlemesine bir analiz içerir. Geniş bir parametre aralığını kapsayarak, çalışma farklı türlerdeki jeopolimerler için geçerli olan yeni bir gerilme-şekil değiştirme modelini geliştirmeyi amaçlamakta, sürdürülebilir yapı uygulamalarını kolaylaştırmayı hedeflemektedir. Bu amaçla, bir gerilme-şekil modeli başlangıçta basınç davranışı üzerine geliştirilmiş ve ardından deneysel bulgulara dayanarak jeopolimerin eğilme davranışının formülasyonu oluşturulmuştur. Nihai moment kapasitelerini başarılı bir biçimde tahmin eden önerilen gerilme-şekil değiştirme modeli literatürden elde edilmiş 36 eğilme testi ile doğrulanmış ve ACI318'e göre hafif sapmalar ve artan doğruluk göstermiştir. Mekanik özellikleri ve donatı detayları değişen 50 kiriş numunesi için bir veritabanı oluşturularak ve tüm olası parametre kombinasyonları için sayısal modeller oluşturularak yük kapasiteleri belirlenmiştir. Önerilen modelin performansı, literatürden gerilme-şekil modelleri ve ACI318 prosedürü ile incelenmiş ve hataların mutlak ortalama yüzdesel hatası %5.13 olarak hesaplanmış, hata yapma biçiminden bağımsız olarak umut verici sonuçlar elde edilmiştir.

Jeopolimer betonun matematiksel modellemesine devamı olarak, Kent ve Park'ın sargılı beton modelinden esinlenerek, jeopolimer kolanların eğilme kapasitelerini tahmin etmek için kapsamlı bir performansa dayalı malzeme modeli geliştirilmiştir. Önerilen gerilme-şekil değiştirme modeli, 41 numunenin test sonucuyla doğrulanmış ve moment kapasitesini doğru bir şekilde tahmin etmiştir. Ek olarak altı numunenin testinden elde edilen moment-eğrilik eğrileriyle karşılaştırılarak, modelin performans temelli tasarım hesapları için doğruluğu ortaya konmuştur. Ayrıca, dört uluslararası koddan (ACI318, BS8110-97, TS500 ve AASHTO) gelen eğilme kapasitesi hesaplarıyla karşılaştırıldığında, önerilen modelin deneysel verilerle güçlü bir korelasyon sergilediği ve geopolimer kolonlar için doğru tahminler sağladığı görülmüştür.

Anahtar Kelimeler: Üretim ve Montaj için Tasarım, Dekonstrüksiyon için Tasarım, İnşaat ve Yıkıntı Atıkları, Sökülebilir Yapı Sistemleri, Döngüsel Ekonomi

ACKNOWLEDGEMENT

TABLE OF CONTENTS

LIST OF FIGURES

LIST OF TABLES

SYMBOLS AND ABBREVIATIONS

Symbols

b	Beam Width
h	Beam Height
fck	Concrete Compressive Strength
fy	Steel Yield Strength
M_{fck}	Model Coefficient
f_{cc}	Compressive Strength of Confined Concrete
ε_{cu}	Ultimate Strain
ε_{ccu}	Ultimate Strain of Confined Concrete
ρs	Stirrup percent density
bk	Big Size of the Core Concrete (area inside the stirrup)
hk	Small Size of the Core Concrete
s	Spacing of Stirrup
GHG	Greenhouse Gas
CO_2	Carbon Dioxide
NaOH	Sodium Hydroxide
Na_2SiO_3	Sodium Silicate

Abbreviations

AASHTO	American Association of State Highway and Transportation Officials
ACI	American Concrete Institute
AFAD	Disaster and Emergency Management Presidency
BC	Boundary Conditions
BIM	Building Information Modeling
BS	British Standards
CABR	China Academy of Building Research
CE	Circular Economy

CDW	Construction and Demolition Waste
CRB	Concrete Rubble
CVC	Conventional Concrete
DfA	Design for Assembly
DfM	Design for Manufacturing
DfMA	Design for Manufacturing and Assembly
DfMA&D	Design for Manufacturing, Assembly, and Deconstruction
DfD	Design for Deconstruction
FEM	Finite Element Model
EM-DAT	Emergency Events Database
EU	European Union
G	Waste Glass
GDP	Gross Domestic Product
GPC	Geopolymer Concrete
HB	Hollow Brick
LCA	Life Cycle Assessment
LVDT	Linear Variable Differential Transformer
OECD	The Organization for Economic Co-operation and Development
OPC	Ordinary Portland Cement
OSC	Off-site Construction
PC	Portland Cement
RAG	Recycled Aggregates
RCB	Red Clay Brick
RT	Roof Tile
SEM	Scanning Electron Microscope
TS	Turkish Standards
XRD	X-ray Diffraction
XRF	X-ray Fluorescence

OVERVIEW

The frequency and severity of natural disasters globally are steadily escalating. In the last decade alone, more than 300 natural disasters have been recorded worldwide, impacting millions of individuals [1]. Over a 20-year period spanning from 1998 to 2017, earthquakes occurring worldwide led to approximately 750,000 fatalities and affected over 125 million individuals [2]. A retrospective analysis of the disasters over the past two decades reveals that globally, there were 552 earthquakes, constituting 8% of all disasters, trailing behind floods (3254 occurance, 44% of total) and storms (2043 occurance, 28% of total) [3]. These catastrophic events span a wide spectrum, encompassing floods, earthquakes, forest fires, and hurricanes. The aftermath of these disasters often leaves millions displaced, lacking basic necessities, and suffering significant economic setbacks. Moreover, political instability in many countries around the world has forced millions of people to leave their houses. Considering the extreme population growth worldwide, the need for rapid, safe, and sustainable urbanization to meet housing needs has reached unprecedented levels. Among natural disasters, earthquakes emerge as the most catastrophic, exposing the urgent need for emergency shelter due to the damage inflicted upon buildings upon occurrence. For instance, in the southern Kant region of Japan, a magnitude 7.9 earthquake resulted in over 460,000 buildings being completely destroyed or incinerated [4]. In Haiti, a single earthquake led to the collapse of over 300,000 buildings [5]. In Turkey, on February 6, 2023, a 7.8 magnitude earthquake struck Kahramanmaraş. According to the Ministry of Environment, Urbanization, and Climate Change's Directorate General of Construction Services, recent data indicates that 197,825 buildings sustained mild to moderate damage, with a total of 18,200 buildings demolished, and 61,890 establishments deemed severely damaged and requiring urgent demolition [6].

Turkey is one of the most critical countries in terms of plate tectonics and is located in a vital seismic belt. There are more than 500 active faults known in Turkey, and 92% of the current population resides in cities where these active faults are present. [7]. As presented in a recent report by the Kandilli Observatory and Earthquake Research Institute, it is estimated that in the event of an earthquake scenario of Mw=7.5, which was analyzed over 1,166,330 buildings, approximately 43% of the buildings in Istanbul, where the highest population resides in Turkey, would sustain damage [8]. It is expected that 26% of the buildings will sustain minor damage,

13% moderate damage, 3% severe damage, and 1% very severe damage. In the earthquake scenario, it is estimated that approximately 17% of the buildings in Istanbul (approximately 194,000 buildings) will sustain moderate to severe damage, necessitating reconstruction of moderately to severely damaged buildings. Additionally, calculations indicate that approximately 25 million tons of debris may result in Istanbul following the scenario earthquake. It is estimated that approximately 640,000 households will require emergency shelter in the event of a possible earthquake. With an assumed population of 3 persons per household, approximately 2,000,000 individuals are expected to be in need of emergency shelter.

In addition to earthquakes, climate change, which is intensely felt worldwide, brings with it natural disasters such as floods, flash floods, and inundations, resulting in significant financial damage and loss of life. Floods are the second most common type of disaster after earthquakes [9], and like earthquakes, floods have destructive effects on the construction. Furthermore, the potential for flooding due to damage to dam structures after major earthquakes further increases the danger. Data from the Emergency Events Database (EM-DAT) indicate that floods are the cause of most disasters, with storms being the second most common type of disaster. Observations show that the number of flood disasters has doubled in the past two decades, rising from 1,389 to 3,254 [9]. According to research, 1.47 billion people worldwide, or 19% of the global population, are directly exposed to significant risks during floods that occur once every hundred years. The majority of those exposed to flood disasters (approximately 1.36 billion people) are located in South and East Asia, with China (329 million) and India (225 million) accounting for more than one-third of global risk [9]. Nearly 30% of all natural disasters in Turkey consist of flood events. According to the EM-DAT, between 1950 and 2007, there were 34 flood events in Turkey, resulting in 1,016 deaths and affecting approximately 1.5 million people [10]. When evaluating statistics shared by the Disaster and Emergency Management Presidency (AFAD) regarding natural disasters in Turkey, it is observed that there were 905 natural disasters in 2020. Among these disasters, floods/flash floods accounted for 19.56%. The latest updated report is for the year 2022. According to the July 2023 report shared by AFAD, there were 450 flood/flash flood natural disaster events in Turkey in 2022 alone. The total

number of natural disasters was 22,982, with floods/flash floods accounting for a rate of 1.96% [11].

Although infectious diseases like COVID-19 do not directly damage constructions like natural disasters such as earthquakes, the experiences gained during the COVID-19 pandemic, which the whole world has faced, have shown the need for emergency shelter facilities for various purposes. The urgent need for testing centers, hospitals, and healthcare facilities highlights the importance of emergency shelter facilities in pandemic situations. Following the onset of the COVID-19 pandemic, it was observed that numerous new healthcare facilities, such as testing centers, patient rooms, accommodations for healthcare workers, and quarantine facilities, were immediately constructed for emergency use [12]. In Wuhan, the epicenter of COVID-19 in China, two emergency hospitals and 16 Fangcang shelter hospitals were constructed. Through careful treatment in these emergency facilities, the mortality rate of patients significantly decreased in subsequent periods. This recent example underscores the importance of rapid production facilities for places such as general hospital treatment centers when faced with infectious diseases [13].

War and political issues worldwide are among the primary factors leading to an urgent need for housing. Recent conflicts in Ukraine have resulted in the destruction of more than 1.4 million dwellings, with one-third of these dwellings being severely damaged [14]. Additionally, the influx of people forced to leave their countries due to war has led to a significant increase in housing demand in countries such as the United Kingdom, European countries, and Turkey [14]. Turkey, due to its geographical location and the uncertain political climate it faces from neighboring countries, is confronted with a refugee problem resulting from conflicts and wars in neighboring countries. Refugees displaced from their countries as a result of conflicts constitute a significant portion of these vulnerable groups. The United Nations Refugee Agency has reported the number of registered Syrians in Turkey as 3,652,000 as of August 2022 [15]. Furthermore, the total official number of Afghan and Ukrainian refugees is approximately 320,000. Rapid solutions implemented for the housing of these groups may subject them to undesirable living conditions, such as thermal discomfort, disease, fire hazards, and security vulnerabilities, due to ongoing wars and economic fluctuations. Additionally, while these

shelters are intended to be temporary housing for these individuals, conditions may render them permanent. Currently, nearly 70% of the world's refugees sustain their life outside regular camps, and more than 65% live in this situation for much longer than anticipated [16]. Moreover, according to the [17], over 80% of refugee crises last for ten years or more; 40% last for 20 years or more; and in countries with conflict-driven or forcibly displaced persons, it takes over 23 years for internally displaced persons to stabilize.

The inevitable increase in demand for housing structures is paralleled by a rise in the consumption of construction materials. Concrete, serving as the backbone of the construction sector worldwide, entails significant consumption of natural resources and emits greenhouse gases into the atmosphere during its production, exacerbating one of the most critical contemporary issues, global warming. Portland cement (PC), the essential component of traditional concrete, is the most energy-intensive, costly, and environmentally unfriendly element. Generally, the production of 1 ton of Portland cement (PC) requires 1.5 tons of raw materials and emits approximately 800 kg of carbon dioxide (CO_2) into the atmosphere [18]. The cement industry alone is responsible for 5-8% of the total anthropogenic CO_2 emissions [19]. Concrete production, in addition to depleting natural resources, is an energy-intensive process that necessitates the use of various sizes of aggregates, resulting in significant waste generation.

In recent years, despite concrete and effective measures being taken, the concentration of CO_2 in the atmosphere continues to rise, contributing to global warming. In response to increasing pressure from national and international environmental issues and policies, both academia and the industry have undergone a significant paradigm shift to reduce CO_2 emissions. However, the scope remains limited, and the construction industry must exert further efforts to seek alternative methods to definitively reduce or eliminate CO_2 levels. In this context, realistic and feasible solutions are needed for every component of the sector to eliminate CO_2 and ensure future circularity, thereby reducing their climate impacts. This includes not only solutions aimed at reducing the high CO_2 emissions from cement production through greener alternative building materials but also efforts directed towards the elimination of CO_2, which is an inevitable consequence of mitigating its impacts on climate.

Construction activities and natural disasters give rise to Construction and Demolition Waste (CDW), comprising materials like concrete, wood, glass, wall units, among others, posing challenges for disposal. These wastes, often destined for landfills and potentially containing hazardous substances, pose risks to both individual health and environmental integrity if not managed properly. Hence, addressing CDW appropriately is crucial for its environmental, social, and economic benefits [20]. In this context, the utilization of CDW for the development of greener construction materials emerges as an environmentally friendly and attractive strategy. Effective CDW utilization not only reduces landfill waste and alleviates strain on depleted natural resources but also curtails reliance on Portland cement (PC) and traditional concrete production in constructing, renovating, reinforcing, repairing, and safeguarding infrastructure. Geopolymers, emerging as potential alternatives to cementitious binders, are gaining traction in the construction sector [20]. Geopolymer binders, activated by alkali activators from aluminosilicate source binders, facilitate the utilization of industrial by-products like blast furnace slag, fly ash, as well as minerals such as silica fume and metakaolin as construction materials, offering binder options capable of reducing cement consumption to zero [20]. Despite the wider adoption of geopolymers for their superior strength and durability over traditional cementitious binders, their adoption may entail higher costs compared to cement-based alternatives. Considering these merits, the integration of CDW-based geopolymer binders into the construction industry assumes a pivotal and promising role in mitigating the adverse environmental impacts associated with cement production and CDW accumulation, potentially transitioning the construction sector's linear economic model into a fully circular framework.

Circular economy principles, enabling waste reduction, must be addressed not only at the material level but also in the production phase. In this regard, prefabrication emerges as a significant technique to reduce waste and shorten construction times. Prefabrication's application-focused sub-approach, known as Modular Construction, considers the entire lifecycle of a building, making it an acknowledged sustainable building methodology. It enhances cost-effectiveness and, through its design, facilitates a construction cycle devoid of waste. Sustainable construction should be achieved by reducing environmental impacts throughout the entire lifecycle of a building and all components of the value chain, while moving

towards a circular economy. In this context, approaches like Design for Manufacturing and Assembly (DfMA) and Design for Deconstruction (DfD) stand out. These methodologies are crucial for maximizing the benefits derived from modular construction techniques aligned with circular economy principles and simplifying processes to minimize drawbacks.

The urgent and cost-effective provision of shelter for vulnerable groups affected by natural disasters and political crises, the ability for such structures to be used for extended periods and even rapidly relocated to desired locations as needed, the design of existing building systems to be adaptable and expandable based on demand, and the development of building elements that allow for the use of region-specific natural materials or recycled construction waste as building materials will enable the implementation of sustainable measures against disasters. With this motivation, the current thesis addresses the design approaches necessary to develop a building system consisting of elements that enable circular economy principles in the construction sector, maximize waste recycling, and allow for reuse for different purposes or the same function after the end of their service life. The study focuses on the in-depth analysis of the mechanical behavior of CDW-based geopolymers, which form the basis of the building elements used, to generate mathematical models for capacity predictions of the building elements. By utilizing a wide parameter range, the study aims not only to create a model specifically for CDW-based geopolymers but also to focus on developing a model that can be adapted to different types of geopolymers. These focal points are conveyed through three main chapters.

Chapter 1 provides insight into the increasing need for rapid construction structures and offers a comprehensive overview of studies in the construction sector that address the principles of Design for Manufacture and Assembly (DfMA) and Design for Deconstruction (DfD) as sustainable, rapid, and circular economy-compliant techniques. As the fundamental reasons behind the demand for rapid construction of shelter structures are examined, the necessity of developing new-generation methods becomes apparent due to the significant demand encountered. In line with this necessity, a case study synthesizing the principles of DfMA, which significantly enhances efficiency in the production process, and DfD, which enables reuse for sustainable production, has been conducted. Within the scope of the case study conducted by the project team of the Hacettepe University Department of Civil Engineering, demountable

structural elements based on geopolymers produced using CDW were manufactured. These elements were utilized for the construction of a single-story residential building, with the structural systems completed in less than one day and exterior claddings installed in less than four days. At the conclusion of the study, a product evaluation was conducted, confirming the benefits of the DfMA and DfD guidelines and principles. While the mechanical performance of the geopolymer structural elements produced for this case study appears to be comparable to that of Ordinary Portland Cement (OPC)-based concrete structural elements, the structural differences between these materials necessitate a more in-depth examination of the mechanical behavior of geopolymer, which contains components distinct from OPC-based concrete. Considering that concrete is accepted as suitable for capacity predictions, reliable predictions are essential for geopolymer concrete, which exhibits performance comparable to concrete, to be widely and confidently used. Focusing on this need, Chapter 2 emphasized the versatility of geopolymer binders as alternative materials to cementitious binders, highlighting the limited number of accurate mathematical models available to predict the capacities of structural elements produced with these binders. Mathematical models predicting the capacity of beams made from construction and demolition waste (CDW)-based geopolymer concrete were developed, drawing upon experimental and numerical studies conducted on these beams. The accuracy of the mathematical model derived from numerical studies was validated through a parametric study, yielding promising results. Subsequently, Chapter 3 delved into a comprehensive analysis of the stress-strain characteristics exhibited by column structural elements made from CDW-based geopolymer concrete subjected to axial loads. Studies were conducted to develop a comprehensive geopolymer concrete material model to predict the bending capacities of column elements. Inspired by the Kent and Park confinement model, a stress-strain model that considered the confinement effect was proposed to accurately predict the moment capacity of geopolymer columns. In this section, numerical modeling was conducted to evaluate the accuracy performance of the formula, comparing it with experimental studies and literature reviews to carry out a parametric study. Promising results were obtained for the performance-based design calculations of the proposed model. Additionally, in the subsequent stages of the study, the performances of the leading international four codes (ACI318, BS8110-97, TS500, and AASHTO) were compared with the proposed model. Notably, the flexural capacity calculated using the code formulations exhibited significant

deviations from the experimental results. In contrast, the proposed model demonstrates a strong correlation with the experimental data, substantiating its effectiveness in accurately predicting the flexural capacities of geopolymer columns.

CHAPTER I: A REVIEW OF DESIGN FOR MANUFACTURING AND ASSEMBLY AND DESIGN FOR DECONSTRUCTION PRINCIPLES WITHIN THE FRAMEWORK OF THE INCREASING NEED FOR RAPID CONSTRUCTION

1.1.   Introduction

In recent years, the escalating demand for housing worldwide has emerged as a critical global issue. The increasing demand for housing arises from various factors, including population growth, frequent natural disasters, unexpected pandemics, political instability, and migration patterns. Despite a decreasing rate of population growth, the actual population continues to rise, driving the imperative for rapid urban development. It is estimated that currently, one out of every eight people globally is in need of housing, with projections suggesting that over three billion individuals will require suitable housing within the next decade [21]. With the continual expansion of the global population, particularly in developing regions, the need for housing has intensified [22]. Furthermore, rapid urbanization, driven by rural-to-urban migration, has resulted in the proliferation of informal settlements and slums in many cities, exacerbating the housing crisis [23]. Additionally, economic development and increasing incomes in emerging economies have elevated expectations for improved living conditions, further fueling the demand for housing [24]. As a consequence, governments, policymakers, and international organizations are confronted with the daunting task of delivering affordable, secure, and sustainable housing solutions to meet the escalating global demand [25]. Addressing this imperative is crucial not only for enhancing living standards but also for advancing broader sustainable development objectives and reducing inequalities [26]. Consequently, the global surge in housing needs highlights the critical importance of devising comprehensive strategies and policies to ensure equitable access to adequate housing for all individuals. However, considering the current linear economic structure of the construction industry, the required material, energy, and time consumption to meet this demand could reach alarming levels.

The linear economic model has traditionally followed the concept of taking, making and disposing of waste. This means that raw materials are collected, then transformed into products,

and they are finally discarded as waste. In the economic system, value is created by producing and selling as many products as possible [27]. This model has, however, led to a sudden increase in the use of natural resources. The rise in resource use has been coupled with growth in waste and emissions, contributing to a series of pressure points including climate change, reduced food security, water scarcity, and air pollution. It is estimated that one-fifth of the raw materials extracted worldwide end up as waste, corresponding to over 12 billion tonnes of waste per year [28]. Following the current patterns of consumption and production, The Organization for Economic Co-operation and Development (OECD) estimates that we will reach 167 Gigatonnes (Gt) material usage by 2060. This would mean that by 2060, materials used per capita per day will reach 45 kg exacerbating environmental challenges [29]. As of today, the extraction and processing of resources are already causing 90% of biodiversity loss and water stress.

The impacts of the climate crisis on the earth and humanity and the urgency of actions to address these impacts reveal the necessity for radical changes in resource utilization, production and economic activities [30]. However, the construction industry is failing to identify problems in resource use, waste generation, carbon emissions and energy use at both global and local levels, and is therefore failing to find appropriate solutions. Responsible for 40% of natural resources consumed globally and 25% of global waste, this industry is the third largest daily waste generator per capita, at around 1.70 kg per person per day [31]. The construction industry has long been under the spotlight for its outrageously high share of global energy consumption and greenhouse gas (GHG) emissions, and is at the center of efforts to reduce this environmental burden. At the scale of buildings, the sector is responsible for 30-40% of primary energy consumption and 40-50% of GHG emissions worldwide [32]. The concept of circularity is still limited to a quite low level, around 9% worldwide. Despite having a perspective on the concept of recycling and reusability of materials, it is estimated that 57% of the total value of materials is lost due to the lack of consolidation of the concept of circularity [33].

In 2020, approximately 2.24 billion tons of solid waste were generated globally [31] with Construction and demolition waste (CDW) constituting at least 30% of this total [34]. This figure is expected to escalate due to urban sprawl [35]. CDW poses a global threat to urban development, given the rapid globalization and urbanization of cities worldwide, leading to

substantial demands on construction projects, resulting in CDW generation and environmental challenges [36]. While CDW is significant in developing countries, developed nations are not absolved from this challenge, necessitating effective management throughout the construction process [37].

The quantity and composition of CDW vary worldwide, with China, the United States, and the European Union being the primary global generators [38]. Recovery rates for CDW fluctuate significantly across different regions, ranging from 7% to 90% [59], yet approximately 35% of the world's CDW ends up in landfills despite its potential added value [40]. Projections on CDW suggest that global waste generation will double by 2025 compared to 2000 levels, and by 2050, it will double compared to 2016 figures [31]. However, a notable concern remains the scarcity of waste data from developing regions [41]. CDW also presents numerous other adverse impacts, including its tendency to be landfilled rather than separated or recycled, with instances of illegal dumping further exacerbating the issue [42]. Both landfilling and illegal dumping not only deplete land resources but also pose significant risks of environmental pollution [43], threatening human health due to pollutants and gas emissions [42]. Additionally, it's estimated that 2.5 billion people worldwide lack adequate sanitation due to current levels of solid waste [44]. These challenges are compounded by the limited levels of recycling and resource conservation, which could mitigate the need for further raw material extraction, ultimately leading to various emissions and pollutants that strain the environment.

These statistics have motivated the construction industry to actively pursue alterations in its methodologies and reconsider notions like Circular Construction to foster greater sustainability. At the European level, endeavors to mitigate the building sector's impact are embedded within the comprehensive European Green Deal policy framework, designed to render the EU economy wholly sustainable. The ultimate ambition is for the EU to attain climate neutrality by 2050, facilitated by an array of initiatives spanning every sector of the economy, with a significant focus directed towards the construction sector [45]. The EU has implemented comprehensive measures to ensure the sustainability of the construction sector, with particular emphasis placed on the operational phase of buildings, recognized for their significant environmental impacts. To this end, extensive efforts have been made to develop policies aimed at reducing energy

consumption and its associated environmental impacts. Initiatives like the Energy Performance of Buildings Directive [46], and the New Renovation Wave [47] are primarily focused on enhancing building energy efficiency and reducing carbon emissions. However, the efforts and measures implemented as part of these breakthroughs have also led to undesirable increases and consequences in waste generation. In order to mitigate/eliminate these side effects of the increasing focus on the energy efficiency of buildings, it is also important to focus on materials and their embodied impacts in the transition of the construction industry towards a circular economy. On the other hand, regulation 305/2011 of the European Commission, "Laying down harmonized conditions for the marketing of construction products", contains provisions on the notification of the main characteristics of products on the market and the use of circular economy indicators to alleviate technical barriers on the market [48]. The Waste Framework Directive, introduced by the European Commission in 2018, promotes selective demolition and sustainable management of construction and demolition waste [49]. In alignment with this directive, the Circular Economy Action Plan, unveiled in 2020, includes a dedicated section on buildings and construction, aiming to extend building lifespans, minimize waste generation throughout their lifecycle, and optimize resource utilization within the construction sector [50].

The concept of the circular economy (CE) aims to transform current consumption and production patterns and is widely explored globally as an alternative to the traditional economic model of "take, make, and dispose of," addressing resource efficiency and environmental concerns [51]. At its core, the CE entails moving away from the linear notion of products reaching the end of their lifespan, instead focusing on the strategic and economic integration of elements back into systems after their useful life. In the construction sector, its objective is to minimize or eliminate waste, prolong building lifespan, and improve resource management, with the principles of "reduce, reuse, recycle" (the 3-R principles) shaping CE practices. The concept of the CE offers significant guidance and impetus to the construction industry in its pursuit of sustainability, emphasizing the importance of designing products for longevity, optimizing resource use, and implementing efficient recycling and waste management strategies. Embracing these principles is crucial for advancing sustainability objectives, as industries and communities can minimize waste, enhance resource efficiency, and contribute to a more sustainable future.

The idea of CE is closely linked with the effective management of CDW, as it optimizes material usage across their lifecycle, leading to waste reduction [52]. Prefabrication strongly aligns with the objectives of the circular economy as a robust method of minimizing on-site waste and reducing construction times. The prefabrication technique improves the quality of the final product, ensures a safe construction process and can reduce waste by 50%-70%. Furthermore, a 70% reduction in formwork is possible compared to traditional on-site construction [53]. Through these advantages, this construction technique minimizes various waste streams such as concrete and wood, which are inevitable wastes of the construction process, and contributes to ultimately enabling the circular economy. As an implementation-oriented approach of prefabrication considering the whole life cycle, Modular construction, acknowledged as a sustainable building methodology, enhances cost-effectiveness and is esteemed for its waste-free design, uncoupling construction cycles from finite material usage. It significantly contributes to sustainability by minimizing material waste and mitigating environmental influence through offsite manufacturing, while its modular nature facilitates effortless deconstruction and reconfiguration. This transformative technology embodies a paradigm shift, accelerating construction speeds, ensuring safer manufacturing processes, enhancing quality control, and reducing construction time and costs by up to 50% and 20%, respectively. Furthermore, its environmental benefits outstrip those of traditional onsite construction methods.

Moving towards a circular economy and reducing the environmental impacts of the construction sector while building sustainably should be achieved at all stages of a building's life cycle and in all components of the value chain. In this context, Design for X (DfX) methodologies have recently attracted great interest in research, innovation and manufacturing. DfX is a set of approaches to product and process design with the goal of cost optimization and quality improvement throughout the entire life cycle of a product. Applicable to all industries, DfX aligns product design and related processes with specific aspects of product development to meet specific requirements. Within the construction industry, more specialized iterations of this approach, such as Design for Manufacturing and Assembly (DfMA) and Design for Deconstruction (DfD), come to the forefront. These methodologies are crucial for maximizing

the benefits of modular construction techniques in line with circular economy principles, while also minimizing drawbacks through streamlined processes. In light of these considerations, this study undertakes an in-depth examination of DfMA and DfD techniques, which fully embrace the imperatives of circular economy to integrate sustainability into the construction sector at a modular scale. The objective is to significantly contribute to existing theoretical knowledge and advance comprehension of the concrete impacts of sustainable construction practices. Additionally, the study aims to offer valuable insights for practitioners looking to implement modular construction techniques efficiently and responsibly, thus making meaningful contributions to societal betterment.

1.2. Design for Manufacturing and Assembly (DfMA) and Design for Deconstruction (DfD)

The principle of Design for Manufacturing and Assembly (DfMA) is an approach based on optimizing the integration of components, considering design for manufacturing (DfM) and design for assembly (DfA) [54]. Since the 1980s, it has been widely used to simplify product design and reduce manufacturing time and costs. While DfM focuses on minimizing the number of parts, DfA concentrates on simplifying assembly. These methods aim to produce easily assembled and cost-effective products without compromising production quality. The fundamental difference lies in DfM focusing on manufacturing individual components, whereas DfA highlights how these elements can be assembled [55]. In both sub-approaches, based on historical data or simulations, they provide cost and time savings and offer pioneering solutions to minimize environmental concerns [56]. Generally, for the term off-site construction, terminologies such as prefabrication systems, panel systems, modular systems, and modular integrated systems are used, and the application of the DfMA principle is feasible for all these terms. **Fig. 1.1** illustrates the procedural flow applied for DfMA. Through this procedure, design, construction, and even production stages become more efficient and predictable [57].
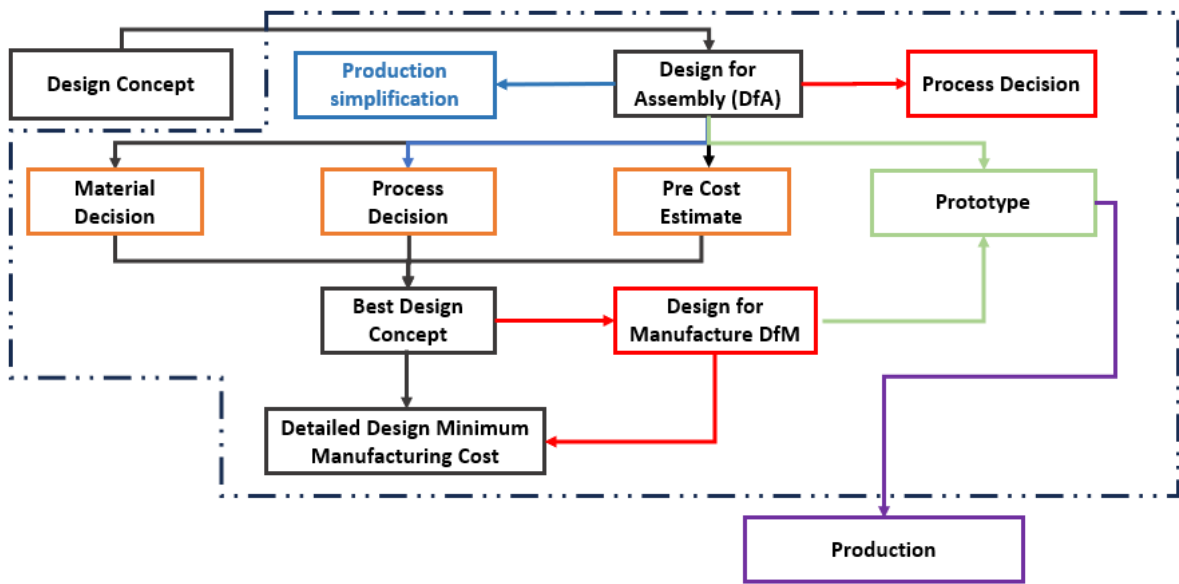
Fig. 1.1. Procedure flow implemented for DfMA

DfMA methodology adopts a collaborative decision-making procedure encompassing all implementation activities. The product system is simplified, thus reducing potential costs. The process begins with the design phase to ensure the product is easy to assemble. At this stage, various strategies are used to decrease system complexity, organize connections between parts, and plan assembly procedures. Subsequently, suitable materials are selected, and economic requirements are determined through cost estimates, aiming to minimize expenditures. In summary, the comprehensive implementation of DfMA brings various advantages such as waste reduction, improved production time, and cost reduction [58]. For instance, the ability to make early cost estimates during the design phase contributes to sustainable environmental practices by eliminating waste by-products and significantly reducing production time. Thus, DfMA is a principle that enhances the design for production, assembly, cost, and circular economy, while preserving the integrity of the basic product function. DfMA is commonly associated with prefabrication, where construction works are completed off-site as much as possible, and some researchers even consider DfMA equivalent to prefabrication. DfMA principles can be applied to all off-site construction systems. Perspectives of DfMA guidelines and their potential benefits are presented in **Table 1.1**.

The lack of standard DfMA guidelines in the construction industry, despite the widespread adoption of this design methodology, has been highlighted. In applying DfMA during the design phase, studies have generally utilized DfMA guidelines that they have tailored based on previous research. Various authors have proposed policies aimed at promoting the use of DfMA in construction practices, which typically include rules such as minimizing, standardizing, and modularizing assembly parts. While these approaches may focus on different lifecycle stages within the value chain, they generally offer similar contributions. However, the establishment of standardized DfMA rules based on construction-oriented design methodologies will contribute to maintaining the current technique on solid ground.

Table 1.1. Perspectives of DfMA guidelines and their benefits

Guidelines	Perspectives	Benefits	References
Aim for mistake-proof design	SD	Avoids unnecessary re-work, improve quality, reduce time and costs	[59,60,61,62]
Design for ease of fabrication	F; SP	Reduces time and costs by eliminating complex fixtures and tooling	[59,60,62]
Design for a simple part orientation and handling	F; SP	Reduces time and costs by avoiding non-value adding manual effort	[59,60,62]
Design with a predetermined assembly technique in mind	F	Reduces time and costs when assembling	[59,62]
Design multifunctional and multi-use parts	F; SP; SD	Reduces time with fewer manufacture processes and simplified jointing	[60]
Consider modular designs	SP; M	Reduces time and costs due to simplified design and assembly	[59,60,61,62]
Consider design for mechanized or automated assembly	SP; A	Improves assembly efficiency, quality, and security	[59,61,62]
Use standard and off-the-shelf components	SP; M; SD	Reduces purchasing lead time and costs	[59,60,61,62]
Use as similar materials as possible	SP; M	Reduces time with fewer manufacture processes and simplified jointing	[59,62]
Use as environmentally friendly materials as possible		Reduces harm to the environment and residents	[61]

Minimize the part count	SP	Reduces time and costs with simplified design, manufacture, and assembly	[59,60,61,62]
Minimize and standardize connector types and quantity	SP; SD	Reduces time and costs with simplified design, manufacture, assembly, repair and maintenance	[59,60,61,62]
Minimize the use of fragile parts	SP	Reduces costs due to fewer part failures, and easier handling and assembly	[59,62]
Do not over-specify tolerances or surface finish	F; SP	Reduces time and costs with easier manufacture	[59,62]

Note: A=Automation; F=Flexibility; M=Modularity; SD=Standardization; SP=Simplification.

Design for Deconstruction (DfD) is a methodology that emphasizes the end-of-life phase of a product. It incorporates procedures to disassemble the product into its original components for future reuse, thereby promoting the circular economy [63]. Additionally, DfD is a significant circular lifecycle method and is closely associated with the "reverse construction" principle. Reverse construction can be defined as the deconstruction of building elements into parts to reintegrate them into the cycle for reuse and recycling [64]. **Fig. 1.2** provides a visual representation of the sequential stages encompassed within the DfD principle.

DfD offers four additional alternatives, including dismantling, processing materials, recycling disassembled components for use in other structures, reusing parts, and relocating the whole building for the same or different purposes [54]. These options promote a sustainable construction environment by eliminating the need to construct a new facility each time, thereby supporting the logic of consuming fewer natural resources and generating less waste through the use of DfD. Although studies showcasing the synthesis of these two closely linked principles, DfMA and DfD, into a single design method known as Design for Manufacturing, Assembly, and Deconstruction (DfMA&D) have been exhibited [54,65], research simultaneously evaluating DfMA and DfD remains limited. It is essential to explore the guidelines and advancements of these design methodologies to further their utilization.

With increasing environmental awareness, the construction industry is at the forefront of industries striving to adopt these design methods on a wide scale. However, the adoption of new concepts always presents challenges. Nevertheless, in recent years, the construction industry has

made significant strides in construction application and management by embracing these design methods.
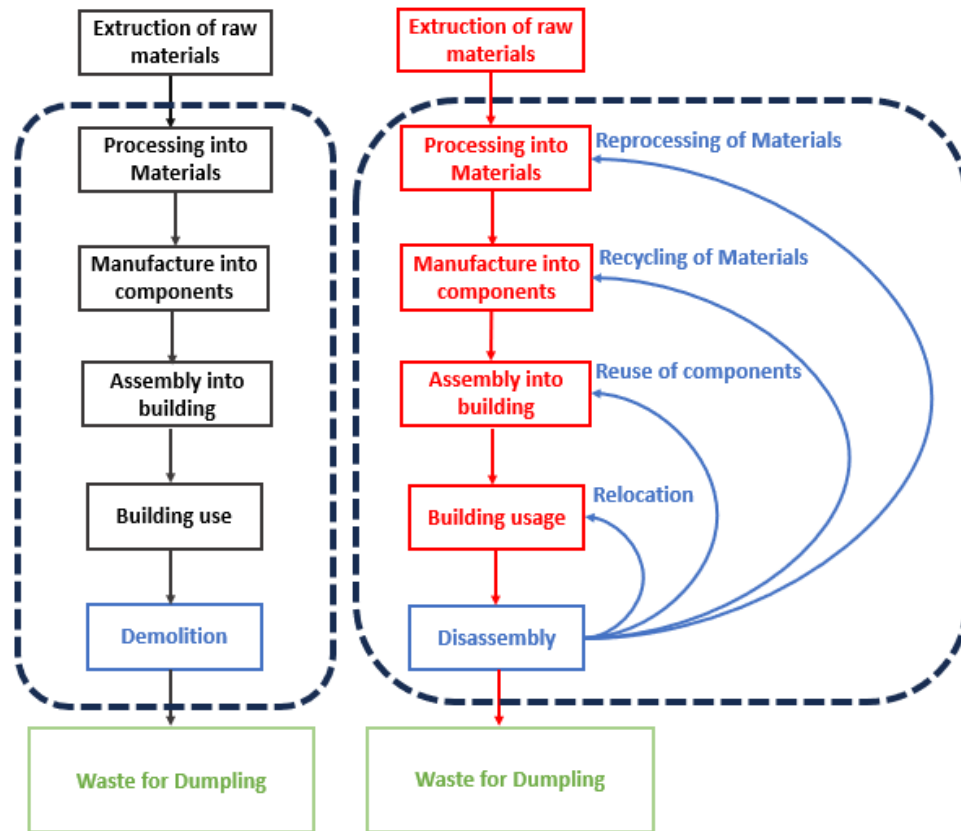
Fig. 1.2. Stages of the DfD approach

Similar to DfMA, there is no directly applicable common understanding or guideline for DfD. Studies in the literature and limited professional guidelines generally embrace approaches to design and construction principles that are suitable for this technique rather than making specific DfD approaches and definitions. In this context, the conducted studies have mainly evaluated DfD based on concepts of collaboration and competence that enable designs encompassing overall building design, material and connection elements, construction and deconstruction works, and all these stages in the design process. The relatively new approach of DfD for the construction industry is also one of the primary reasons for this situation. According to limited studies, perspectives of DfD guidelines and their benefits are presented in **Table 1.2**.

Table 1.2. Perspectives of DfD guidelines and their benefits

Perspectives	Guidelines	References
Design of the Construction	Designing a building as a multi-layered structure with individual life cycles	[65,66,67]
	Formulating a plan for deconstruction and waste management	[67]
	Minimization the number and variety of building components through modularization and standardization	[65,66,67]
	Utilization of off-site construction and prefabrication techniques to the building process	[65,66,67,68]
	Incorporation of lightweight components	[65,66,67]
	Utilization accessible technical installations within an open building design	[66,67]
	Designing the interchangeability of building components for flexibility and ease of maintenance	[67]
	Incorporation of a structural grid	[66,67]
	Establishing a database for materials, parts, and construction data	[65,66]
	Integration of deconstruction type and technique within the design phase	[68]
	Technical plans, schematics, and images documentation	[65]
Design of Materials and Connections	Use of reusable, environmentally safe, non-hazardous materials	[65,66,67,70]
	Use of simple, ease-to-remove connections	[68]
	Use of mechanical, dry connections	[66,67,70]
	Connections and connection types number minimization	[66,67,69]
	Design materials and connections for long service life and durability	[66,67,69]
	Use of accessible components and connections	[68]
	Avoid to use the composites and different types of materials	[65,66,67,70]
	Avoid applying secondary finishes	[66,67]
	Storage of replacement components for unexpected minor revisions	[66]
	Optimization of element size	[66]
	Identification of lifespan of each material and components	[67]
	Determination of the end-of-life performance of each elements	[67]
Determination of Deconstruction Details	Instructions for materials to undergo reuse and recycling	[65,67]
	Identification of components within the building system allocated for deconstruction	[66]
	Consideration of simultaneous deconstruction within the design process	[66]
	Facilitating easy access to the entire building	[66]

1.3.   Sustainability and Principles of DfMA and DfD

Approximately 40% of waste production and 25% of resource consumption are attributed to building construction, while 25% of global carbon emissions derive from the construction sector [71]. The environmental impact of the construction sector arises primarily from the substantial energy required for material production [72]. The ongoing use of new raw materials and energy also leads to adverse economic effects. The construction industry traditionally follows a linear economic model, where industrial production and resource consumption occur without consideration for the physical limitations of raw materials [73]. Due to the prevalence of this model, concerns regarding sustainability persist. Traditional approaches are inadequate in addressing environmental concerns, as supported by numerous studies. Traditional construction methods still rely heavily on large amounts of concrete, scaffolding, formwork, wall, and roof elements, generating considerable waste. Productivity in traditional methods is often hindered by delays and waste due to the direct impact of workers' productivity [74]. Therefore, practitioners and researchers have endeavored to implement new methods embracing the circular economy approach to enhance the construction process. While productivity in the construction industry decreases, the manufacturing sector continues to enhance its productivity [75]. Particularly for rapid production structures, the growing inclination towards sustainable methods, coupled with researchers' heightened attention to environmental issues, has encouraged the adaptation of principles such as DfD and DfMA, which embrace sustainable and circular economy models, to new generation production techniques. In this context, the potential of DfMA and DfD methods to completely transform the construction process and mitigate undesirable effects has emerged prominently.

Developing new products with high quality and speed at low cost, while integrating sustainability into product design to meet environmental standards, is crucial. This relies on reducing the number of parts, operations, assembly, and production times, as well as selecting eco-friendly materials and incorporating options such as reusable connection designs. From the perspective of the design stage and considering the early stages of product development, DfMA methods are often the most impactful methodologies for sustainability, as they typically allow for reducing waste, product complexity and significantly decreasing costs and operating times

[76]. Because it provides significant direct and indirect sustainable environmental benefits, such as reducing emissions, energy consumption, and the amount of required raw materials.

Continuously implementing demolition practices leads to increased waste generation, higher consumption of raw materials, and associated costs. Therefore, it is important to adopt the DfD method to change this traditional practice. DfD significantly enhances the sustainability of the construction industry by shifting from the traditional linear material use model to a circular model where building components are designed to be disassembled, reused, and recycled. Reuse strategies aim to directly utilize old structural components, thereby reducing raw material demands, component production, and waste disposal, thus providing a more sustainable reuse approach. Particularly, it is known that concrete components have a longer service life compared to other components, making them suitable for reuse [77], However, traditional connections hinder the reuse of components. Therefore, DfD, considering the reusability of components during the structural design stage, is created with a design concept that facilitates dismantling/repair.

There is a substantial number of studies focusing on material-phase recycling of products, but efforts need to be scaled up to the structural element level. The use of DfD will help promote circularity and support sustainable development. DfMA and DfD methods can be applied simultaneously to minimize deconstructible components, use lightweight materials, and execute easy process systems such as prefabrication, thus reducing costs and enhancing quality [54,66]. These approaches are commonly employed to reduce costs and enhance quality. Additionally, integrating these methods into the design process has been recognized as a practical strategy to make the asset lifecycle circular and reduce waste. Incorporating DfMA and DfD into the design process is considered a step towards bringing about radical changes and transformation.

1.4.   DfMA in Construction Industry

The utilization of DfMA is particularly thriving in the off-site construction method. The terminology encompassed by off-site construction is quite broad, including terms such as modular construction, modular integrated construction, prefabricated construction, modern construction methods, and industrialized building systems. All these terms are associated with

off-site construction. The benefits of off-site construction and DfMA can be perceived similarly because their goals are aligned. However, from a broader perspective, DfMA can be seen as a tool to maximize the full potential of prefabrication. Many studies consider off-site construction practices that align building components with precast structures, supporting a certain degree of standardization while minimizing environmental impacts. Compared to traditional construction, off-site construction is perceived as a more advanced technique, with aspects such as reduced construction time, increased quality, and anticipation and elimination of potential errors [78].

Implementing the DfMA principle entails a collaborative decision-making process that takes into account all activities related to its application, aiming to streamline the product system and lower potential costs. The process begins with designing the product to be easily assembled. At this stage, strategies are applied to reduce system complexity. Connections between elements are designed, and assembly processes are planned. Then, suitable materials are decided, and cost requirements are finalized through cost estimation. It may seem that incorporating the DfMA approach into these processes would extend the design process. However, it has been observed in many studies that integrating this method enhances efficiency in all other procedures after the design stage and reduces total production time.

The utilization of the DfMA method in the construction industry provides the following benefits: i) Low cost due to predictable expenses, ii) Simplification of modular structure design, iii) Reduced construction time, iv) Improved design, v) Higher quality construction, vi) Safety enhancement. The adoption of DfMA in the construction industry brings contributions such as increased efficiency, reduced costs and waste, optimized safety and quality, and enhanced reliability. Strategies such as minimizing the number of parts, simplification, reducing weights, and minimizing waste generation during the assembly process contribute to these benefits. DfMA guidelines, developed and presented by Boothroyd et al. [79], have been further supplemented by guidelines developed by researchers such as Emmatty and Sarmah [61] and Swift and Brown [62] for the implementation of DfMA. Despite the increasing adoption of DfMA and the continuous improvement of related guidelines, it is important to note that the focus has not been on its implementation in construction projects. For instance, Boothroyd's [79] DfA and DfM-focused DfMA procedures do not address downstream logistics and supply

chain elements critical in offsite prefabrication construction. Therefore, there is an ongoing need for further development of the guidelines [60]. A research conducted by Tan et al. [80] established construction-focused DfMA guidelines, including "context-based design, technology-based design, logistics-optimized design, component-integrated design, and material-lightened design."

Review articles specifically focusing on DfMA are relatively scarce. The article by Gao et al. [81] approached DfMA principles from the perspective of the construction industry. It extensively examined the process, starting from the design phase and evaluating the manufacturing and assembly process, with a detailed analysis of the use of the DfMA model in prefabricated construction. Another article by Razak et al. [55] emphasized that DfMA techniques serve as a design principle to enhance industrialized building methods. It highlighted the current state of this principle in the construction sector, its benefits upon implementation, and the challenges associated with its adoption. Additionally, it underscored the integration of building information modeling (BIM) methods in the implementation of these design principles, revealing the benefits of DfMA usage. In another study, Gbadamosi et al. [82] examined four different assembly parameters for design optimization: (i) ease of assembly, (ii) ease of processing, (iii) assembly speed, and (iv) assembly waste. They identified assembly speed as the most critical category. A case study was conducted to evaluate system performance, and the results were presented to a panel of validation experts. The assessment system was tested in a BIM environment to evaluate the composite optimized assembly score for four BIM materials used in building cladding. Validation results indicated that the assessment system was practical and had the potential to enhance the construction industry's ability to meet efficiency goals. Moreover, a study conducted by Tan et al. [80] suggested three potential functions of BIM integration with DfMA: enabling the DfMA process, serving as a tool for using DfMA techniques, and generating an information model for DfMA.

Lu et al. [83] addressed the integration of Lean construction principles with the DfMA concept, providing an in-depth analysis. Roxas et al. [54] and their colleagues attempted to compile the benefits of studies using the synthesis of DfMA and DfD, along with trends and challenges in their implementation, through a systematic review. Meanwhile, Hyun et al. [84] conducted a

systematic review to explore the promising use of DfMA methods for Off-site construction (OSC), highlighting the lack of a comprehensive design process despite the frequent use of DfMA in OSC methods. They proposed a systematic design process for OSC to address this issue. Numerous researches have been conducted to identify factors hindering the broad adoption of OSC, revealing challenges such as lack of experience and knowledge, resulting in errors such as neglect and conflict in design, as well as a lack of early interventions for critical decisions. To mitigate these issues, the need for design guidelines specific to the OSC process has been emphasized [85].

Case studies often delve into aspects such as efficient assembly processes during the design phase, reduction or simplification, facilitating manufacturing and assembly by minimizing the number of parts [86], simplifying the geometry and reducing the weight of components [87], or reducing complexity in operations [88]. These studies commonly reveal prevalent practices in the implementation of DfMA, such as developing criteria for "manufacturability" and "assemblability," investigating specific challenges addressed in design, involving diverse professionals in the design team, and optimizing design through various principles, aiming at producing simpler yet functional products under the simplification principle.

The utilization of DfMA has significantly reduced application errors, minimized waste production, and increased productivity. In a study conducted by Chen et al. [89], the aim was to achieve a more practical process by incorporating DfMA from the design to the construction phase of a curtain wall system. The guides and approaches used in the study were tailored specifically to the project. Upon examination of the results, a significant improvement in application accuracy was observed. Additionally, the typical assembly time for a curtain wall system unit showed a 50% decrease with the use of DfMA. In terms of cost, Banks et al. [90] demonstrated in their study on a 40-story high-rise residential construction project that the implementation of DfMA principles led to tangible improvements compared to traditional in situ construction methods. Particularly noteworthy was the high controllability of the construction program, which was in line with cost estimates and contract value. Wasim et al. [91] applied DfMA methods to examine the wooden frame wall and plumbing drainage system of a residential building. Field and factory observations were conducted to collect real assembly

times for these components. These data revealed the impact of DfMA-based pre-assembly on design efficiency and its cost implications. Trinder et al. [92] highlighted that DfMA not only brought economic benefits but also contribute to enhancements in health and safety. Numerous research studies investigating the hurdles of implementing DfMA in the construction sector have concentrated on issues like inefficiencies within multidisciplinary teams, limitations in design standards, conventional loading methods, insufficient training, absence of a supportive environment, and delays in involving suppliers in the project's initial phases.

1.5.   DfD in the Construction Industry

DfD offers a sustainable approach by utilizing the dismantling principle when products reach the end of their service life due to any reason, thereby promoting reusability and recyclability instead of traditional demolition. Planning the dismantling procedure before construction begins can yield more environmentally and cost sustainable outcomes. This sustainable practice is feasible through the integration of DfD into modern construction processes. Reusing production elements in a different system after initial use and making this process continuous can significantly contribute to the preservation of natural resources [68]. The increasing environmental pollution and unnecessary depletion of natural resources pose a significant threat to public health and safety. The common denominator of all off-site production approaches is standardization with techniques that consider environmental principles [93]. However, the broader environmental impacts of prefabrication techniques should be taken into account, and policies and standards that consider these impacts need to be developed [60]. The necessity for the construction industry to continue with more sustainable techniques fully supports DfD's cradle-to-cradle approach to reducing environmental impact. This approach embraces a design approach that allows for future changes to structures and extends the lifespan of buildings by enabling the dismantling of materials [94].

DfD enables the possibility of reuse and recycling approaches in the construction industry's value chain, making a circular economy a viable option for a sustainable industry. The transition to a circular economy will not only reduce waste in the construction industry, thus saving resources, but will also contribute to the proliferation of green products. For effective implementation of DfD, a building system should be simplified, suitable materials should be

used, and relevant deconstruction information should be easily accessible. Considering these parameters, efficient DfD implementation in the construction sector can be achieved. Incorporating the DfD stage into the planning phases can eliminate the production of construction and demolition waste [68]. From an environmental perspective, this is among the best options for construction waste management methods. When buildings undergo deconstruction instead of demolition, the structural elements obtained can be reused in the construction of different buildings [95]. Additionally, in terms of supporting sustainable development, DfD can reduce waste generation, enhance resource efficiency, and provide a more adaptable construction technique, thereby increasing the ability of existing structures to adapt to new services and reducing the need for new constructions [96].

At the core of the DfD principle lies the design of demountable and reconfigurable building elements, with the development of supporting structural connection elements being the most crucial factor enabling this capability. Various types of DfD connections, which distinguish DfD structures from traditional prefabricated buildings, have been proposed to facilitate the creation of demountable structures. These include bolted end-plate connections [97], cast-in-place concrete connections [98], embedded steel connections [99], among others. Several studies have explored the suitability of different materials for deconstructable structural elements, highlighting their unique characteristics and implications for sustainable construction practices. In their study, Broniewicz et al. [100] emphasized that steel material is an ideal material for deconstruction due to its sustainable qualities such as low waste generation, reusability, and compatibility with dry construction processes. Similarly, Lu et al., [60] proposed some DfD rules for cold-formed steel structures, listing their outcomes as ease of deconstruction, increased reuse, and enhanced safety. Tingley, [101] presented an examination of DfD for wood, steel, and concrete structures. Wood structures are generally suitable for deconstruction due to their simple construction techniques and standard dimensions. Standard-sized bricks and blocks in wall works, especially when lime mortar is used, are suitable for reuse, while cement mortar may complicate this process. Steel, on the other hand, is typically recyclable, and its reuse depends on the quality of the steel and the connection method; adding fire protection can make deconstruction more challenging.

26

In general, these materials and systems may require high costs and labor. However, it is important for a sustainable construction technique to be cost-effective and to have easily accessible and usable materials. In this context, concrete, as a fundamental material in traditional construction techniques, is considered a building material that should be taken into account for DfD techniques due to its low cost, easy accessibility, and applicability. One of the studies conducted for the integration of DfD, the study by Wang et al., [102] carried out an experimental study to determine the applicability of DfD to a composite beam design constructed with prefabricated concrete beams and clamping connectors. The load-deflection curves of demountable composite beams constructed using concrete planks and clamping connectors indicate a ductile behavior with minimal or no loss in post-yield strength. Under full service loading, the behavior of the beams exhibited slight nonlinearity, possibly attributed to beam flexure, slight displacement of steel beams, or minor slippage of the clamps. However, it is believed that the steel beams and concrete planks in these demountable composite beams can be reused without significant concern for any potential yielding during their service life. Ding et al. [103], introduced a new concrete beam-column connection design developed as DfD connections and investigated their behavior under seismic loads. The findings demonstrated that the designed connections exhibited reasonable performance under seismic conditions and displayed reversible behavior. Xiao et al. [104] examined the effect of coarse aggregate materials on connections. They noted that the connection performance was minimally affected but remained within acceptable limits. Korkmaz and Tankut, [105] examined concrete joints with a specific level of dismantling and suggested that employing hybrid steel joints was the most suitable approach for implementing DfD principles in concrete structures. This approach enables continuity of reinforcement without disturbing the complex reinforcement in the joint core. Leso et al. [106] and others developed wood-steel connection designs to reduce concrete usage and adopted a comprehensive DfD principle by incorporating recyclable materials into their studies. Finally, emphasizing the long service life of structures, it was noted that further research is needed to develop these predictions due to the lack of advanced studies on the application of DfD principles to structures that will be dismantled approximately 60 years later.

To address this knowledge gap, utilizing simulations and virtual models to determine whether a building is demountable at the end of its service life is an important approach. In a study

conducted by Basta et al. [107], Building Information Modeling (BIM) was employed to develop a demountability assessment scoring system. This made it possible for the authors to evaluate the feasibility of deconstruction at the end of a structure's life. The development of various BIM software and international data exchange standards such as IFC can assist in reducing the complexity of deconstruction details. Therefore, BIM programs have been widely utilized to promote DfD principles. Akbarnezhad et al. [108] analyzed information stored in BIM databases to examine potential applications for recycling and reuse of construction materials, proposing a method to select the best deconstruction strategy. They validated their developed procedures by presenting the results of a case study. Similarly, Swift et al. [109] investigated the use of RFID physical tags within the BIM process to change ownership of building components and facilitate lifelong management of component cycles. Marzouk et al. [110], developed a BIM plugin tool to integrate deconstruction practices into building design. Schultmann and Sunke [111], differentiated recycling at the module or component level and recycling at the material level.

One of the notable studies focusing on the DfD principle is the research conducted by Xia et al. [112], which addresses concerns related to the Circular Economy. In this study, it is highlighted that the implementation of DfD provides 1.8 to 2.8 times more environmental benefits compared to structures built without employing DfD principles. Leising et al. [113], identified the Circular Economy approach for buildings as a life cycle approach that optimizes the useful life of buildings, integrates end-of-life stages into design, and employs new ownership models where materials are temporarily stored and reused. In a research by Ortlepp et al. [114], the environmental impact of DfD constructions using dry connections was examined in comparison to those constructed with wet connections. It was determined that the use of dry connections increased material recycling. Eckelman et al. [115] evaluated a new DfD floor system and reported that when the components of the DfD floor system are reused, it becomes a more environmentally beneficial alternative compared to conventional floor systems. It was indicated that the negative environmental impact of traditional floor systems could be reduced by approximately 60% to 70% when the components are used three times. Tingley and Davison [116], developed software for Life Cycle Assessment (LCA) of DfD structures, ensuring that the environmental impacts of the components are equally considered throughout their lifecycle.

1.6.   Case Study: CDW-based Demountable Lego Construction

1.6.1. Introduction

The construction sector stands as one of the largest industries responsible for a significant portion of Turkey's gross domestic product (GDP). The sector's linear economic model, characterized by a "build-use-dispose" approach, poses substantial environmental, social, and economic challenges. CDW resulting from construction and demolition activities contributes to approximately 40% of the total solid waste generation, with these waste materials often being directly disposed of in landfills without undergoing recycling processes, thus creating significant economic and environmental burdens [117]. Particularly in Turkey, recent urban transformation projects are expected to result in the demolition of approximately 6.5 million housing units, leading to a substantial increase in CDW generation [118]. Effectively managing, segregating, classifying, monitoring, improving, and ultimately recycling CDW to integrate into a circular economy stands as one of the paramount goals of today's world. The designation of the construction and demolition sector as one of the five target sectors under the European Union Circular Economy Action Plan underscores the importance of this issue [119].

Apart from urban renewal efforts, earthquakes stand as a significant contributor to the generation of construction and demolition waste in Turkey. Situated in a region with three major fault lines and over 500 active faults, Turkey is highly prone to seismic activity [120]. Unfortunately, on February 6, 2023, a devastating earthquake measuring 7.7 on the Richter scale struck, centered in the Pazarcık district of Kahramanmaraş. This earthquake impacted neighboring provinces, including Adıyaman, Hatay, Kahramanmaraş, Kilis, Osmaniye, Gaziantep, Malatya, Şanlıurfa, Diyarbakır, Elazığ, and Adana, home to approximately 14 million residents. Roughly 9 hours later, a second major earthquake, registering 7.6 in magnitude, hit the region, causing even more severe damage and the collapse of already compromised structures. According to the latest data gathered by the Ministry of Environment, Urban Planning, and Climate Change, approximately 250,000 buildings have been identified as either destroyed, slated for demolition, or severely damaged. With ongoing damage assessments and the anticipated demolition of moderately damaged structures, this figure is expected to rise.

The estimated quantity of waste generated in the aftermath of the earthquake ranges between 100 to 210 million tons, depending on various predictive models.

Factors such as population growth, pandemics, earthquakes, floods, and migrations continue to drive the demand for rapid construction structures. This escalating demand underscores the need to prioritize the more effective implementation of rapid construction techniques based on DfMA principles, as well as applications taking DfD principles as the base, aimed at preventing the demolition of buildings at the end of their service life. In today's context of sustainability and waste reduction efforts, there is an increasing emphasis on the development of building materials using various waste-based materials and the recycling of manufactured building components. From a production standpoint, it is imperative to focus on new generation circular production techniques that allow for optimal automation and manufacturing of structures, thereby facilitating the realization of circular economy principles in the construction sector.

The urgent and economical provision of housing for vulnerable groups, ensuring their long-term usability and even rapid relocation to requested locations when necessary, designing existing building systems to be adaptable and expandable according to need, as well as the design of building components that can utilize region-specific natural materials or construction waste through recycling, and the development of new production techniques, will enable the implementation of sustainable measures against disasters. To achieve this goal, a case study covering all stages of the construction industry value chain was conducted, taking into account the advantages provided by DfMA and DfD principles. In this study, geopolymer-based building elements, entirely derived from construction and demolition waste, were developed and used to manufacture a single-story building.

The DfMA method ensures a predictable optimization of the construction process from both environmental and economic standpoints, while the DfD method aims to facilitate the reuse of structural components of buildings after their service lives, significantly reducing the environmental impacts of construction activities in terms of raw materials, energy, and emissions. When the building's service life ends, large steel components can be recycled through an energy-intensive melting process. Other materials are either stored inactively in waste sites

or inefficiently recycled as fill material in road construction. To significantly reduce and recycle such waste, it should become commonplace to design and construct buildings to be reused after their service lives. To achieve this goal, this case study, which synthesizes the DfMA and DfD principles, has been conducted within the framework of the principles and foreseeable benefits outlined in **Fig. 1.3**.
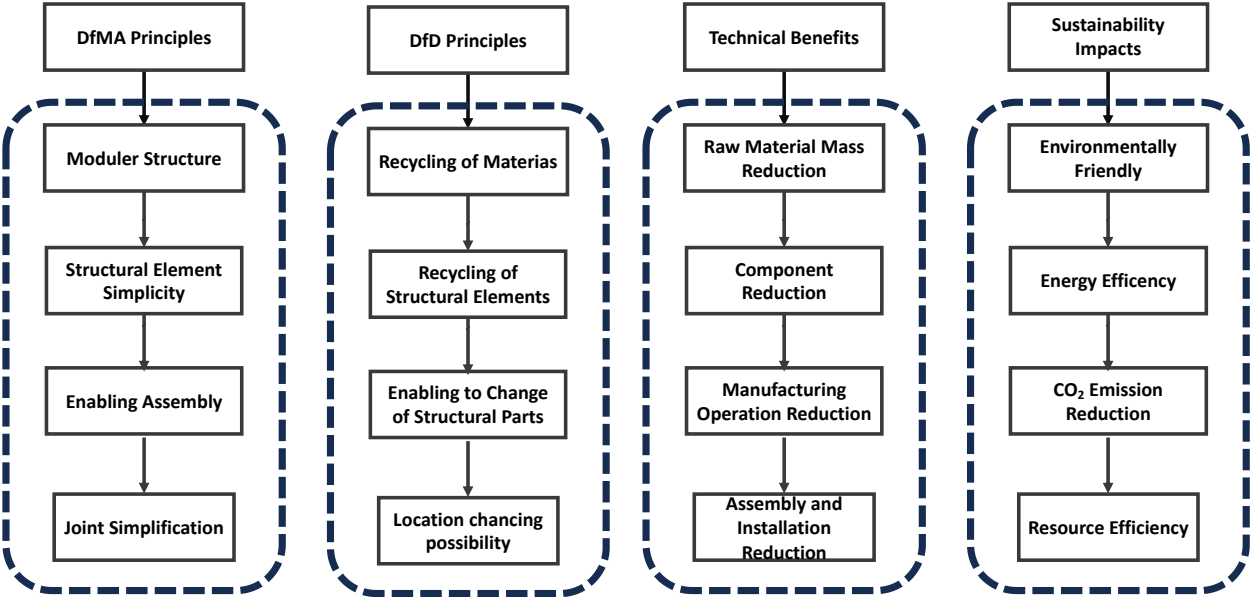
Fig. 1.3. DfMA and DfD principles adopted in the case study and expected benefits and impacts

Reusing reinforced concrete structural elements after their service life should be a priority in material efficiency strategies. The key to the success of reusable structural components lies in conducting a design phase that considers DfMA procedures during production and realizes designs that can easily be made compatible with DfD at the end of the structure's service life. Demountable structural systems offer many sustainable benefits such as construction speed, design flexibility, cost reduction, and energy and material savings. Demountable structural elements provide less interruption and significant savings as they can be assembled or disassembled quickly or expanded. Given the serious natural disasters that leave millions of people homeless in our country, there is a significant need for urgently developing low-cost, sustainable, easily manufacturable, and expandable shelter structures. It is believed that these demands can be easily met by developing demountable prefabricated building systems. In this

context, the study was conducted in light of the construction-focused DfMA guide compiled by Lu et al. [60], considering a design process that simultaneously enables the realization of DfD principles. The Civil Engineering project team at Hacettepe University conducted a study focusing on the development and utilization of green concrete systems, which are produced solely from demolition waste, using a production technique called the disassemble-reassemble Lego concept. As a result of the studies, structural elements (columns, beams, slabs, etc.) that can be demounted and reassembled have been developed using demolition waste-based materials. This has opened up the possibility of using low-quality waste like construction and demolition waste in an innovative production technique to achieve high added value. In this context, the construction process of a single-story structure with an area of approximately 300 m^2 was completed within the campus, and currently, this structure has being used as an administrative building. All structural elements of this building, including columns, beams, and walls, were prepared in advance at the production facility and transported to the site. Thanks to the connections of the prepared elements, they were ready for installation, and the construction was completed after an installation process lasting approximately four days.

1.6.2. Sustainable, Green Geopolymer Concrete

The production of building materials focusing on material recycling, which enables a circular economy and sustainable development, has the potential to significantly reduce greenhouse gas emissions. In this regard, utilizing construction and demolition waste (CDW) in the production of building materials holds great potential [121-123]. This potential contributes to green transformation initiatives by reducing the negative impacts associated with Portland cement production and enabling waste recycling. In this context, the present study designs new geopolymer concrete mixtures by utilizing various CDW-based materials as precursors and aggregates.

The final CDW-based geopolymer concrete developed in the study was produced by activating a combination of sodium hydroxide, sodium silicate, and calcium hydroxide alkali activators with different proportions of CDW and industrial wastes, namely ground granulated blast furnace slag and fly ash. The aggregate phase of the mixture consisted of fine and coarse

recycled concrete aggregates obtained from the concrete waste phase, thus establishing a completely waste-based system (**Table 1.3**).

Table 1.3. Mixture proportion of CDW-based geopolymer concrete

Mixture proportion (kg/m^3)												
HB	RCB	RT	C	G	GBFS	FA	Ca(OH)$_2$	NaOH	Na$_2$SiO$_3$	FRCA	CRCA	Water
150	200	250	100	100	150	50	50	112	224	500	500	202

Following the 28-day ambient curing of the developed CDW-based geopolymer concrete, a compressive strength of 34.2 MPa was achieved, while its shrinkage, water absorption, and porosity performances were comparable to conventional concrete with values of <4000 μɛ, <8.6%, and <9.8%, respectively. Furthermore, structural testing of the developed geopolymer concrete was conducted to compare its behavior with Ordinary Portland Cement (OPC) concrete. Flexural tests on beams and axial and lateral cycling loading tests on columns were performed [124-126]. The results indicated similar behavior to elements produced with OPC concrete in terms of load-displacement capacity. The similarity in curvature capacities and crack behaviors confirmed these observations. When subjected to the dominant bending behavior of the designed structural element, the geopolymer concrete exhibited a significant amount of ductility. The ductility of the geopolymer concrete in curvature was confirmed to be comparable to traditional concrete through the conducted tests. In light of all these findings, geopolimer concrete containing recycled aggregate emerges as a strong candidate against Ordinary Portland Cement, adhering to the principles of DfMA and DfD, for evaluating the structural performance of beam-column, column-foundation, and slab-beam dry connections to be used in the construction of a demountable prefabricated building.

1.6.3. Design and Manufacturing the Demountable Structural Elements

In this case study, which synthesized the principles of DfD and DfMA approaches, demountable connections and structural elements were produced in a way that facilitated easy manufacturing, disassembly, and assembly, enabled modular construction, and allowed for the recycling of waste materials. This was done to create beam-column, column-foundation, and slab-beam

connections based on these fundamental approaches (**Fig. 1.4**). In the design and manufacturing phase of the demountable structure, the following principles of the DfMA approach was considered: (i) Aim for mistake-proof design, (ii) Design for ease of fabrication, (iii) Design for simple part orientation and handling, (iv) Design with a predetermined assembly technique in mind, (v) Consider modular designs, (vi) Use as similar materials as possible, (vii) Use as environmentally friendly materials as possible, (viii) Minimize and standardize connector types and quantity, (ix) Minimize the use of fragile parts, (x) Do not over-specify tolerances or surface finish. On the other hand, considering the DfD approach and the guidelines presented in the literature, the following principles have been taken into account: (i) Formulating a plan for deconstruction and waste management, (ii) Minimization the number and variety of building components through modularization and standardization, (iii) Utilization of off-site construction and prefabrication techniques to the building process, (iv) Designing the interchangeability of building components for flexibility and ease of maintenance, (v) Incorporation of a structural grid, (vi) Integration of deconstruction type and technique within the design phase, (vii) Documentation of technical plans, schematics, and images, (viii) Use of reusable, environmentally safe, non-hazardous materials, (ix) Use of simple, ease-to-remove connections, (x) Use of mechanical, dry connections, (xi) Connections and connection types number minimization, (xii) Design materials and connections for long service life and durability, (xiii) Use of accessible components and connections, (xiv) Avoid applying secondary finishes, (xv) Optimization of element size, (xvi) Instructions for materials to undergo reuse and recycling, (xvii) Identification of components within the building system allocated for deconstruction, (xviii) Consideration of simultaneous deconstruction within the design process, (xix) Facilitating easy access to the entire building.

In order to investigate the capacity of the proposed demountable beam-slab connections, beams measuring 240 mm x 445 mm were placed on top of slabs measuring 240 mm x 800 mm x 3670 mm, as observed in **Fig. 1.4.** Connections between the slab and beam were facilitated using square profiles embedded within the slab. Displacement results were monitored using Linear Variable Differential Transformers (LVDT) during testing. For the proposed column-foundation connection, selected based on performance from three different demountable connection types researched by Akduman et al. [126], ultimate connection tests were conducted under three

different axial compressive loads. The cross-section of the demountable columns was 150 mm x 250 mm with a height of 930 mm. Each column was reinforced with six longitudinal bars of 10 mm diameter and stirrups of 6 mm diameter. The sample containing this connection exhibited behaviors such as cracks induced by plastic hinges, core crushing, and longitudinal bar ruptures under advanced loads during testing. Thus, the testing for column-slab connections was successfully completed.

Following the design and completion of all these connections, the real-scale demonstration process commenced. Located within Hacettepe University Beytepe Campus in Ankara, Turkey, the single-story building composed entirely of demountable structural elements comprised 24 columns, 37 beams, and 19 slabs, all produced in a precast concrete factory. The demountable structural elements were assembled within a short period (less than 6 hours), and the main skeleton of the building was installed. The total construction time, including the facade cladding of the building, was less than 4 days. Construction began with laying the foundation, followed by the placement of columns and beams on the foundation, and finally, the installation of slabs (**Fig. 1.5**). Only bolts were used in the column base and slab-beam sections, yet due to the bolted connections designed for beam-column connections, assembly was easily accomplished without the need for screws. Thus, the completed structure was constructed entirely from environmentally friendly materials and designed to be fully demountable.

	Demountable Structural Element	Testing of Connection Performance	Dry Connection Elements
Beam-Column Connection			
Slab-Beam Connections			
Column-Foundation Connection			

Fig. 1.4. Demountable structural elements and connections

Fig. 1.5. Completely demountable housing construction with CDW-based geopolymer concrete

1.7.   Conclusion

In this chapter, the aim is to in the main theme, background, benefits, applications, and impact of Design for Manufacture and Assembly (DfMA) and Design for Deconstruction (DfD) on sustainable development within the construction industry. In this context, a comprehensive literature review was conducted, providing an overview of the current position of DfMA and DfD techniques in the construction industry. Process flows, fundamental principles, existing guidelines were examined, and research gaps were assessed. In addition to this literature review, a synopsis of a planned case study involving CDW-based geopolymer demountable structural elements, which are detailed in the subsequent chapters of the thesis, was presented within the framework of rapid and sustainable construction, which was the main motivation of the thesis. The findings obtained from this chapter of the thesis are listed below:

DfMA aims to enhance efficiency in the production process for the final product by making moves such as increasing productivity, reducing costs, and minimizing waste. DfD principles center around developing components that can be reintegrated into the system at the end of their service life for the same or different purposes during the design phase, designing them to allow for easy and rapid manufacturing, and maximizing reusability.

While widely adopted in various industries, the integration of DfMA and DfD techniques in the construction industry, despite the use of prefabrication techniques, has not yet become widespread enough. Therefore, there is a lack of standard DfMA and DfD guidelines for the construction industry, and it is important for future studies to develop standard construction-oriented DfMA and DfD guidelines. Additionally, integrating these design methods with emerging technologies like BIM can bring significant benefits, as such technologies can be utilized as tools and information models for these methods.

More comprehensive studies are needed to integrate DfMA and DfD, which are important approaches supporting sustainable development and the circular economy, into the construction sector. Conducting studies on the synthesis of these systems, maximizing the benefits obtained, and comprehensively researching their effects compared to traditional construction techniques are crucial steps towards the widespread adoption of these techniques.

Within the scope of the examined case study, demountable connections developed for structural prefabricated elements such as beams, columns, and slabs, produced with CDW-based geopolymer, synthesizing the DfMA and DfD approaches, exhibited successful performances under various loading conditions, enabling their use in prefabricated buildings. The use of demountable connections in the construction of prefabricated buildings reduces the time and labor cost of on-site assembly while maximizing the CDW-based geopolymer waste recycling.

CHAPTER II: COMPRESSIVE STRESS-STRAIN MODEL FOR THE ESTIMATION OF THE FLEXURAL CAPACITY OF REINFORCED GEOPOLYMER CONCRETE MEMBERS

2.1. Introduction

The rapid progress of the construction sector has shown that the demand for construction materials, especially concrete, increases without slowing down. The primary binding phase for concrete is the Portland Cement (PC), and its production consumes a lot of energy. Worse, the reactions occurring during this production cause enormous carbon dioxide emissions. In this context, considering demand intensity and environmental awareness, geopolymer concrete is a leading candidate for research seeking a green alternative to conventional concrete (CVC) [127-129]. Geopolymer concrete is a more environmentally friendly and comparably similar-cost new generation construction material. It is formed from the reaction between aluminosilicate compounds and alkaline solution and has been proved to have good binding properties [130]. Although based on the material cost, the cost of geopolymer concrete is greatly superior to the conventional concrete due mainly to the used alkali activators and, in addition, fly ash and GGBS are hardly available in several regions of the globe, its positive effect to the environment is one of its driving reason for preference over CVC. Thus, researchers try to come up with new sources to be utilized in the construction practice other than CVC and ordinary steel [131-134]. Globally, there are many ongoing research and development studies on the geopolymer concrete as a promising alternative to CVC [135-138]. While these studies have mainly positioned on the investigation of thermal characteristics, microstructural properties, electrical conductivity, and durability, some limited research on structural performance have been conducted by testing large-scale structural components [139,141]. In addition, applications of geopolymer concrete became more widespread by the inclusion of hybrid fibers inside the mixture or even 3D printing [142,143].

Fly ash, blast furnace slag, calcined clays, and metakaolin are the most commonly used precursors as aluminosilicate precursors in producing both CVC and geopolymers [136,144]. Because of their substantial demand in the industry, these by-products are tried to be eliminated from the geopolymer mixtures. In this context, construction and demolition wastes (CDWs)

produced in high quantities by the construction industry are seen as essential candidates for geopolymerization. CDW is a collective term used for all waste generated during the construction, demolition, or reconstruction of any buildings. With the acceleration of urban population growth, CDWs have started to turn into a serious problem, frequently referred to as global waste. According to official data published by the European Union (EU), CDWs constitute the largest source of waste in Europe [141]. It is stated that global aggregate demand was increasing by approximately 5.2% annually to reach 51.79 billion tons as of 2019 [145]. Considering the situation in China, extensive urban renewal projects throughout the country have resulted in the large-scale demolition of existing buildings. According to a report by the China Academy of Building Research (CABR), the total area of demolished urban buildings reached 3 billion m^2 over the 11th National Five-Year Plan period, with the ratio of demolished buildings to newly constructed buildings approaching one-quarter, at 23%. During the 12th Five-Year Plan period, about 130 million m^2 of residential buildings were demolished [146]. Numerical data clearly shows how much danger CDW poses. If CDW could not be adequately controlled, depleted storage areas would adversely affect the environment and reach large amounts that threaten public health and the global economy [150]. It is necessary to prevent the rate of waste accumulation by developing more effective ways than the traditional ways used for the disposal of this pile of waste, which is predicted to increase more and more every year. The utilization of CDW for concrete mixtures is a more cost-effective and environmentally friendly solution; however, usage rate as recycled aggregate or substitution to reduce cement content has remained limited [121,151-159]. In recent studies, researchers also investigated possibly replacing a part of geopolymer paste with other waste materials like coke dust waste [157].

Like Conventional Concrete (CVC), the structural properties of CDW based Geopolymer Concrete (GPC) components are not easy to model since the mechanical behavior changes depending on the level of stress and interaction of different loading types. Therefore, it is, of great importance, to determine the stress-strain relation, which definitely helps define the relationship between the equilibrium equations and the compatibility conditions [160-163]. Many studies have been carried out on the investigation of stress-strain relations and stress block variables for CVC, i.e., Kent and Park [163], Hognestad [164], Sheik and Uzumeri [165], Roy

and Sözen [166], Saatcioglu and Ravzi [167], etc. In addition, many equations, rules, and design suggestions are given in the current codes and standards applicable for reinforced CVC components. However, attempts to propose stress-strain relations for geopolymer concrete are limited in number [148,149]. All these researchers attempted to derive mathematical equations representing experimentally-obtained compressive stress-strain equations. In none of these studies, the ability of the proposed stress-strain relation to estimating the flexural capacity was investigated.

Therefore, this study focused on the formulation of the stress-strain model for estimating the load capacities of reinforced GPC members. To this end, a novel mathematical model for the stress-strain characteristics of GPC was formulated by utilizing recent flexural tests [124,125]. Then, the performance of the proposed stress-strain model in estimating the capacities of 36 test beams from the literature was investigated. After that, a soft database composed of 50 different beams with varying compression steel ratio, tensile steel ratio, concrete compressive strength, etc. was formed in order to double check the accuracy of the proposed model. This test database was also analyzed using both the verified finite element model and the proposed mathematical model to estimate the flexural and shear capacities. In addition, the ACI318 [168] formulation was used to estimate the ultimate moment capacities of all the beams. The results of the comparison revealed that the proposed stress-strain model could estimate the flexural capacity with less than %5.13 error on average. In addition, this new model is suitable for numerical sectional analysis applications as the mathematical model was designed to be differentiable in its definition range.

2.2.   Details on the proposed stress-strain model for geopolymer concrete

In this study, the aim is to propose a mathematical model for the compressive stress-strain relation of GPC concrete. This new mathematical model was proposed based on several flexural tests of geopolymer concrete beams by formulating the required relation in order to mimic the flexural behavior. The assumptions during the formulation of the stress-strain relation for the compression behavior are listed below:

a.   The contribution of the concrete in tension was neglected in calculating the flexural strength of the cross-section (**Fig. 2.1**),

b. Third-order polynomial was used to define the compressive stress-strain relation of GPC (Eq. 1),

c. Strain distribution over the cross-section was assumed to be linear (i.e., shear deformations were neglected),

$$\sigma_{GPC}(\varepsilon) = a\,\varepsilon^3 + b\,\varepsilon^2 + f\varepsilon + g \tag{1}$$
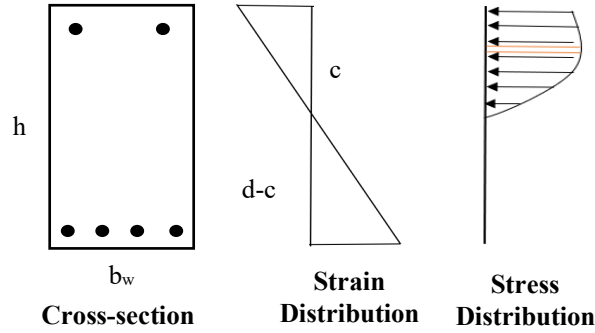
Fig. 2.1. Diagrams utilized in formulating compressive stress-strain relation of GPC concrete

In addition, the unknown coefficients in the proposed stress-strain equation (Eq. 1) were determined by imposing the following boundary conditions (BC).

i. Stress at zero strain should be zero (i.e., $\sigma_{GPC}(\varepsilon = 0) = 0$).

ii. No stress values over the distribution exceed the compressive strength of the GPC concrete (i.e., $\sigma_{GPC}(\varepsilon) \le f_{ck}\ for\ \forall \varepsilon\ \in Q$).

iii. Stress converges to zero at the ultimate strain (i.e., $\sigma_{GPC}(\varepsilon = \varepsilon_{cu}) = 0$).

The first BC resulted that the constant *g* should be zero (i.e., g=0). Besides, the last BC could be imposed on the model by modifying the polynomial so that it has a double root at the ultimate strain. This mathematical manipulation resulted in one more BC on the proposed model. In other words, all the roots of the equation were parametrized ($\sigma_{GPC}(\varepsilon_1 = 0) = 0\ and\ \sigma_{GPC}(\varepsilon_{2,3} = \varepsilon_{cu}) = 0$). Consequently, Eq. 1 could be rewritten as follows:

$$\sigma_{GPC}(\varepsilon) = a\,(\varepsilon - 0)(\varepsilon - \varepsilon_{cu})^2 \tag{2}$$

Therefore, Eq. 2 had two unknown parameters (i.e., a and ε_{cu}) that should be found by imposing the BCs and by optimizing the flexural strength estimations. To this end, flexural tests from recent studies [124,125] were utilized. The details on the test specimen and the utilized material are given in the following section.

2.3. Details on the Flexural Tests

2.3.1. GPC Mixture

The used GPC concrete was originated from recycled construction demolition wastes (CDWs). In this context, masonry units (including red clay brick (RCB), hollow brick (HB), waste glass (G), concrete rubble (CRB), and roof tile (RT)) were procured from an urban transition zone in Eskişehir province in Turkey. Crushing and grinding techniques were performed sequentially on the CDWs acquired. The preparation of CDW-based materials for the grinding process was the first part of this two-stage method. For that purpose, the CDWs (i.e., masonry units, concrete rubble, glass, etc.) were embedded in a laboratory-type jaw crusher for the first size reduction phase, followed by the second step. Then, the crushed CDWs were placed in a ball mill and milled for about an hour. Furthermore, recycled aggregates (RAG) were produced by crushing demolition concrete rubble and separating crushed particles using sieves with varied openings.

The particle size, crystalline nature, and chemical compositions of CDW-based materials could differ much. Therefore, in another phase of this research, scanning electron microscope (SEM), X-ray diffraction (XRD), and X-ray fluorescence (XRF) analysis were used to obtain information about the particle size distributions, analyze the crystalline nature, and determine the chemical composition of the CDW-based precursors, respectively. Detailed information about these analyses could be found in Yildirim et al. [121]. The preparation of geopolymer mixes consists mainly of two phases. The prepared liquified alkaline activator is mixed with the remaining materials in the second stage, which include powdered alkaline activators (such as calcium hydroxide and sodium silicate), ground CDWs, aggregates, and water. In light of this procedure, the liquified alkaline activator was prepared by dissolving sodium hydroxide flakes in water at a Na^+, which corresponded to an overall NaOH molarity of 8M; this mixture was allowed to cool to ambient temperature for one day. Preliminary studies show that when only

sodium hydroxide is used as an alkali activator, the setting time of the mixtures is prolonged, and low mechanical properties are obtained due to insufficient geopolymerization. For this reason, other alkaline activators (such as calcium hydroxide and sodium silicate) were added to increase the mechanical qualities of the combinations while also reducing the setting time (i.e., less than 2hrs). In addition, adding slag and fly ash (other manufacturing wastes) to the concrete mixture improved the combination's strength and workability. These modifications of the geopolymer concrete enabled it to cure at ambient temperatures (i.e., 20°C) since calcium hydroxide, sodium hydroxide, and sodium silicate have sufficient reactive silica content and also acted as an additional source of sodium. A water/binder ratio of 0.35 was chosen in the geopolymer combination. **Table 2.1** provides information on the proportions of all the elements in geopolymer concrete. The procedure given in Yildirim et al. [121] and Ulugol et al. [150] results in concrete compressive strength values up to 30MPa under ambient temperature curing conditions. However, it is commonly encountered fact that the compressive strength of geopolymer could be enhanced using only special curing conditions, i.e., high temperature curing. To reach comprehensive study results on geopolymer concrete compositions, see recent studies by Yildirim et al. [121] and Ulugol et al. [150].

Table 2.1. Proportions for completely CDW-based geopolymer concrete and conventional concrete mixtures

Material (kg/m³)	Hollow Brick	Red Clay Brick	Roof Tile	Glass	Concrete	Portland	Slag	Fly Ash	Ca(OH)$_2$	NaOH	Na$_2$SIO$_3$	NAG (Fine)	NAG (Coarse)	RAG (Fine)	RAG (Coarse)	Water	Water/Binder
NGC-R	150	200	250	100	100	-	150	50	50	112	224	-	-	500	500	202	0.35

2.3.2. Experimental Results

This study aims to propose a mathematical model for the stress-strain relation of CDW-based geopolymer concrete. Beam tests on GPC concrete were presented in Akduman et al. [124] and Aldemir et al. [125]. In summary, a total of six large-scale beam specimens (i.e., 100×250×1000mm) were tested. In these studies, both shear-dominant and flexure-dominant

behavior was simulated by testing specimens with different shear-span-to-depth (a/d) ratios (i.e., 0.50, 1.00, and 1.65) and different transverse reinforcement patterns. Four-point bending tests were conducted to determine the load-displacement curves. The test setup, which is prepared to represent a closed system, had an electrohydraulic servo valve with a displacement application speed range of 0.10–1.00 mm/min. Each test was carried out with a constant displacement velocity of 0.30 mm/min. The schematic diagram of the test setup and the instrumentations is presented in **Fig. 2.2** Only flexural-dominant specimens were used in the formulation of the stress-strain model (i.e., GPC-NA-1.65, GPC-RA-1.65, NGC-1.65, and NGC-R-1.65).

Firstly, the parameter ε_{cu} was determined from the average strain records at the top chord of the tested specimens (**Table 2.2**). It is apparent that the ultimate strain was around 0.006 for the tested specimens. After that, the section analysis of the tested specimens was performed by using Eq. 2 for the GPC concrete in compression. As usual, the section was sliced into 1000 pieces, and the ultimate moment capacity of the section was estimated for each specimen. Therefore, the unknown parameter a in Eq. 2 was determined for each specimen and listed in **Table 2.2**.

Fig. 2.2. Schematic view of the four-point bending test and the instrumentations [125]

Table 2.2. Summary of experimental results and numerical estimations

Specimen	Compressive Strength (f_{ck}, MPa)	Top Strain at the Failure	Ultimate Moment (kN.m)	Calculated Parameter a	Estimated Ultimate Moment (kN.m)	Error in Moment Capacity (%)
GPC-NA-1.65	37.50	0.00609	20.48	1171875000	20.56	0.39
GPC-RA-1.65	36.60	0.00598	20.18	1155264176	20.38	0.99
NGC-1.65	37.50	0.00601	20.26	1149487866	20.26	0.00
NGC-R-1.65	36.60	0.00596	19.23	1195628507	19.01	-1.14

The calculated parameter a could be rewritten in terms of f_{ck} and ε_{cu} to obtain a generic equation for the stress – strain relation (**Fig. 2.3** and Eq. 3). Therefore, the proposed stress-strain relation has its ultimate strength value defined (i.e., f_{ck}) at a strain value of $\varepsilon_{co} = \varepsilon_{cu} / 3$.

$$\sigma_{GPC}(\varepsilon) = \frac{6.75\, f_{ck}\, \varepsilon}{\varepsilon_{c}}$$

(3)
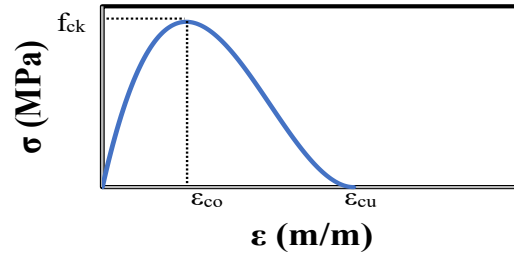
Fig. 2.3. Proposed stress – strain relation for geopolymer concrete

$$\sigma_{GPC}(\varepsilon) = \frac{6.75\, f_{ck}\, \varepsilon\, (\varepsilon - \varepsilon_{cu})^2}{\varepsilon_{cu}^{\,3}}$$

(3)

It should be noted that the modulus of elasticity of the geopolymeric paste and the aggregates would also affect the stress-strain relation. In this regard, the proposed mathematical model has some limitations as the geopolymer has a wide variety of different ingredients, several different alkali-activators, and different curing techniques. These differences generate different rigidities of the end product, i.e., geopolymer concrete. Therefore, the proposed stress – strain relation was formulated to base on global parameters f_{ck} and ε_{cu}. It should be reminded that the proposed formulation is specific to geopolymer concrete whose f_{ck} and ε_{cu} values would not differ too much from the selected experimental and soft database batch.

The proposed stress-strain relation was derived by utilizing the experimental findings of bending tests of several specimens, but its accuracy should be tested using other experiments from the literature. To this end, 36 different tests from recent studies [124,125, 169-176] were utilized (**Tables 2.3 and 2.4**). It could easily be inferred that the used test database has a very large range of compressive strength, tensile reinforcement ratio, compressive reinforcement ratio, section sizes, etc. The ranges for the different parameters in this experimental database is summarized in **Table 2.3**. In addition, the geopolymer materials are all different in the selected test specimens (i.e., slag-based geopolymer, fly ash-based geopolymer, fully recycled geopolymer, etc.). Therefore, it is aimed to have amathematical model for the stress-strain relation of geopolymer concrete with different orientations. All the material and physical properties of the test specimens are available in the referred papers. The ultimate moment capacities of all test specimens were estimated by using the proposed stress-strain relation and the performance of the estimations are listed in **Table 2.3**. To check the need for a new kind of stress-strain relation for the geopolymer concrete, the estimation performance of ACI318 [168] was also presented in **Table 2.3**. The ultimate moment capacities from the ACI318 [168] formulation did not include material factors (i.e., $\phi=1$). From **Table 2.3**, it was found that the absolute mean and the standard deviation of the ultimate moment capacity estimation error of the proposed stress-strain model is 2.66% and 1.92%, respectively. Whereas the absolute mean and the standard deviation of the ultimate moment capacity estimation error of the ACI318 [168] model is 18.08% and 10.41%, respectively. In addition, the percentage errors of the proposed model are significantly less than the currently utilized model (**Fig. 2.4**). It is apparent that the deviations, as well as the accuracy, were enhanced by the use of the proposed stress-strain model, implied by the less deviations from the horizontal line (**Fig. 2.4**).

Table 2.3. Ranges of the selected variables in the experimental database

Parameter / Range	f_{ck} (MPa)	f_{yk} (MPa)	ρ	ρ'	b_w (mm)	h (mm)	a / d
Minimum	17.0	330	0.0031	0.0013	100	150	1.5
Maximum	71.6	561	0.0310	0.0230	203	400	5.8

In summary, the procedure followed in this study is that, firstly, tested specimens that showed flexure-dominant failure, manifesting itself with flexural crack formations at the midspan and clear post-yield zone in the load-displacement curves were used at the initial stage of the study. After that, 36 beam test specimens from the literature were collected. At this stage, it should be noted that these specimens were intentionally selected so that they were produced by using geopolymer concrete with different origins like fly ash-based, slag-based, CDW-based geopolymers, etc. (**Table 2.4**). In addition, the shear-span-to-depth ratios of the selected test specimens ranged from 1.50 to 5.80 and all the specimens were claimed to be failed in flexure-dominated actions. Therefore, the proposed stress-strain relation was derived and tested by using experimental results that failed due to flexure-dominated actions. Finally, a soft database was formed to include beam specimens having a range of 3-8 for a/d ratio and the performance of the proposed model was checked.

At this point, it should be mentioned that geopolymer concrete inherently has a large deviation of chemical components. Therefore, the performance of any proposed stress-strain material models should be tested against possible geopolymer orientations. To this end, the test beams collected from the literature (**Table 2.4**) were selected to have different geopolymer concrete origins like fly-ash based, slag-based, construction demolition waste based, etc. The results clearly indicated that the effect of different origins of geopolymer concrete has a limited influence on the estimation performance of the flexural capacity (**Table 2.4**). This may be attributed to the conventional concrete response. For instance, the conventional concrete could be produced by using cement-only, cement+fly ash from different sources, cement+slag from different sources, or cement+fly ash+slag, etc. Similar diversity is valid for fly ash, slag, etc. However, the flexural capacity of conventional concrete is calculated by using material models incorporating only mechanical properties like compressive strength, strain at ultimate strain, modulus of elasticity, etc. [164, 165, 167]. In addition, other proposed material models for geopolymer concrete [148,149] have only peak stress (f_{ck}), strain at peak stress (ε_{co}), and modulus of elasticity (E_c) as their parameters. Therefore, the same approach was used for geopolymer concrete calculations in the study.

Table 2.4. Summary of test database

Reference	Specimen	bw (mm)	h (mm)	a / d	Material	f_{ck} (MPa)	ρ	ρ'	f_y (MPa)	M_{max} (Ganesan et al. [148])	Error (%)	M_{max} (Noushini et al. [149])	Error (%)	$M_{u,exp}$ (kN.m)	$M_{max,pro.}$ (kN.m)	Error (%)	$M_{u,ACI318}$ (kN.m)	Error (%)
Yacob et al. 2019 [169]	GL6-2.4	203	305	2.40	Fly ash based GPC	43.4	0.0137	0.0025	561	111.30	12.28	112.04	11.70	126.88	122.59	3.38	113.95	10.19*
	GS6-2	203	305	2.00	Fly ash based GPC	41.2	0.0137	0.0025	561	110.51	10.33	111.33	9.66	123.24	121.76	1.20	113.35	8.02
Wu et al. [170]	O3-N1.8-I	200	400	2.50	Slag-based GPC	64.2	0.0159	0.0013	480	200.50	11.56	204.27	9.90	226.71	220.47	2.75	204.13	9.96
	G3-N1.8-D	200	400	1.50	Slag-based GPC	71.6	0.0159	0.0013	480	203.47	3.45	203.71	3.34	210.74	208.28	1.16	192.86	8.48
	G3-N1.8-I	200	400	2.50	Slag-based GPC	66	0.0159	0.0013	480	201.25	4.25	204.85	2.54	210.18	206.4	1.80	191.63	8.82
	G3-N2.7-S	200	400	4.00	Slag-based GPC	70	0.0238	0.0013	416	264.72	0.43	261.81	1.52	265.86	262.71	1.18	242.08	8.94
	G1-N2.5-I-S	200	300	2.50	Slag-based GPC	32.6	0.0212	0.0017	480	126.29	-4.69	126.99	-5.27	120.63	123.87	-2.69	115.38	4.35
	G3-N2.5-I-S	200	300	2.50	Slag-based GPC	71.2	0.0212	0.0017	480	141.06	2.64	140.67	2.91	144.88	140.39	3.10	131.7	9.09
Akduman et al. [124]	GPC-NA-1.65	150	250	1.65	CDW-based GPC	37.5	0.0042	0.0018	456	15.19	25.83	14.51	29.15	20.48	20.49	-0.07	15.58	23.91
	GPC-RA-1.65	150	250	1.65	CDW-based GPC	36.6	0.0042	0.0018	456	15.10	25.17	14.43	28.49	20.18	20.39	-1.03	15.57	22.85
Aldemir et al. [125]	NGC-1.65	150	250	1.65	CDW-based GPC	37.5	0.0042	0.0018	456	15.19	25.02	14.51	28.38	20.26	20.26	-0.02	15.57	23.15
	NGC-R-1.65	150	250	1.65	CDW-based GPC	36.6	0.0042	0.0018	456	15.10	21.48	14.43	24.96	19.23	19.04	0.99	15.58	18.17
Dattatreya et al. [171]	FAB-I	100	150	1.90	Fly ash and Slag based GPC	17	0.0151	0.0067	450	8	5.21	8.14	3.55	8.44	8.88	-5.24	4.63	45.13
	FAB-II	100	150	1.90	Fly ash and Slag based GPC	49	0.0226	0.0067	450	12.67	33.56	12.75	33.14	19.07	17.95	5.86	16.39	14.04

	FAB-III	100	150	1.90	Fly ash and Slag based GPC	52	0.0268	0.0067	450	13.30	*34.19*	12.78	*36.76*	20.21	20.88	-3.34	18.79	7.00
	GGB-I	100	150	1.90	Fly ash and Slag based GPC	63	0.0268	0.0067	450	13.62	*33.20*	13.14	*35.56*	20.39	21.38	-4.88	17.57	*13.81*
	GGB-II	100	150	1.90	Fly ash and Slag based GPC	57	0.0268	0.0067	450	13.46	*29.97*	12.95	*32.62*	19.22	18.08	5.95	17.32	9.90
	GGB-III	100	150	1.90	Fly ash and Slag based GPC	52	0.0268	0.0067	330	8.48	*45.95*	9.81	*37.48*	15.69	15.99	-1.90	13.09	*16.58*
Lisantano et al. [172]	I	120	240	4.10	Fly ash based GPC with Bauxite as coarse aggregate	32.22	0.0140	0.0092	506.5	28.57	*23.81*	27.67	*26.21*	37.50	37.13	0.99	38.64	-3.04
"Kumaravel [173]	I	125	250	4.00	Low-calcium Fly ash based GPC	26.36	0.0050	0.0018	415	10.94	*52.43*	12.45	*45.87*	23.00	21.87	4.91	16.37	*28.83*
Amer Hassan [174]	I	100	150	5.80	Fly ash based GPC	28.4	0.0105	0.0067	512	6.25	*30.55*	6.63	*26.33*	9.00	8.98	0.22	7.9	*12.22*
Ninthya [175]	GPCSC-D1	150	230	4.05	Slag-based GPC	32.6	0.020	0.005	518	53.48	*-39.81*	54.07	*-41.35*	38.25	38.84	-1.53	54.12	*-41.48*
	GPCSC-D2	150	230	4.05	Slag-based GPC	32.6	0.031	0.017	518	69.40	*-12.69*	66.29	*-7.64*	61.58	62.97	-2.26	80.99	*-31.52*
	GPCSC-D3	150	230	4.05	Slag-based GPC	32.6	0.018	0.023	518	55.55	*22.82*	55.76	*22.38*	71.84	77.92	-8.46	85.24	*-18.65*
	GPCC-D1	150	230	4.05	Slag-based GPC	35.2	0.020	0.005	518	32.16	*17.9*	28.70	*26.76*	39.19	40.75	-3.99	54.62	*-39.39*
	GPCC-D2	150	230	4.05	Slag-based GPC	35.2	0.031	0.017	518	62.23	*17.94*	62.20	*26.77*	63.44	63.48	-0.06	81.72	*-28.81*
	GPCC-D3	150	230	4.05	Slag-based GPC	35.2	0.018	0.023	518	72.58	3.86	72.57	3.96	75.57	77.93	-3.12	85.63	*-13.31*
	GPCSC-S1	150	230	4.05	Slag-based GPC	32.6	0.0046	0.0029	518	10.71	3.96	11.61	3.97	13.06	12.64	3.23	15.88	*-21.57*

	GPCSC-S2	150	230	4.05	Slag-based GPC	32.6	0.0131	0.0029	518	11.95	*17.99*	11.35	*11.10*	17.73	17.85	-0.69	22.29	*-25.74*
	GPCSC-S3	150	230	4.05	Slag-based GPC	32.6	0.0197	0.0029	518	35.21	*32.60*	30.17	*35.98*	25.19	25.83	-2.54	32.56	*-29.25*
	GPCC-S1	150	230	4.05	Slag-based GPC	35.2	0.0046	0.0029	518	14.31	-2.21	13.27	5.21	14.00	14.33	-2.39	15.94	*-13.90*
	GPCC-S2	150	230	4.05	Slag-based GPC	35.2	0.0131	0.0029	518	21.84	3.21	18.15	-5.14	18.66	18.3	1.93	22.38	*-19.94*
	GPCC-S3	150	230	4.05	Slag-based GPC	35.2	0.0197	0.0029	518	27	0.02	23.57	*12.89*	27.06	26.63	1.58	32.74	*-21.00*
Pham et. al. [176]	D1	200	300	2.50	Low-calcium Fly ash based GPC	30.4	0.0038	0.0017	356.5	25.14	-3.88	22.83	5.66	24.20	25.23	-4.26	20.66	*14.63*
	D2	200	300	2.50	Low-calcium Fly ash based GPC	39.1	0.0067	0.0017	415.6	38.78	*19.04*	39.42	*17.70*	47.9	46.06	3.84	41.69	*12.96*
	D3	200	300	2.50	Low-calcium Fly ash based GPC	48.2	0.0134	0.0017	415.6	74.33	*19.29*	79.47	*13.71*	92.1	88.98	3.39	80.88	*12.18*
										Absolute Mean	17.61	**Absolute Mean**	18.97		**Absolute Mean**	2.66	**Absolute Mean**	18.08
										Std. Dev.	14.22	**Std. Dev.**	14.02		**Std. Dev.**	1.92	**Std. Dev.**	10.41

Absolute error values greater than 10% are marked with red itali
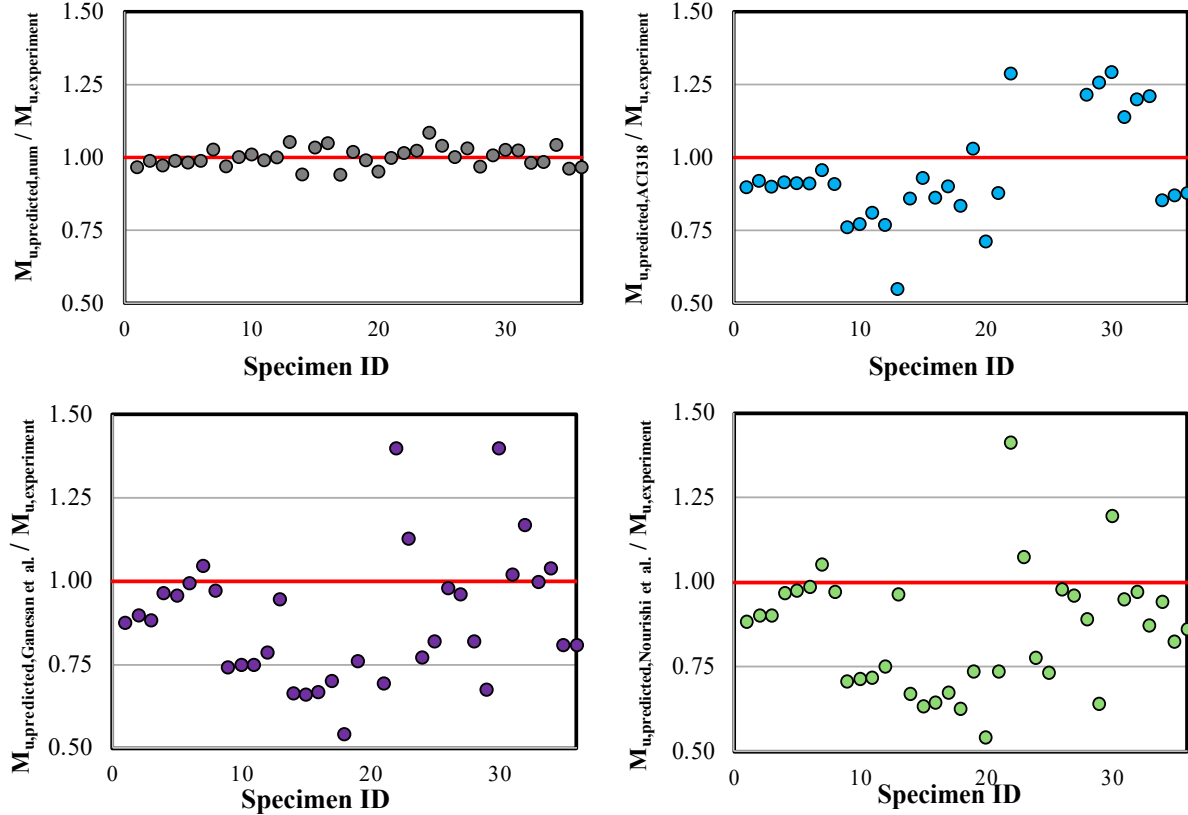
Fig. 2.4. Comparison of the estimation performances for the test database

Although the performance of the proposed stress-strain model is promising, the estimation accuracy is further examined in the following section using a soft database composed of 50 different specimens having a wide range of parameters that are not covered in the test database.

2.4. Details on the Numerical Model

This section includes calibration studies for the numerical model to be created based on the test results presented in the previous sections. The numerical models were generated in the program ANSYS (2016) [177]. The 8-node solid element (i.e., Solid65), which has the ability to simulate both cracking and crushing of the concrete material, is assigned [177]. Thus, the cracking behavior in the tensile zones and the crushing behavior in the compression zones of the geopolymer concrete could appropriately be simulated. In addition, the transverse and longitudinal reinforcements were represented by link elements (i.e., Link180). The selected link element has three translational degrees of freedom at each node.

The observations on the fact that the bonding behavior of geopolymer concrete is similar to that of conventional concrete [178,179]. Like CVC, GPC is a nonlinear material with properties that change with time and pressure. Thus, the nonlinear behavior was mimicked using the Drucker-Prager model [180] combined with William-Warnke [181] plasticity surface in the study. The cohesion (c) and the internal friction angle (ϕ) values in the model were determined from the concrete compressive strength (f_{ck}) and concrete tensile strength (f_{ctk}) using Eqs. 4-5. The shear transfer coefficients for open and closed cracks had a significant impact on the estimations. Therefore, during the calibration phase, open-shear and close-shear coefficients were optimized, and the same value was utilized for all beams (**Table 2.5**). Besides, the steel reinforcement was characterized as an elastic-perfectly plastic material. The numerical model is presented in **Fig. 2.5**.

$$\phi = \text{asin}\left(\frac{f_{ck}-f_{ctk}}{f_{ck}+f_{ctk}}\right) \tag{4}$$

$$c = f_{ck} * \frac{1-\sin(\phi)}{2\cos(\phi)} \tag{5}$$

Table 2.5. Crack parameter values of geopolymer concrete

Concrete Parameters	
Open Shear Transfer Coefficient	0.2
Closed Shear Transfer Coefficient	0.8
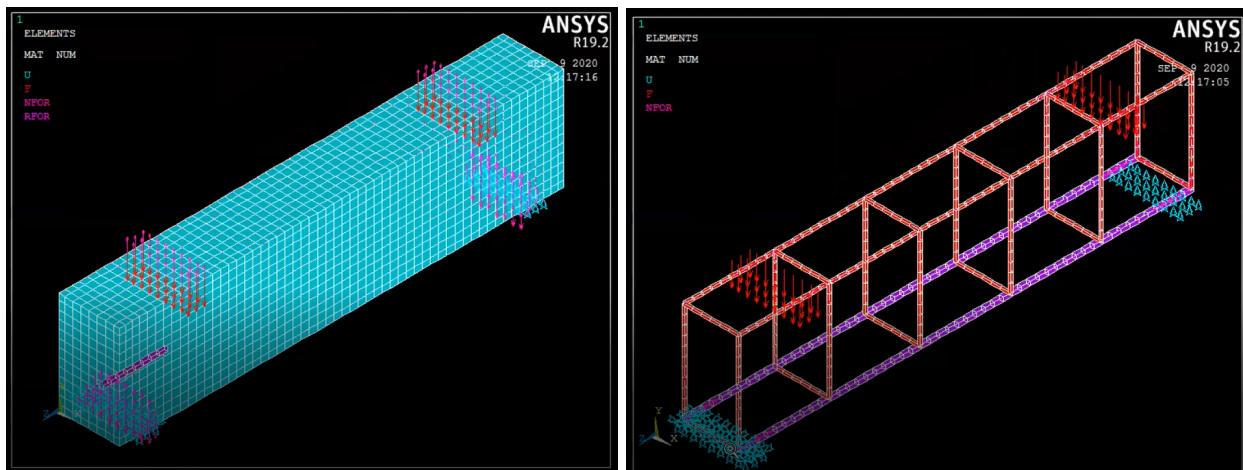
Fig. 2.5. Numerical model: (a) 3D solid model and its support conditions and (b) Steel reinforcements

The boundary conditions of the models were assumed to be roller-supported and pin-supported at ends (**Fig. 2.5a**). Due to rectangular volume of each beam element, beams were meshed by using rectangular prismatic elements. The maximum mesh size was calculated by following an adaptive mesh procedure. In this procedure, an initial mesh was chosen, and a modal analysis was run. Then, the mesh size was halved, and the model was solved once again. The coarse mesh (i.e., the mesh used in the previous analysis) was accepted as the optimum mesh when the change in the predicted vibration period obtained in consecutive models was found to be less than 1% (**Fig. 2.5a**). Several researches in the literature [182-186] adopted this numerical methodology. Since the difference in the predicted periods from numerical models with 10mm and 20mm maximum mesh sizes were less than 1%, it was concluded that the most appropriate mesh sizes for beams were 20mm after mesh sensitivity analysis. Subsequently, similar to the tests, the vertical load was applied to utilize displacement-controlled loading. Two locations at a distance equal to the shear span were used to load the simulated beams. The described numerical model was calibrated using tests given in Akduman et al. [124] and Aldemir et al. [125]. The Finite Element Model (FEM) model estimation results are summarized in **Table 2.6** and **Figs. 2.6-2.7**.

Table 2.6. Comparison of FEM model estimations

Specimen	Ultimate Moment (kN.m)	Estimated Ultimate Moment (kN.m)	Error (%)	Ultimate Displacement (mm)	Estimated Ultimate Displacement (mm)	Error (%)
GPC-NA-1.65[*]	20.48	20.88	-1.95	35.69	36.51	-2.30
GPC-RA-1.65[*]	20.18	20.17	0.05	13.66	15.83	-15.89
NGC-1.65[**]	20.26	20.88	-3.06	34.92	38.55	-10.40
NGC-R-1.65[**]	19.23	18.66	2.96	13.64	13.73	-0.66

[*] Specimen was adopted from Aldemir et al. [125].

[**] Specimen was taken from Akduman et al. [124].
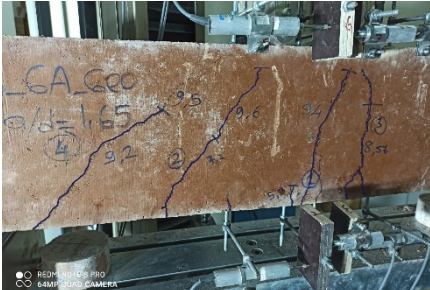
Test Specimen	Initial Crack	Final Stage
GPC-NA-1.65		
GPC-RA-1.65		
NGC-1.65		
NGC-R-1.65		

Fig. 2.6. Crack patterns of the used tests [124,125]
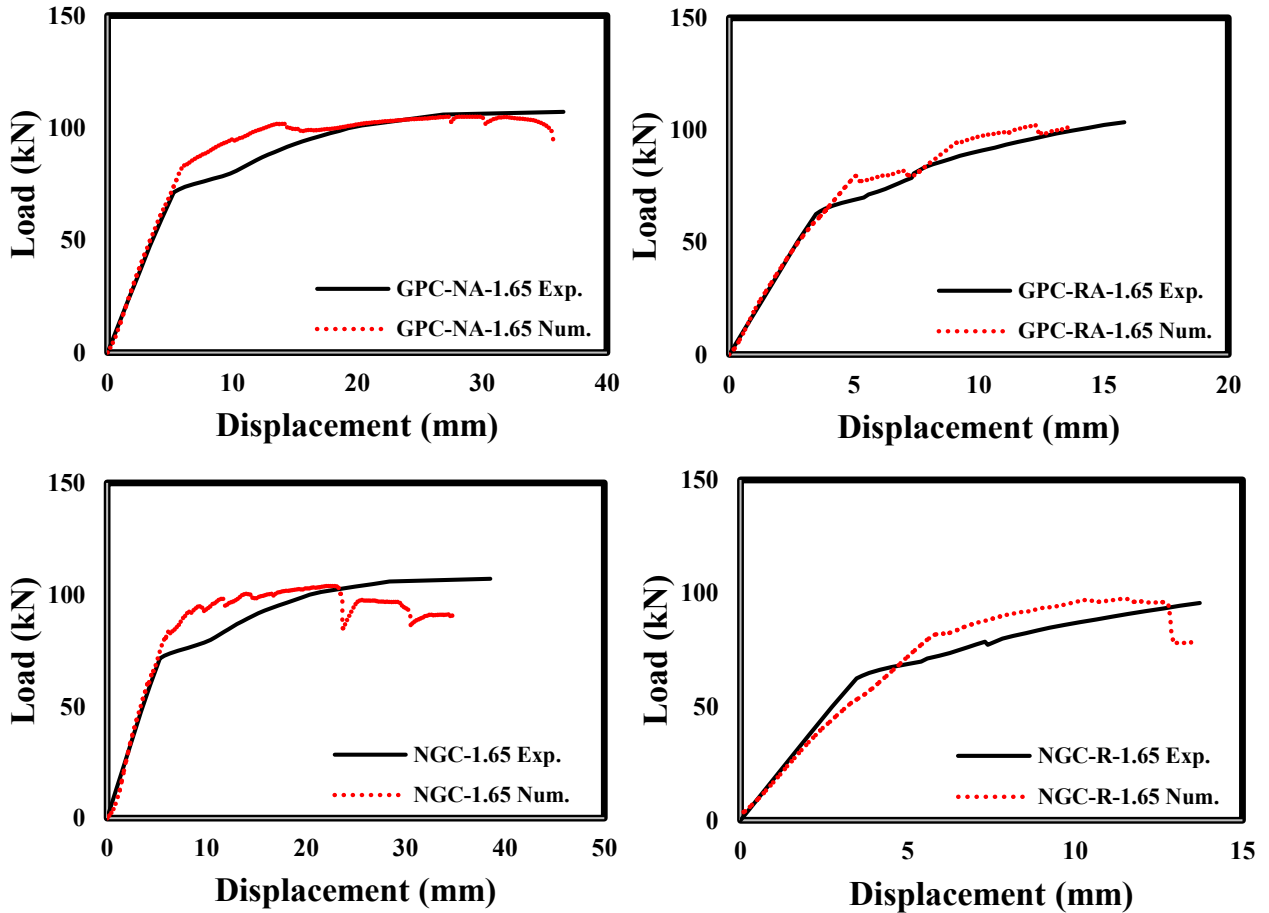
Fig. 2.7. Comparison of load – displacement curves

In the literature, there are several load-displacement curves of geopolymer concrete beams reported to be failed in flexure and, those literature-available curves are very similar to the ones given in the study. In all of the tests, the general characteristics of the load-displacement curves are that i. they have no clear cracking points, ii. they have a point where a significant change in stiffness is observed (this could be attributed to yield point or cracking point), iii. they don't have zero stiffness after yield. Those observations could be attributed to the fact that the capacity of the under-reinforced beams is dominated by the behaviour of the reinforcement, which has a clear strain hardening region. Therefore, a positive slope after yielding is expected as observed in tests conducted in this study and in the literature. In addition, the shapes of the literature-available load-displacement graphs are similar to the reported ones in this study. It could easily be inferred that the maximum percentage errors for the ultimate moment and ultimate

displacements are 3.06% and 15.89%, respectively. And the general outlook of the load – displacement curve estimations is very similar for all specimens (**Fig. 2.6**).

2.5.   Numerical Database to Test the Proposed Model

The proposed models' performance was double checked by using a new database consisting of unscaled specimens. For this purpose, a soft database of 50 different beam specimens was formed and the ultimate moment capacities of all specimens were determined by using the verified numerical model. After that ultimate moment capacities of each specimen were determined by using both the proposed model and ACI318 [168] model. Finally, the estimation performance of the proposed stress-strain model was investigated. The selected variables were concrete compressive strength (f_{ck}), tensile reinforcement ratio (ρ), compressive reinforcement ratio (ρ'), section width (b_w), and section height (h). The soft database was formed to represent a wide range of variables. To this end, firstly, possible ranges for parameters f_{ck}, f_{yk}, ρ, ρ', b_w, h, and a/d ratio were decided to simulate beam geometries that could be encountered in real designs. From those possible ranges, parameters were selected by using uniform-randomly distribution [187]. After that, the numerical models were solved to obtain the moment capacities of each beam specimen in the soft database. Then, the capacities were estimated by utilizing the proposed stress – strain model, and the estimations were compared. The ranges for each selected variable are listed in **Table 2.7**. All the specimens were enforced to exhibit flexure-dominated failure by taking a shear-span-to-depth ratio (a/d) of more than 3.

Table 2.7. Ranges of the selected variables

Parameter / Range	f_{ck} (MPa)	f_{yk} (MPa)	ρ	ρ'	b_w (mm)	h (mm)	a / d
Minimum	25	400	0.005	0.003	250	500	3
Maximum	80	600	0.040	0.030	600	800	8

The results are summarized in **Table 2.8**. In **Table 2.8**, all the physical and mechanical properties of specimens are also presented. It could be stated that the proposed stress-strain model could yield satisfactory ultimate moment capacity estimations with a maximum absolute

percentage error and absolute mean percentage error of %5.07 and %3.47, respectively. Likewise, the estimation performance of ACI318 [168] is presented in **Table 2.8**. From **Table 2.8**, it was observed that the absolute mean and the standard deviation of the ultimate moment capacity estimation error of the ACI318 [168] model is 30.61% and 17.35%, respectively. Thus, it was double checked that the percentage errors of the proposed model are significantly less than the currently utilized model (**Fig. 2.8**). It is apparent that the deviations, as well as the accuracy, were enhanced by the use of the proposed stress-strain model (**Fig. 2.8**).

Table 2.8. Summary of test soft database

Specimen	b_w (mm)	h (mm)	a/d	f_{ck} (MPa)	ρ	ρ'	f_y (MPa)	$M_{u,num}$ kN.m)	Mmax (Ganesan et al. [148])	Error (%)	Mmax (Noushini et al. [149])	Error (%)	$M_{max, pro.}$ (kN.m)	Error (%)	$M_{u, ACI318}$ (kN.m)	Error (%)
1	336	573	6	57	0.031	0.018	577	1686	1607	4.69	1652	2.02	1721	-2.06	2543	-47.81*
2	531	777	7	59	0.015	0.028	589	2709	2515	7.16	2516	7.12	2495	7.91	4594	-84.13
3	424	517	5	77	0.029	0.021	452	1282	1237	3.51	1241	3.20	1516	-13.86	1919	-26.58
4	268	618	4	70	0.028	0.007	407	1107	988	10.75	976	11.83	1099	0.79	1609	-46.41
5	479	710	7	62	0.039	0.022	599	4950	3330	34.09	3868	23.45	5053	-2.08	7159	-41.68
6	323	552	7	50	0.034	0.019	424	1191	1186	0.42	1188	0.25	1324	-11.10	1886	-42.45
7	338	789	8	27	0.031	0.02	536	3146	3072	2.35	3014	4.20	3182	-1.14	4143	-30.20
8	333	768	6	60	0.022	0.011	413	2284	1578	30.91	1579	30.87	2133	3.24	2639	-15.54
9	414	557	5	30	0.018	0.004	496	1244	775	37.70	914	26.53	1240	0.34	1351	-8.60
10	464	558	7	53	0.028	0.013	536	1943	1795	7.62	1675	13.79	1976	-1.69	2780	-40.69
11	593	727	7	52	0.037	0.006	544	5069	4887	3.59	4726	6.77	5071	-0.03	6712	-32.36
12	444	507	5	44	0.017	0.01	489	1006	788	21.67	789	21.57	927	7.76	1296	-28.86
13	258	760	6	67	0.031	0.014	595	2270	2360	-3.96	2369	-4.36	2368	-4.31	3651	-54.18
14	590	657	5	52	0.023	0.019	491	3265	2467	24.44	2491	23.71	3328	-1.92	4175	-25.45
15	530	570	4	77	0.018	0.026	527	1356	1338	1.33	1391	-2.58	1432	-5.60	1969	-37.50
16	558	590	5	42	0.008	0.007	596	1172	796	32.08	796	32.08	1148	2.04	1353	-17.86
17	515	698	7	45	0.026	0.009	567	3074	3051	0.75	3039	1.14	3046	0.91	3178	-3.38
18	252	607	5	80	0.035	0.017	448	1313	1238	5.71	1233	6.09	1410	-7.32	2027	-43.76
19	450	516	7	76	0.008	0.011	486	484	395	18.39	394	18.60	437	9.88	536	-22.65

20	279	597	6	31	0.02	0.019	403	1068	685	*57.77*	626	*41.38*	1048	1.92	1158	*-10.50*
21	364	673	8	69	0.019	0.014	559	1767	1525	*13.70*	1525	*13.70*	1893	-7.12	2564	*-35.45*
22	286	749	8	70	0.022	0.027	444	1522	1387	8.87	1387	8.87	1437	5.63	1676	*-16.63*
23	302	606	4	50	0.022	0.006	444	991	904	8.78	894	9.79	990	0.05	1452	*-46.67*
24	275	508	5	71	0.04	0.028	420	1260	976	*22.54*	976	*22.54*	1239	1.66	1637	*-32.12*
25	570	750	8	58	0.036	0.024	420	5980	4226	*29.33*	4219	*29.45*	6212	-3.87	6994	*-12.59*
26	346	528	5	31	0.02	0.005	420	898	650	*27.62*	648	*27.84*	833	7.16	990	*-18.85*
27	289	554	5	54	0.029	0.005	583	1306	1163	*10.95*	1146	*12.25*	1228	5.99	1689	*-37.54*
28	507	639	5	38	0.009	0.022	453	1136	733	*35.48*	732	*35.56*	1149	-1.11	1738	*-51.26*
29	445	530	6	48	0.013	0.005	581	846	786	7.09	786	7.09	904	-6.75	1285	*-42.15*
30	335	695	3	42	0.027	0.011	474	2065	1706	*17.38*	1762	*14.67*	1801	*12.78*	2679	*-48.75*
31	413	640	5	68	0.032	0.03	481	3180	2245	*29.40*	2248	*29.31*	3399	-6.88	3803	*-19.59*
32	300	565	5	45	0.01	0.025	445	634	364	*42.59*	363	*42.74*	572	9.65	879	*-53.67*
33	480	582	6	60	0.007	0.012	473	756	464	*38.62*	463	*38.76*	727	3.85	781	-7.43
34	394	674	4	29	0.029	0.021	472	2676	2112	*21.08*	2114	*21.00*	2451	8.40	3221	*-31.42*
35	574	590	6	33	0.015	0.03	592	2640	1516	*42.58*	1260	*52.27*	2391	9.43	2905	*-21.50*
36	390	771	8	56	0.016	0.008	420	2151	1378	*35.94*	1384	*35.65*	2220	-3.16	2340	-8.79
37	403	626	7	35	0.034	0.01	490	2181	1992	8.67	1991	8.71	2088	4.26	2714	*-29.98*
38	432	542	7	44	0.037	0.029	413	1887	1622	*14.04*	1622	*14.04*	2061	-9.22	2646	*-28.38*
39	526	691	4	46	0.025	0.005	457	2744	2377	*13.37*	2363	*13.88*	2532	7.72	3651	*-44.19*
40	564	571	3	26	0.016	0.014	459	1693	1137	*32.84*	1145	*32.37*	1618	4.43	1896	*-17.18*
41	393	516	7	60	0.017	0.005	578	987	848	*14.08*	848	*14.08*	952	3.61	1373	*-44.22*
42	332	688	6	61	0.021	0.019	533	2054	1537	*25.17*	1539	*25.07*	2224	-8.27	2598	*-16.82*
43	284	607	4	58	0.021	0.02	500	1204	944	*21.59*	940	*21.93*	1303	-8.22	1602	*-22.95*
44	342	640	8	37	0.034	0.008	478	1912	1724	9.83	1752	8.37	2015	-5.35	2363	*-17.27*

45	312	784	4	26	0.007	0.008	427	545	511	6.24	510	6.42	558	-2.28	575	-3.05
46	570	552	3	80	0.022	0.003	471	1636	1509	7.76	1510	7.70	1513	7.51	2473	*-63.45*
47	279	542	3	67	0.025	0.009	409	803	704	*12.33*	886	*-10.34*	809	-0.74	1161	*-43.51*
48	501	573	6	42	0.027	0.005	514	1710	1773	-3.68	1786	-4.44	1787	-4.45	1792	-4.80
49	556	616	6	39	0.012	0.013	532	1102	1160	-5.26	1161	-5.35	1165	-5.6	1234	-5.92
50	531	777	7	59	0.015	0.028	589	2709	2515	7.16	2516	7.12	2779	-2.56	4000	*-43.94*
									Absolute Mean	19.47	**Absolute Mean**	18.75	**Absolute Mean**	5.07	**Absolute Mean**	30.61
									Std. Dev.	15.04	**Std. Dev.**	14.58	**Std. Dev.**	3.47	**Std. Dev.**	17.35

* Error values greater than 10% are marked with red italics.
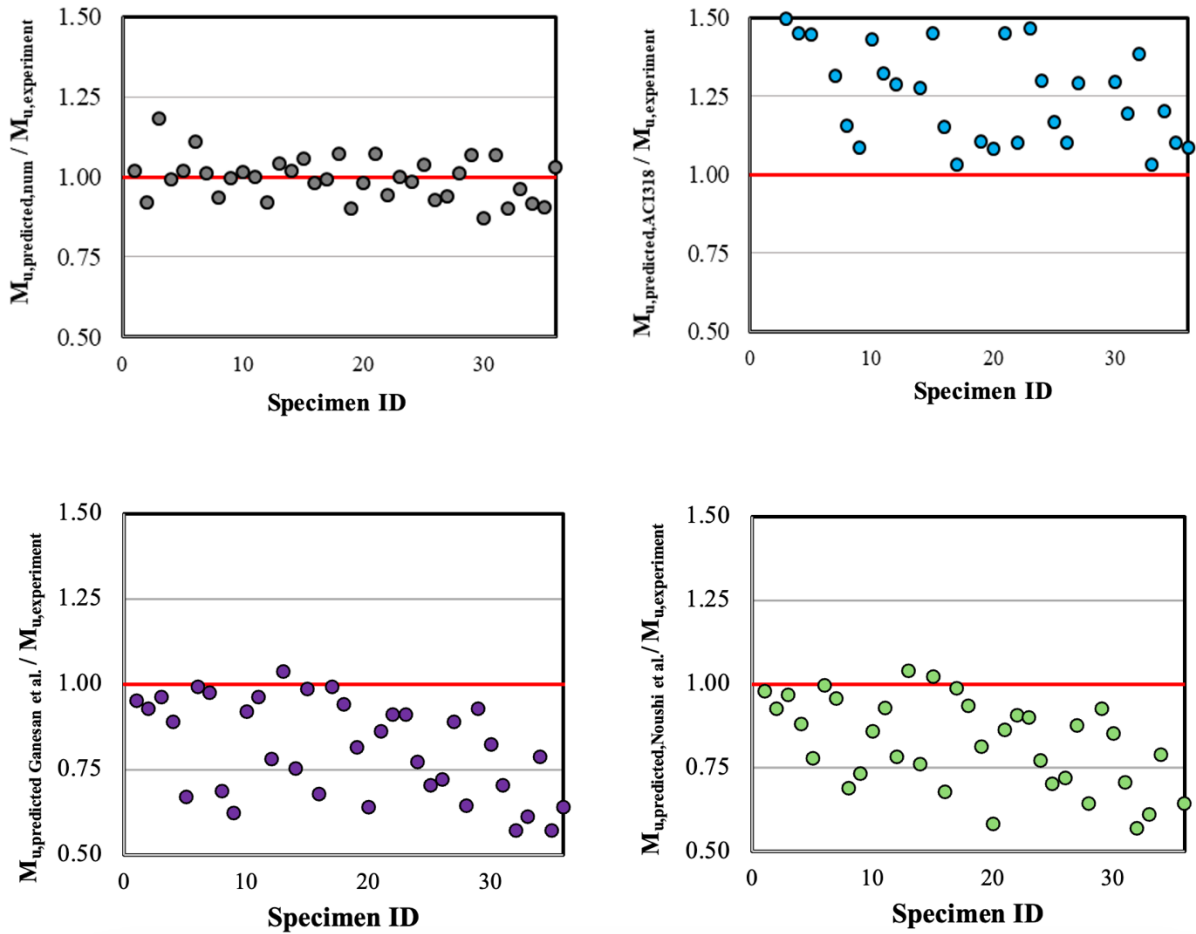
Fig. 2.8. Comparison of the Estimation Performances for the Test Soft Database

2.6. Discussions

In this study, a new mathematical model describing unconfined stress-strain behaviour of geopolymer concrete under compression is proposed. A higher-order polynomial is utilized to represent the stress-strain behavior of geopolymer concrete as polynomials are one of the most easily integrable and differentiable mathematical models. Consequently, this mathematical model results in more rapid evaluation of sectional response. The proposed model is intended to be utilized to estimate the flexure capacity of geopolymer concrete structural elements in lack of confinement. Therefore, formulations of the stress-strain model are based totally on beam tests conducted in the scope of this study and recent studies from the literature. Firstly, tested specimens that showed flexure-dominant failure, manifesting itself with flexural crack

63

formations at the midspan and clear post-yield zone in the load-displacement curves were used at the initial stage of the study. Therefore, only specimens with an a/d ratio of 1.65 were used in the formulations (**Table 2.2**). After that, 36 beam test specimens from the literature were found. These specimens were intentionally selected so that they were produced by using geopolymer concrete with different origins like fly ash-based, slag-based, CDW-based geopolymers, etc. (**Table 2.3**). In addition, the shear-span-to-depth ratios of test specimens ranged from 1.50 to 5.80 and all the specimens were claimed to be failed in flexure-dominated actions. Therefore, the proposed stress-strain relation was derived and tested using experimental results failed that due to flexure-dominated actions. Finally, a soft database was formed to include beam specimens having a range of 3-8 for a/d ratio. Therefore, all the formulations are derived and tested using flexure-dominant beam specimens as stress-strain relation is not limited to a few tests conducted in the scope of this study but several tests from both literature and this study.

The estimation performance of the proposed model is compared with the use of two distinct databases: i. experimental and ii. soft database. In order to double check the estimation performance of the proposed model, two different material models generated for geopolymer concrete in the literature [148,149] are also used. In experimental tests, all specimens failed in flexure-dominant action, manifesting themselves by nearly vertical cracks concentrated at the midspan. In other words, it was observed that GPC specimens failed with a significant post-yield response due to several flexure cracks at the midspan. In all of these tests, there exists a significant amount of ductility, implied by the large yield plateau in load-displacement and moment-curvature curves in **Fig. 2.7**.

The estimation performances of the literature available formulation [148,149] revealed that these two material models resulted in moment capacity estimations ranging from 0.5 to 1.5 times the measured moment capacity from the experiment. The capacity estimations of these formulas are largely scattered as shown in **Fig. 2.4**. Although on average, these literature-available formulations have similar percentage errors to the ACI318 [168] estimations, they have more standard deviations (more than about 40%) than the ACI318 [168] formulation (**Table 2.4**). On the contrary, the proposed material model resulted in moment capacity estimations ranging from the experiment 0.94 to 1.08 times the measured moment capacity from the experiment. In

64

addition, the average percentage error, as well as the standard deviation of the estimations of the proposed material model, are calculated as 2.66% and 1.92%, respectively, which are the least among the other alternatives (**Table 2.4**). The most important observation from these experimental estimations is that the proposed model not only has better accuracy but also has less deviations, which is more crucial when a dependable capacity estimation tool is sought.

The second comparison is made by using a soft-database. In this case, the real capacity of the selected database is assumed to be obtained by using the verified numerical model in the scope of this study. Afterwards, the capacities of each beam element in the soft-database are estimated by using the proposed mathematical model, the formulation given in ACI318, and the material models proposed by Ganesan et al. [148] and Noushini et al. [149]. The observations from the comparison of estimations are similar to ones from the experimental findings. In other words, the formulations of Ganesan et al. [148] and Noushini et al. [149], as well as, ACI318 resulted in a large scatter and the percentage error reach as large as 50% (**Fig. 2.8** and **Table 2.7**). In contrast, the proposed formulation resulted in much less deviations and more accurate estimations, implied by the standard deviation of 3.47% and the largest percentage error of 13% (**Fig. 2.8** and **Table 2.7**).

However, the mathematical model in this study neglects the strain-gradient effects as no equivalent stress block is intended to be proposed. In this study, a full stress-strain curve valid for compressive actions of geopolymer concrete under no confinement is given. This stress-strain relation is used during the section analysis. Therefore, the proposed stress-strain curve does not need any modifications regarding equivalent compressive stress and its resultant, depending on the level of eccentricity. In other words, the equilibrium equations in the section analysis handle the effects due to eccentricity (i.e., strain-gradient) provided that stress-strain relation is not simplified to a rectangular distribution. Yet, the maximum stress at the section could not exceed the ultimate compressive strength (f_{ck}). In addition, this comment is also verified when the estimation of ACI318 procedure (i.e., equivalent stress block application) is examined (**Tables 2.4 and 2.8**). It is clear from **Tables 2.4 and 2.8** that ACI318 procedure had significant errors in the flexural strength estimations.

2.7.   Conclusions

The need for less greenhouse gas emissions to slow down the speed of global warming necessitates the development of new generation materials with less carbon footprint in any sector. Consequently, researchers struggle to update conventional concrete to cause less harm to the environment. Geopolymer concrete is one of the most promising candidates for this issue as it has less amount of CO_2 emission and the production stage of it includes the use of waste materials. However, the use of structural elements produced from geopolymer concrete requires accurate methods for estimating their sectional responses like ultimate moment, ultimate shear, and ultimate axial load capacities. Nearly every design engineer uses ACI318 or similar formulations developed for conventional concrete in order to design their geopolymer concrete structural elements, which clearly fails to estimate capacity with reasonable accuracy. This is because; geopolymer concrete is more complex than conventional concrete. In addition, there are some limited efforts to propose stress-strain relation for geopolymer concrete in compression. Therefore, the proposed the stress - strain model is a significant contribution to the existing literature as it enables to estimation of the flexural capacity of geopolymer concrete structural elements with acceptable accuracy. Therefore, this study proposed a novel compressive stress-strain model in order to capture the ultimate moment capacities of geopolymer concrete.

The study initiated the formulation of the mathematical model by applying the necessary boundary conditions and by utilizing recent bending test results of reinforced geopolymer concrete beams. After calibrating the proposed mathematical model, a large test database was formed from the literature. Then, the performance of the proposed model in estimating the ultimate moment capacities was investigated. The results showed that the proposed model could estimate the ultimate moment capacities with an absolute mean and a standard deviation of the estimation errors of 2.66% and 1.92%, respectively. In addition, the percentage errors of the proposed model are significantly less than the currently utilized model recommended by the ACI318.

The estimation performance of the proposed model is investigated by referring to i. experimental and ii. soft database. In these checks, two different material models generated for geopolymer

concrete in the literature [148,149] are also used. The estimation performances of the literature available formulation [144,145] revealed that the capacity estimations of these formulas are largely scattered as shown in **Figs. 2.4 and 2.8**. Although on average, these literature-available formulations have similar percentage errors to the ACI318 estimations, they have more standard deviations (more than about 40%) than the ACI318 formulation (**Tables 2.4 and 2.8**). On the contrary, the proposed material model resulted in moment capacity estimations ranging from the experiment 0.94 to 1.08 times the measured moment capacity from the experiment. In addition, the average percentage error, as well as the standard deviation of the estimations of the proposed material model, are calculated as 2.66% and 1.92%, respectively, which are the least among the other alternatives. The most important observation from these experimental estimations is that the proposed model not only has better accuracy but also has less deviations, which is more crucial when a dependable capacity estimation tool is sought.

Finally, the proposed models' performance was double checked by using a new database consisting of unscaled specimens. For this purpose, a soft database of 50 different beam specimens was formed and the ultimate moment capacities of all specimens were determined by using the verified numerical model. After that ultimate moment capacities of each specimen were determined by using both the proposed model and ACI318 model. Finally, estimation performance of the proposed stress-strain model was investigated. It could be stated that the proposed stress-strain model could yield satisfactory ultimate moment capacity estimations with a maximum absolute percentage error and absolute mean percentage error of 5.07% and 3.47, respectively. Therefore, the proposed mathematical model is a promising candidate to estimate the flexural capacity of geopolymer elements.

CHAPTER III: CONFINED COMPRESSIVE STRESS – STRAIN MODEL FOR RECTANGULAR GEOPOLYMER REINFORCED CONCRETE MEMBERS

3.1.   Introduction

Concrete production is a process that requires the use of aggregates of different sizes, the production process of which is quite energy-intensive and creates a significant amount of waste, as well as the consumption of natural resources. Conventional concrete (CVC), despite its disadvantages such as low ductility and durability, is still the most widely used building material (the second most consumed material in the world after water) [188], and its production process causes serious carbon emissions. Although concrete and effective measures have been taken in recent years, the concentration of CO_2 in the atmosphere is still increasing and contributes to global warming. Academia and the construction industry have undergone a major paradigm shift in recent years to reduce CO_2 emissions as a result of increasing pressure from national and international environmental problems and policies. However, the scope is still very limited, and the construction industry should make more efforts to look for alternative methods to definitively reduce-eliminate CO_2 levels. In this context, in addition to the solutions developed to reduce the production of high CO_2 production to which cement is responsible for producing greener alternative building materials, realistic and applicable solutions are needed for each component of the sector. These solutions should be geared towards eliminating CO_2 and ensuring future circularity, which is an unavoidable requirement to reduce the construction industry's carbon cycle and climate impacts. At this point, geopolymer binders, an alternative binding material developed by Davidovits [189] as an innovative solution, come to the forefront among popular solutions. Geopolymer binders produced by activating aluminosilicate source binders employing alkali activators are binder candidates that can reduce the use of cement to zero by enabling industrial by-products such as blast furnace slag, fly ash and minerals such as silica fume and metakaolin to be used as building materials [138,190-192]. However, the literature lacks of necessary amount of research on the mathematical models devoted to estimating the capacity of this newly-practiced material. It should be noted that this kind of research is a must for new materials to become useful in practice.

Analytical models are required for numerical simulation of the behavior of structural members and for detecting the exact stress-strain relationship of confined and unconfined concrete under compression. Thanks to the models that define the stress-strain relationship of CVC, the load-deflection behavior and ultimate load capacity of reinforced concrete elements can easily be calculated during the design stage. There are methods proposed by Hognestad [193], Popovics [194], Sargin [195], Wang [196], Kent and Park [163], Sheikh and Uzumeri [165], Saatcioglu and Razvi [167], Mander [197], Scott [198], Roy and Sözen [166], which are still valid for reinforced members.

As mentioned above, while the studies on stress-strain models for CVC have reached a maturity level , geopolymer concrete (GPC) is still in the development stage and therefore, there are significant gaps in the literature [199,200]. In addition, whether or not mathematical models based on conventional concrete are valid to predict the behavior of geopolymer concrete for large structural elements, which are structurally different from CVC, remains a controversial issue [125]. Similar to CVC, determining the behavior of geopolymer concrete requires modeling the structural properties of its components; because the mechanical behavior changes depending on the stress level and the interaction of different loading types [160,161].

According to the findings of experimental studies, a lower elastic modulus of GPC has been reported compared to ordinary Portland concrete (OPC) with the same compressive strength [159,161,201-204]. Therefore, the stiffness mechanism of the geopolymer is different from that of the OPC binder. Therefore, the equations required to calculate the current standards overestimate the elastic modulus of the GPC. In addition, experimental studies have shown that GPC has a more brittle structure [205]. This underlines the need for the in-depth investigation and the development of new formulations for the mechanical properties of GPC. In this context, Prachasare et al. [206] developed a new stress-strain model based on the stress-strain curve of fly ash-based GPC and the design equations proposed by Thorenfeldt [207]. The results indicated very close results to the experimental test data of the proposed stress-strain model. Tung et al. [204] suggested stress block parameters for fly ash and slag-based geopolymer concrete in their study. As a result of the study, it was proved that the accuracy of using the ACI formulation for concrete structures in the design of GPC beams is quite satisfactory, but at the

same time, in some cases, the calculated axial parameters differ significantly from the experimental results. However, to the best of the author's knowledge, there are no studies that have been proposed to address a broad framework consisting of different types of components in general. In addition, Kocaer and Aldemir [208] proposed a novel compressive stress-strain formulation for unconfined GPC with different orientations referring to a large test database from the literature [125, 176, 140-168]. They proved that the proposed material model helped predict the moment capacity of reinforced concrete GPC members in the absence of confinement. As the results were promising, as a follow-up study to this work, a new research was performed to simulate the confinement effect on the compressive stress – strain model of rectangular GPC columns.

The significance of the research could be explained in the following sense that reinforced concrete columns subjected to axial and flexural loads are subject to a rapid deterioration in strength due to lateral expansion of the internal concrete following delamination of the concrete cover. In this context, confinement is one of the most effective methods to improve the ductility of concrete and transverse reinforcement of columns increases the compressive strength and ductility under lateral loading by limiting the lateral expansion of the core concrete [211-213]. The effectiveness of the confinement effect varies according to the arrangement of the reinforcement (such as length, shape, distance between lateral reinforcement, reinforcement ratio, etc.) and the quality of the concrete. This phenomenon of confining the concrete by proper arrangement of transverse reinforcement results in a significant change in the behaviour of concrete base material. In the literature, there are only a limited amount of attempts to understand the confined compressive stress-strain models of GPC. For instance, Ganesan et al. [148] aimed to investigate the effects of the confiment mechanism on OPC and GPC by conducting compressive tests on cylinder samples. For this purpose, 36 cylinders were tested under monotonic loading, with 24 of them made with GPC and the rest made with OPC. The study focused on the volumetric ratio of confinement as the variable, and an analytical model was suggested to explain the stress-strain behavior of confined GPC. As a result of the evaluations in the study, it was seen that the model proposed by Mander et al. [197] gives a better representation of the stress-strain behavior of the bounded GPC. Therefore, they obtained the most optimum stress-strain graph for geopolymer concrete by applying a modified parameter

(r) to this model. However, there is no other research on this subject, to the best of the authors' knowledge. Therefore, this study aimed to propose a new confined compressive stress–strain model for GPC to estimate the flexural capacity of GPC structural members. The study selected the unconfined compressive stress–strain model proposed by Kocaer and Aldemir [208] as the base curve and introduced a modification to the confinement mechanism for rectangular columns. To this end, the formulation for the confinement mechanism given in Kent and Park [163] was modified using experimental data. Then, the performance of the proposed confinement concrete model to estimate the flexural capacity of rectangular columns with different GPC orientations, different axial lad ratios, different sizes, and different concrete and steel qualities were investigated. The results were also compared with the equations from four different codes (i.e., American Concrete Institute (ACI318), British Standart (BS8110-97), Turkish Standart (TS500), and American Association of State Highway and Transportation Officials (AASHTO)). The results showed that the proposed mathematical model had better accuracy and fewer deviations as far as the flexural capacity estimation performances were considered. In addition, the ability of the proposed model to estimate the full moment–curvature curves were studied using experimental results. The comparison of the experimental moment–curvature curves from three different tests revealed that the proposed model also predicts the full moment–curvature curve satisfactorily.

3.2.   Material Method

Research on the behavior of structural members subjected to both axial and moment date back to the early 1900s [212-214]. One of the most important properties of concrete is that it exhibits different behavior in confined and unconfined states. While confined concrete exhibits larger ductility, unconfined concrete is brittle. For this reason, examining the behavior of confined and unconfined concrete using different stress-strain models is an important element in obtaining more accurate results. Various confinement models have been developed to predict the stress-strain behavior of normal and high-strength concrete. In this context, many linear and non-linear stress-strain models make it possible to predict concrete behavior. In addition, the strength improvement obtained from the confinement and the descending slope of the stress-strain curve has a significant effect on the flexural strength and ductility of the reinforced

concrete members. The moment-curvature curve is critical to evaluate the stress-strain behavior of concrete, and the ductility and deformability of reinforced concrete members.

Early works by Hognestad [193] and Desayi and Krishnan [213] with the stress-strain curve equation suggested basic models for stress-strain in concrete. In order to simulate Hognestad's proposed post-peak behavior under the effect of confinement, Kent and Park [163] proposed a set of equations to modify the stress-strain curves. This approach along with other examples (i.e., Sheikh and Uzumeri [165], Mander et al. [197] etc.) thoroughly based on the improvement of strength and strain due to passive confinement. These models commonly develop formulations for enhanced mechanical properties due to the effect of confinement from the lateral reinforcements. Keeping in mind the fact that the amount of enhancement in mechanical properties of both CVC and GPC is dependent on the confinement mechanism to a large extent, it is wise to utilize similar confinement mechanisms for CVC and GPC. Therefore, in this study, the confinement equations given by Kent and Park [163] are decided to be utilized with slight modifications. And, the base material response (i.e., compressive behaviour of unconfined GPC) is also taken from the study of Kocaer and Aldemir [208]. In their studies, they proposed a stress-strain relation based on two global parameters (i.e., f_{ck} ve ε_{cu}) for the compressive behavior of GPC (**Fig. 3.1** and Eq. 3.1).

$$\sigma_{GPC}(\varepsilon) =$$
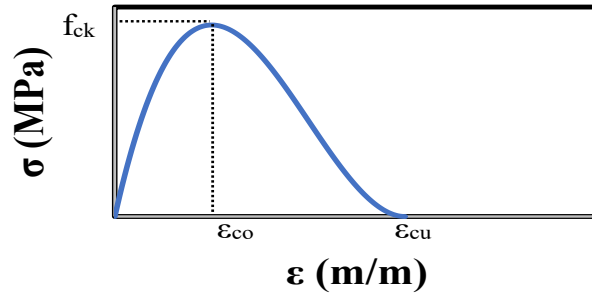
Fig. 3.1. Stress – strain relation for unconfined geopolymer concrete [125]

$$\sigma_{GC\_unconfined}(\varepsilon) = \frac{6.75\, f_{ck}\, \varepsilon\, (\varepsilon - \varepsilon_{cu})^2}{\varepsilon_{cu}{}^3} \tag{3.1}$$

It should also be repeated that the main parameters affecting the confinement mechanism are the amount of stirrup, stirrup spacing, unsupported length of stirrups, etc. Therefore, it could be assumed that the confinement mechanisms in GPC and CVC are similar. And, a small

modification should result in a satisfactory representation of the change in the base material (i.e., a shift from CVC to GPC). The confined concrete formulations proposed by Kent and Park [163] are given in Eqs. 3.2-3.8. In this study, only a modifier is applied in front of the confined strength estimation formula given by Kent and Park [163].

$$K = 1 + \frac{\rho s. fyh}{fck} \tag{3.2}$$

$$\varepsilon_{50u} = \frac{2\varepsilon_{cu}}{3} \tag{3.3}$$

$$ls = 2(bk + hk) \tag{3.4}$$

$$\rho s = dia_{lat}^2 * \frac{\pi}{4} * \frac{ls}{s*bk*hk} \tag{3.5}$$

$$\varepsilon_{50h} = \frac{2\rho s\sqrt{bk/s}}{3} \tag{3.6}$$

$$\varepsilon_{ccu} = \frac{4.8(\varepsilon_{50u}+\varepsilon_{50h})}{3.6} \tag{3.7}$$

$$f_{cc} = M_{fck} * K * f_{ck} \tag{3.8}$$

The proposed confined material model (Eq. 9) is obtained only modifying the f_{ck} and ε_{cu} with f_{cc} and ε_{ccu} in Eq. 3.1, respectively (**Fig. 3.2**). Optimization of the applied modifier coefficient was first established in light of the results obtained from experimental tests carried out in the scope of this study. Details on the tests are presented in Section 3. The coefficient M_{fck} was determined to optimize the capacity estimations of flexural test results. The optimum value for M_{fck} value was obtained as 0.7 from these three experimental results.
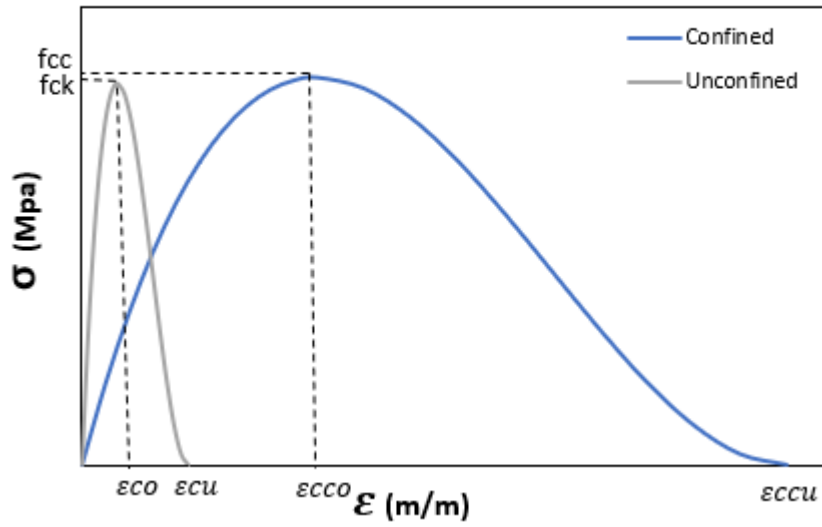
Fig. 3.2. Proposed stress – strain relation for confined geopolymer concrete

$$\sigma_{GPC\_confined}(\varepsilon) = \frac{6.75\ f_{cc}\ \varepsilon\ (\varepsilon - \varepsilon_{ccu})^2}{\varepsilon_{ccu}{}^3} \tag{3.9}$$
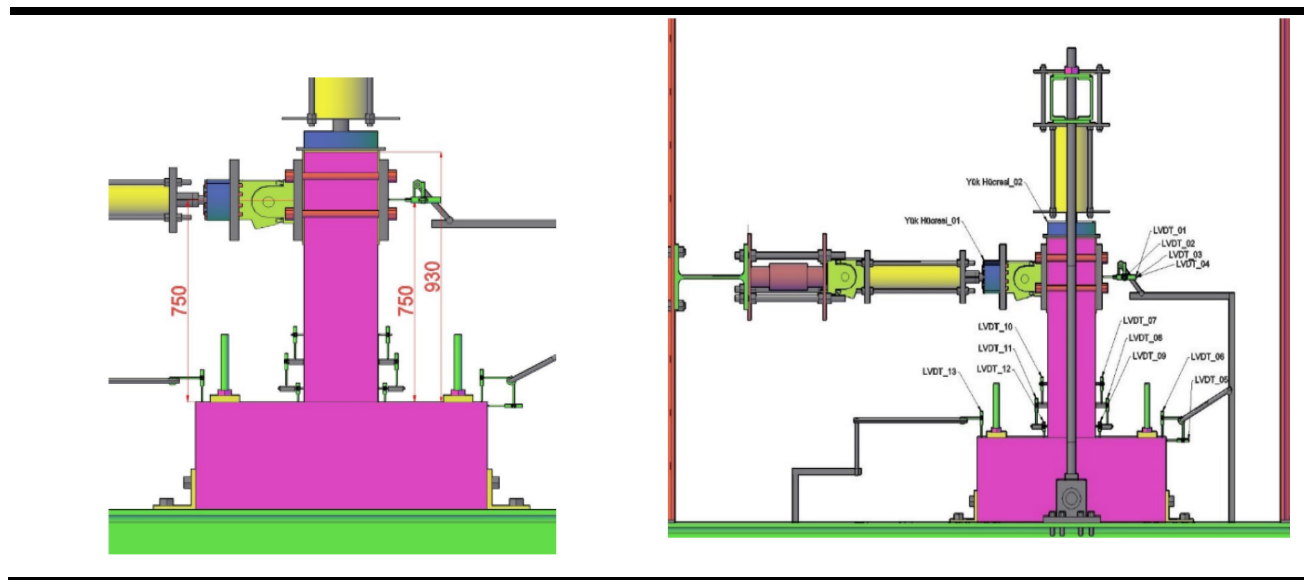
3.3.   Experimental Tests

Geopolymer columns designed and tested within the scope of this study were produced by considering the mixture design with the best compressive strength as a result of extensive studies [125,208,151,152]. The mixture proportions of geopolymer concrete produced within the scope of experimental studies are shown in **Table 3.1**. During the experiment, the tip displacement, applied lateral load and base curvature distributions were recorded using linear variable displacement transducers (LVDTs) and load cells (**Fig. 3.3**).

Table 3.1. Mixture proportions of geopolymer columns

Ingredients*	BW	GW	CW	S	FA	CH	NH	NS	AF	AC	W
Amount (kg/m³)	600	100	100	200	50	50	112	224	250	750	202

*BW: Brick-based wastes, GW: Glass waste, CW: Concrete waste, S: Slag, FA: Fly ash, CH: Ca(OH)$_2$, NH: NaOH, NS: Na$_2$SiO$_3$, AF: Aggregate fines, AC: Aggregate coarses, W: Water

The test setup prepared to perform lateral and axial loading tests on geopolymer column samples is presented in **Fig. 3.3**. Two types of geopolymer ½ scaled column tests were carried out in this study (i.e., monolithic and demountable). The tested columns are 250 × 150mm rectangular columns. The longitudinal bars used in all specimens are 6ϕ10. The lateral reinforcement at the confinement zone (i.e., at the bottom 500mm zone) is ϕ6/50mm whereas the lateral reinforcement at the rest of the column height is ϕ6/100mm. The shear span of the columns was 750 mm. The concrete cover was 25 mm. The experiment was carried out with displacement-controlled loading protocols. 3 samples were tested under 0.10, 0.20, and 0.30 $A_g f_{ck}$ axial loading ratios. Cyclic lateral displacement excursions were applied till a capacity drop of 20% was observed. The crack behavior, energy absorption capacity, and fracture load of the columns under these movements were investigated.

Fig. 3.3. Experimental setup

The first and last views of the geopolymer column test specimens are shown in **Fig. 3.4**. P_{max}, Δ_{max}, and axial load values obtained as a result of the tests are shown in **Table 3.2**.

Initial Stage	Final Stage	Initial Stage	Final Stage
GEO_0.10CAP_D**		GEO_0.10CAP_M*	
GEO_0.20CAP_D**		GEO_0.20CAP_M*	
GEO_0.30CAP_D**		GEO_0.30CAP_M*	

Fig. 3.4. Experimental results

As can be seen from the results of the experimental data (**Fig. 3.4**), no failure occurred on the demountable specimens (i.e., the failure zones formed not on the joint but on the plastic zone of the concrete column). Therefore, although some of the test samples are produced with

demountable joints, they all are suitable to be used as a database for the proposed mathematical model.

Table 3.2. Summary of experimental results and numerical estimations

Test ID	Axial Load (kN)	P_{max} (kN)	Δ_{max} (mm)
GEO_0.10CAP_M*	101.25	51.23	16.96
GEO_0.20CAP_M	202.50	71.33	14.47
GEO_0.30CAP_M	303.75	76.71	14.85
GEO_0.10CAP_D**	117.00	43.67	17.36
GEO_0.20CAP_D	234.00	47.77	18.61
GEO_0.30CAP_D	351.00	47.78	18.91

* GEO_0.10CAP_M denotes monolithic column specimen under 0.10 $A_g f_{ck}$ axial loading.

** GEO_0.10CAP_D denotes demountable column specimen under 0.10 $A_g f_{ck}$ axial loading.

3.4. Experimental Database

The proposed modification was derived by utilizing the experimental findings of experimental tests of several specimens, but its accuracy should be tested using other experiments from the generated database. Therefore, 41 various tests from recent studies [215-220] were utilized (**Tables 3.3 and 3.4**). It could easily be inferred that the used test database has a very large range of compressive strength values, eccentricity values, section sizes, etc. The ranges for the different parameters in this experimental database are indicated in **Table 3.3**. In addition, the geopolymer materials in the formed experimental database are all different in the selected test specimens (i.e., slag-based geopolymer, fly ash-based geopolymer, fully recycled geopolymer, etc.).

Table 3.3. Ranges of the selected variables in the experimental database

| Parameter / Range	f_{ck} (MPa)	f_{yk} (MPa)	Longitudinal Reinforcement Diameter	Lateral Reinforcement Diameter	Eccentricity (mm)	Width (mm)	Height (mm)
Minimum	25	392.5	10	6	0	150	120
Maximum	72.5	710	14	10	145	260	250

Table 3.4. Summary of the test database

Reference	Specimen	Length (mm)	Width (mm)	Height (mm)	Geopolymer Material	fck (MPa)	Longidutional Reinf.	Lateral Reinf.	fy (MPa)	Eccen. (mm)	Cover (mm)	Failure Load (kN)
Sumajouw et. al. [215]	GCI-1	1500	175	175	Fly-Ash Based	42	4φ12	φ6/100	519	15	25	940
	GCI-2	1500	175	175	Fly-Ash Based	42	4 φ 12	φ6/100	519	35	25	674
	GCI-3	1500	175	175	Fly-Ash Based	42	4 φ 12	φ6/100	519	50	25	555
	GCI-4	1500	175	175	Fly-Ash Based	43	8 φ 12	φ6/100	519	15	25	1237
	GCI-5	1500	175	175	Fly-Ash Based	43	8 φ 12	φ6/100	519	35	25	852
	GCI-6	1500	175	175	Fly-Ash Based	42	8 φ 12	φ6/100	519	50	25	666
	GCII-1	1500	175	175	Fly-Ash Based	66	4 φ 12	φ6/100	519	15	25	1455
	GCII-2	1500	175	175	Fly-Ash Based	66	4 φ 12	φ6/100	519	35	25	1030
	GCII-3	1500	175	175	Fly-Ash Based	66	4 φ 12	φ6/100	519	50	25	827
	GCII-4	1500	175	175	Fly-Ash Based	59	8 φ 12	φ6/100	519	15	25	1559
	GCII-5	1500	175	175	Fly-Ash Based	59	8 φ 12	φ6/100	519	35	25	1057
	GCII-6	1500	175	175	Fly-Ash Based	59	8 φ 12	φ6/100	519	50	25	810
Danda et. al. [216]	8M	1000	150	150	GGBS	48.04	4 φ 12	φ8/100	595.45	26.2	25	575.2
	10M	1000	150	150	GGBS	50.14	4 φ 12	φ8/100	595.45	24.5	25	593.7
	12M	1000	150	150	GGBS	51.44	4 φ 12	φ8/100	595.45	23.8	25	605.1
	14M	1000	150	150	GGBS	54.93	4 φ 12	φ8/100	595.45	22.8	25	635.9
	16M	1000	150	150	GGBS	60.03	4 φ 12	φ8/100	595.45	23	25	680.9
Elchalakani et. al. [217]	G150-25	1200	260	160	Unspecified	26	6 φ 14	φ8/150	708	25	35	657
	G75-25	1200	260	160	Unspecified	26	6 φ 14	φ8/75	708	25	35	804
	G150-50	1200	260	160	Unspecified	26	6 φ 14	φ8/150	708	50	35	353
	G75-50	1200	260	160	Unspecified	26	6 φ 14	φ8/75	708	50	35	454

Reference	ID											
	G150-75	1200	260	160	Unspecified	26	6 φ 14	φ8/150	708	75	35	234
	G75-75	1200	260	160	Unspecified	26	6 φ 14	φ8/75	708	75	35	244
Saranya et. al. [218]	I	1100	200	200	GGBS Dolomit	72.5	4 φ 12	φ8/60	580	0	25	53
Albitar et. al. [219]	SHC2-10	1600	150	150	Fly-Ash Based	35	4 φ 12	φ6/85	510	10	32	545
	SHC3-35	1600	150	150	Fly-Ash Based	35	4 φ 12	φ6/85	510	35	32	354
	SHC4-50	1600	150	150	Fly-Ash Based	35	4 φ 12	φ6/85	510	50	32	272
	SHC5-85	1600	150	150	Fly-Ash Based	35	4 φ 12	φ6/85	510	85	32	170
	SLC7-30	1600	150	150	Fly-Ash Based	30	4 φ 12	φ6/85	510	30	32	302
	SLC8-125	1600	150	150	Fly-Ash Based	30	4 φ 12	φ6/85	510	125	32	91
	SLC9-145	1600	150	150	Fly-Ash Based	30	4 φ 12	φ6/85	510	145	32	76
Experimental Study Data	GEO_0.10CAP_M	930	150	250	CDW	31.2	6 φ 10	φ6/50	456	0	15	43.67
	GEO_0.20CAP_M	930	150	250	CDW	31.2	6 φ 10	φ6/50	456	0	15	47.77
	GEO_0.30CAP_M	930	150	250	CDW	31.2	6 φ 10	φ6/50	456	0	15	47.78
	GEO_0.10CAP_D	930	150	250	CDW	27	6 φ 10	φ6/50	710	0	15	51.23
	GEO_0.20CAP_D	930	150	250	CDW	27	6 φ 10	φ6/50	710	0	15	71.33
	GEO_0.30CAP_D	930	150	250	CDW	27	6 φ 10	φ6/50	710	0	15	76.71
Kumar et. al, [220]	GCII	1000	120	120	GGBS	33.78	4 φ 10	φ6/100	500	15	328	15
	GC III	1000	120	120	GGBS	33.78	4 φ 10	φ6/100	500	30	288	15
	GCV	1000	120	120	GGBS	33.78	6 φ 10	φ6/100	500	15	376	15
	GC VI	1000	120	120	GGBS	33.78	6 φ 10	φ6/100	500	30	296	15

In addition, a comparative analysis was made using different design codes in order to make a more comprehensive analysis. Thus, it was aimed to investigate the performance of the proposed model compared to other available code equations. The results obtained with the ACI318, TS500, BS8110-97, and AASHTO codes used for comparison are shown in **Fig. 3.5 and 3.6**. In **Fig. 3.5**, the accuracy of the proposed model and the four design code equations to estimate the flexural capacity of the test data is summarized. In this figure, the ordinate is designed as the ratio of the estimated moment capacity to the experimental moment capacity. Therefore, any estimation close to unity represents an accurate result (i.e., values close to the dashed horizontal line). The estimations of the proposed model range between 0.80 and 1.20 whereas the other design code equations resulted in estimations ranging between 0.20 to 1.80. The average (standard deviations) of the normalized moment capacity values for the proposed model, ACI318, TS500, BS8110, and AASHTO are 1.003 (0.101), 0.758 (0.355), 0.943 (0.425), 0.729 (0.431) and 0.499 (0.232), respectively. Besides, from **Fig. 3.6**, it could be stated that the proposed model has the least percentage error for each specimen in the test database. The absolute average percentage errors (standard deviations) for the proposed model, ACI318, TS500, BS8110, and AASHTO are 7.39 (5.39), 37.3 (17.2), 37.18 (21.05), 42.96 (20.53) and 47.38 (23.34), respectively. Consequently, these results indicate that the proposed model estimates the test results with the most accuracy and the least deviations.
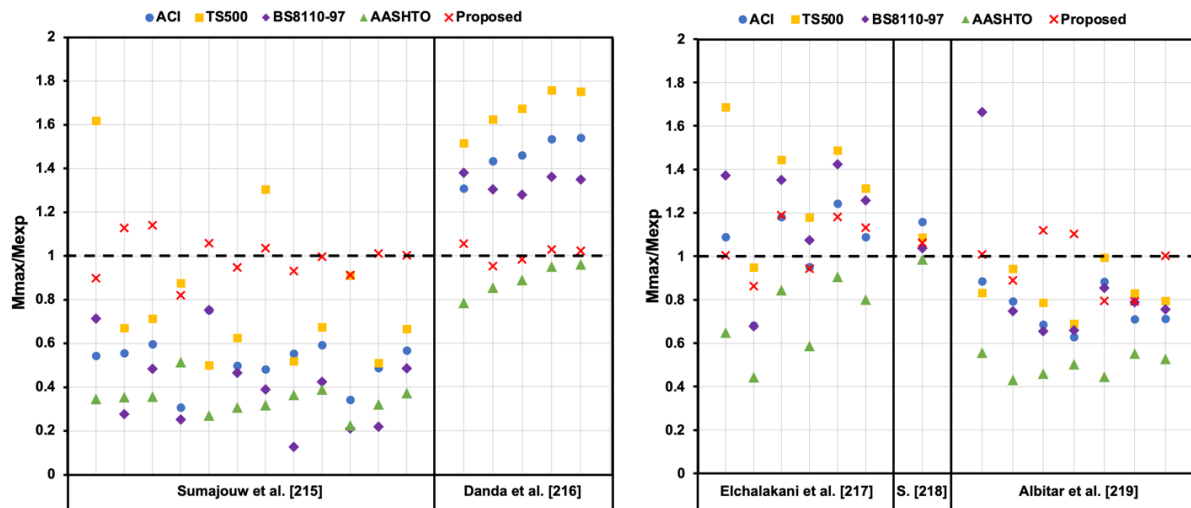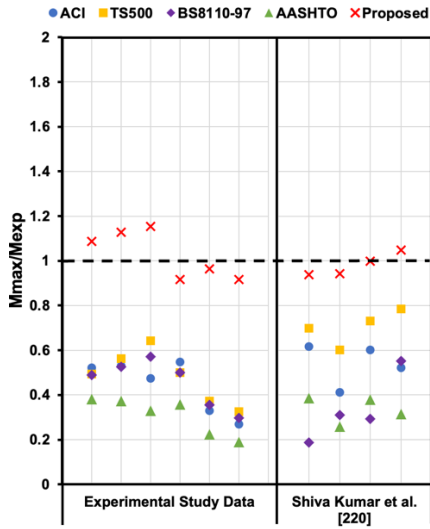
Fig. 3.5. Comparison of Performances of Different Equations for the Test Database
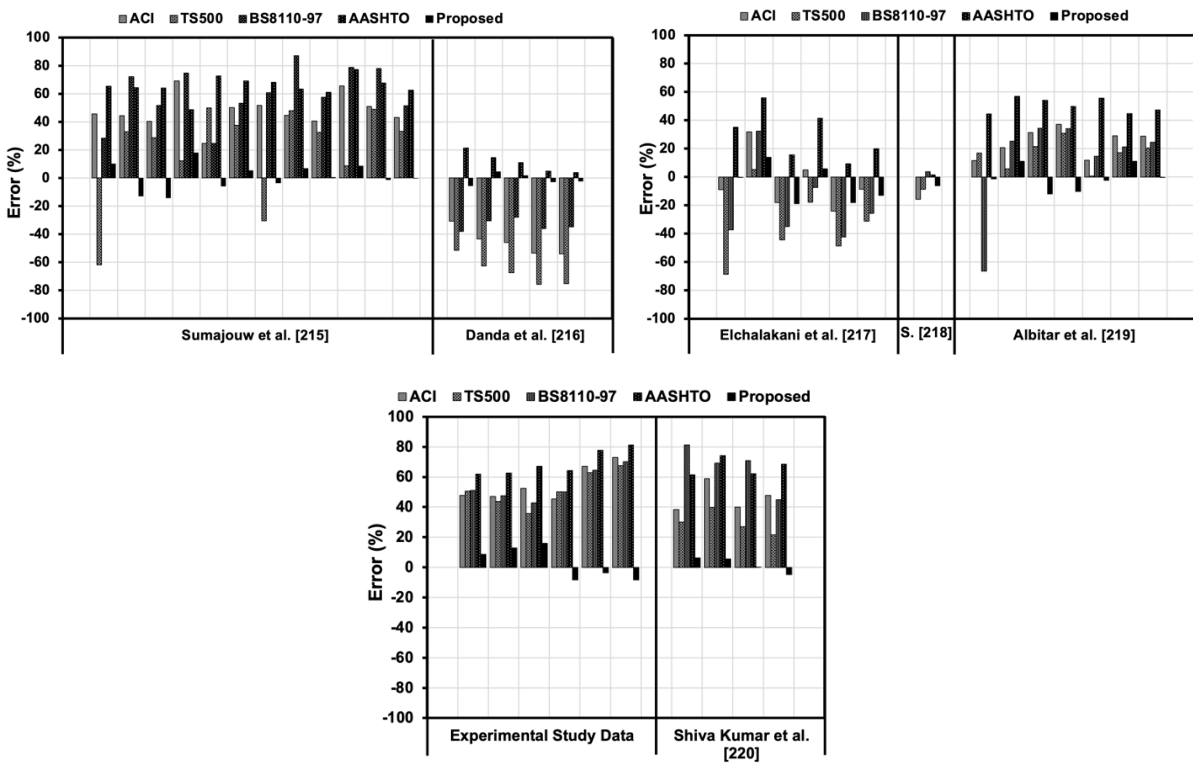

Fig. 3.6. Percentage Error Distributions of Different Equations for the Test Database

3.5.   Comparison of Results

The proposed model was double-checked with the database obtained from the literature. For this purpose, the final moment capacities obtained using the proposed model and 4 different codes were determined with the test results compiled from 41 different column samples in a wide range of f_{ck}, b, h, f_y longitudinal and lateral reinforcements. Then, the prediction performance of the proposed stress-strain model was examined. In the selected test specimens, all of the geopolymer column specimens were selected to accommodate different structural contents. (i.e., slag-based geopolymer, fly ash-based geopolymer, fully recycled geopolymer, etc.). Thus, it was aimed to have a comprehensive mathematical model for the stress-strain relationship of different content of geopolymer concrete. In order to interpret the data obtained in **Fig. 3.7 and 3.8** more accurately, scatter charts were obtained.
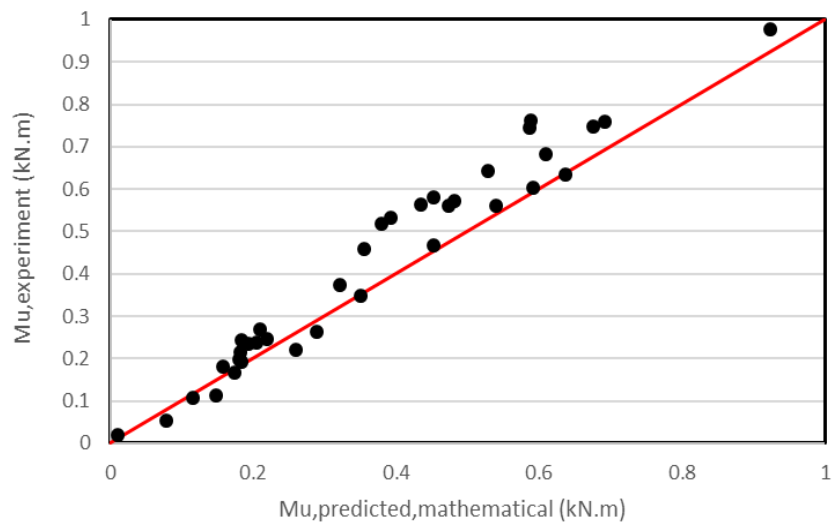
Fig. 3.7. Comparison of the estimation performance of the proposed model for the test database
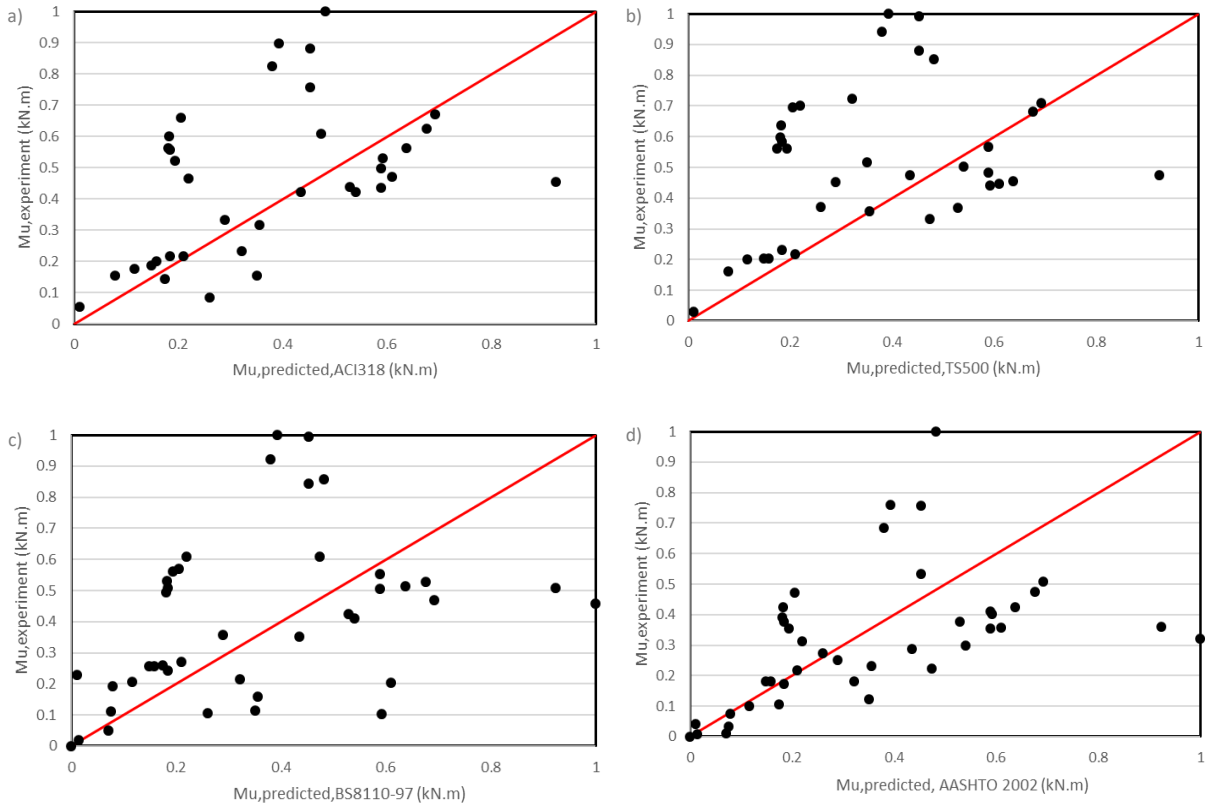
Fig. 3.8. Comparison of the estimation performances of code equations: (a) ACI318, (b) TS500, (c) BS110-97, (d) AASHTO 2002

It is seen from **Fig. 3.7 and 3.8** that the estimation performance of the proposed model is quite better compared to the code-based formulations as the estimations of the proposed model are closely distributed to the diagonal solid line, indicating the perfect match between the estimation and the experimental value.

Finally, the moment-curvature estimation performances of the proposed model were studied using the experimentally obtained moment – curvature curves for specimens given in **Table 3.2**. The envelops of moment-curvature values from the cyclic experiments are utilized as the proposed model is suitable for monotonic calculations. The moment – curvature values from the experiment were obtained from the LVDT measurements at the base of the tested specimens. It is clear from **Fig. 3.9** that the proposed material model not only estimates the moment capacities accurately but also predicts the moment-curvature distributions satisfactorily. Therefore, it is a

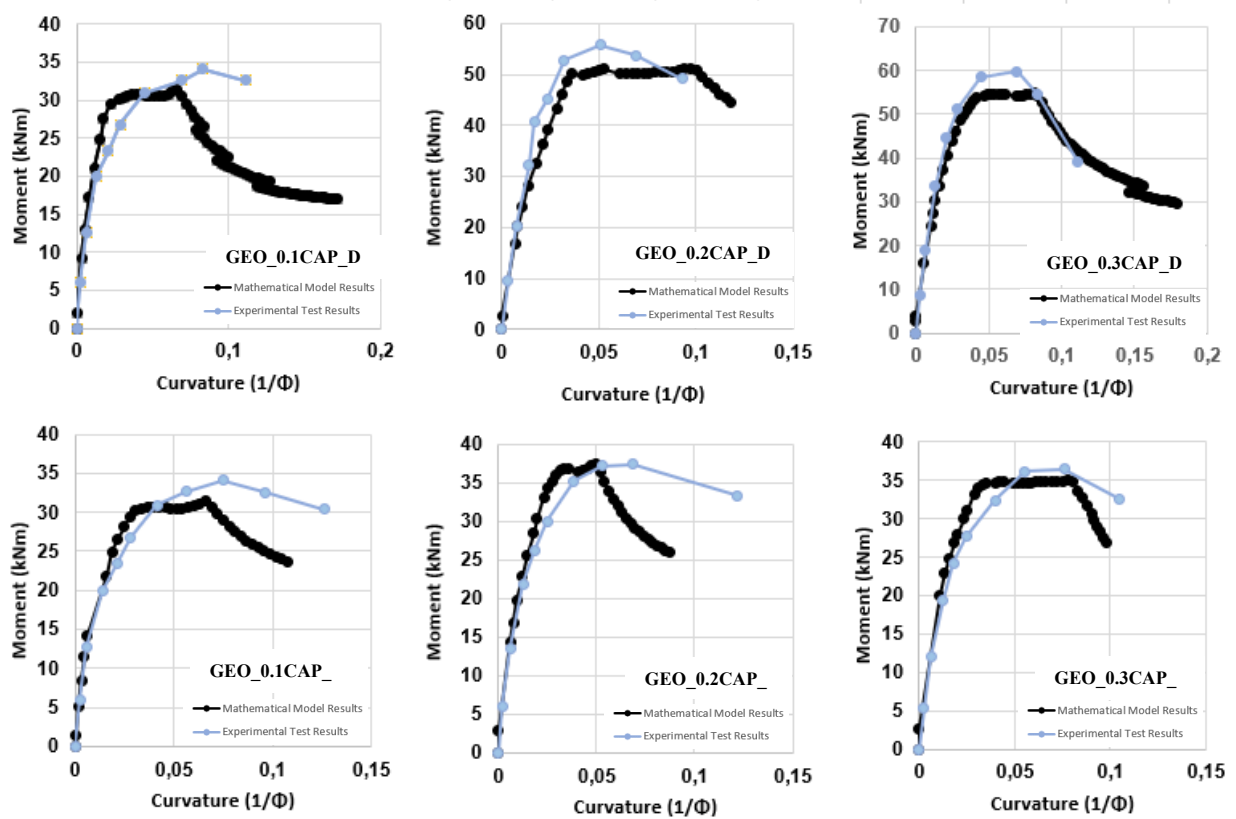good candidate for the robust design calculations during both force-based and performance-based designs.

Fig. 3.9. Comparison of the moment-curvature estimation performances of the proposed model

3.6. Conclusion and Discussions

In this study, a new mathematical model for the compressive behaviour of the confined geopolymer concrete is proposed. The proposed confined model selects an unconfined material model for GPC and applies some modifications due to the effect of confinement. The proposed confined concrete model is intended to be used to estimate the moment capacity of geopolymer concrete column elements. Therefore, the formulations of the stress-strain model are completely based on the column experiments conducted within the scope of this study. Experimental tests of a total of six geopolymer columns (three monolithic and three demountable columns) were carried out under different axial loads (0.1, 0.2, and $0.3A_gf_{ck}$) in order to incorporate the interaction between the axial load nad the moment. The proposed model was then validated by generating a large experimental database. The test database has consisted of 41 test samples from the literature with different material contents of GPC and wide mechanical and geometrical

parameter ranges. The generated test database constituted only rectangular or square cross-sections because the proposed model had a restriction on circular column calculations. The confined GPC compressive stress – strain model took the unconfined GPC compressive stress – strain model of Kocaer and Aldemir [208]. Then, the enhancement due to confinement was taken into account by the modified versions of the formulations given by Kent and Park [163]. The modification coefficient (M_{fck}) for the Kent and Park [163] model was determined from the limited number of tests conducted in the scope of this study. However, M_{fck} was validated for a large test database, too.

In addition, a comparative analysis was made using different design codes in order to make a more comprehensive analysis. Thus, it was aimed to investigate the performance of the proposed model compared to other available code equations. As a result of the comparisons, the absolute mean percent error and standard deviation of the estimations of the proposed material model were calculated as 7.39% and 5.39%, respectively, giving the least among other alternatives. In addition, while these values are followed by the ACI318 code with 37.30 absolute mean and 17.20 standard deviation as the best value closest to the proposed model, it is followed by the TS500 code with 37.18 absolute mean value and 21.05 standard deviation value. BS8110-97 code and AASHTO code, respectively, 42.96 and 20.53, 47.38 and 23.34 absolute mean values and standard deviation values gave results far from the experimental results. The most important observation from these experimental predictions is that the proposed model not only has better accuracy but also has less bias; this is more important for a reliable capacity estimator.

The moment-curvature curve estimation performance of the proposed model was also studied using the experimentally obtained moment – curvature curves for specimens given in **Table 3.2**. The envelops of moment-curvature values from the cyclic experiments are utilized as the proposed model is suitable for monotonic calculations. It is apparent from **Fig. 3.9** that the proposed material model could satisfactorily estimate both the moment capacities and the moment-curvature distributions. Therefore, it is a good candidate for the robust design calculations during both force-based and performance-based designs. In conclusion, the results obtained from the comparative analysis proved that the proposed model shows very promising results.

CONCLUDING REMARKS AND FUTURE RECOMMENDATIONS

The construction of urgent and cost-effective shelter structures for vulnerable groups affected by natural disasters and political crises, the capability for these structures to be used for extended periods and quickly relocated to desired locations when needed, their flexibility and expandability, and the use of region-specific natural materials or recycled construction waste as the primary building materials are important common issues. The current thesis presents a series of studies to provide design guidelines and model the behavior of waste-based concrete to be used in such structures in order to enable building systems that adopt the principles of circular economy in the construction industry, increase waste recycling, and consist of building elements that can be reused for different purposes or for the same function even after the end of their service life.

With this motivation, the main theme, background, benefits, applications, and impacts of Design for Manufacture and Assembly (DfMA) and Design for Deconstruction (DfD) techniques in the construction sector for sustainable development were aimed to be explored. Process flows, fundamental principles, and existing guidelines were examined, and research gaps were assessed. In addition to this literature review, a synopsis of a building constructed with demountable structural elements produced by Construction and Demolition Wastes-based (CDW) geopolymer at Hacettepe University, designed based on the synthesis of DfMA and DfD principles within the framework of rapid and sustainable construction, was presented. The study also aims to develop mathematical models for capacity predictions of the building elements by focusing on the in-depth analysis of the mechanical behavior of CDW-based geopolymers, which form the basis of the building elements used. By utilizing a wide parameter range, the study does not only aim to create a model specifically for CDW-based geopolymers but also focuses on developing a model that can be adapted to different types of geopolymers.

In the first chapter of this study, benefits, and impact of Design for Manufacture and Assembly (DfMA) and Design for Deconstruction (DfD) on sustainable development in construction industry was explored. Their current position, principles, and gaps were outlined. DfMA was found to be enhanced production efficiency, cost reduction, and waste minimization, while DfD

focused on component reintegration for multiple purposes alongside these benefits. Despite prefabrication use, DfMA and DfD integration in construction is limited, lacking standard guidelines. Future research should conduct construction industry-specific standards and integrate these methods with technologies like BIM. More studies are needed to fully integrate DfMA and DfD into construction, supporting sustainable development and the circular economy. This further research should include synthesizing systems, maximizing benefits and comparing impacts with conventional techniques. Additionally, the case study conducted at Hacettepe University demonstrated that CDW-based geopolymer demountable structural elements can be easily applicable for DfD and aligned with the sustainable construction principles of DfMA. Case study also demonstrated successful performances of demountable connections in prefabricated buildings, reducing on-site assembly time and labor costs while enhancing CDW-based geopolymer waste recycling.

In the second chapter, considering the limited availability of accurate mathematical models to predict the capacities of structural elements based on geopolymers, a novel stress-strain model was proposed to estimate the flexural capacity of geopolymer structural elements originated from CDW. The study was initiated by formulating a novel stress-strain model applicable for defining the compressive behavior of geopolymer concrete. Thereafter, a mathematical model incorporating fundamental boundary conditions was developed, and further refined using flexural test findings related to reinforced geopolymer concrete beams. An evaluation of the proposed model's performance in predicting ultimate moment capacities was conducted through a substantial test dataset compiled from existing literature. The findings revealed that the proposed model achieved estimations of ultimate moment capacities with an absolute mean error and standard deviation of estimation errors amounting to 2.66% and 1.92%, respectively. Additionally, the percentage errors associated with the proposed model were significantly lower compared to those of the currently endorsed model by ACI318. To further validate the model, a new database comprising 50 different unscaled beam specimens was utilized, and their ultimate moment capacities were determined using the verified numerical model. It was established that the proposed stress-strain model could produce satisfactory estimations of ultimate moment capacity with a maximum absolute percentage error and absolute mean percentage error of

5.07% and 3.47%, respectively. Therefore, the proposed mathematical model stands as a promising candidate for estimating the flexural capacity of geopolymer elements.

The third chapter summarized an in-depth analysis of the stress-strain properties exhibited by CDW-based geopolymer concrete columns and developed a comprehensive material model of geopolymer concrete to predict the flexural capacities of columns. Inspired by Kent and Park's confinement model, a stress-strain model incorporating the effect of confinement, aiming to accurately predict the moment capacity of geopolymer concrete columns, was proposed. The performance of the proposed formulation was validated using 41 different test results obtained from previous research on geopolymer concrete columns, yielding promising results. Additionally, moment-curvature curves obtained from experiments conducted on six manufactured monolithic and demountable columns were compared with moment-curvature curve estimations using the proposed stress-strain model. The obtained results, showing close estimations, substantiate the model's capability to be a good candidate for performance-based design calculations. Furthermore, the performance of existing formulations from four prominent international codes (ACI318, BS8110-97, TS500, and AASHTO) was compared with the proposed model. Specifically, significant deviations were observed between the flexural capacities calculated using code formulations and experimental results. On the other hand, the proposed model demonstrated a strong correlation with experimental data, validating its effectiveness in accurately predicting the flexural capacities of geopolymer columns.

In the context of sustainable development in the construction industry, promising areas for innovation and advancement are clearly seen in the synthesis of Design for Manufacture and Assembly (DfMA) and Design for Deconstruction (DfD) approaches for rapid urbanization. Building upon the insights gained from the study's first chapter, urgent need for the establishment of construction industry-specific standards is evident considering the limited integration of DfMA and DfD principles in construction practices and the identified gaps. Future research efforts should focus on formulating comprehensive guidelines tailored to the unique requirements and challenges of the construction sector. These standards should encompass not only technical aspects but also considerations related to project management, procurement, and regulatory compliance.

The integration of DfMA and DfD methodologies with advanced technologies such as Building Information Modeling (BIM) holds significant potential for enhancing efficiency and effectiveness in construction projects. Future research efforts should explore ways to seamlessly incorporate DfMA and DfD principles into BIM workflows. This integration can enable real-time optimization and decision-making, leading to improved project outcomes and resource utilization by facilitating collaborative design, visualization, and simulation across project stakeholders.

To fully realize the potential of DfMA and DfD in construction, future research should prioritize the synthesis of systems and the maximization of associated benefits. This entails a holistic approach that considers the entire lifecycle of built assets, from design and fabrication to operation and deconstruction. By systematically identifying synergies and trade-offs between DfMA and DfD strategies, researchers can develop integrated frameworks that optimize resource efficiency, cost-effectiveness, and environmental performance throughout the construction lifecycle.

Within the scope of this study, it is considered that the mathematical modeling of the mechanical behaviors of beam and column elements based on CDW-based geopolymer concrete is an important foundational study in understanding the behaviors of structure materials with very different compositions, and thus very different micro and macro mechanical properties, such as geopolymers. It is recommended to further experimentally validate the proposed models to strengthen their reliability and credibility. In this context, evaluating the model by different researchers and integrating their own datasets into the model would be beneficial. This may involve conducting additional flexural tests on various geopolymer concrete samples under different environmental conditions, loading rates, and curing regimes. Such experiments will provide a more comprehensive dataset to assess the performance of the model under different scenarios.

Geopolymer materials have the potential to provide enhanced durability compared to traditional Portland cement-based concrete. However, long-term durability studies are important to assess

the performance of geopolymer structural elements when exposed to aggressive environments for extended periods. Integrating data obtained from durability studies into the stress-strain model can enhance the accuracy and reliability of the model during long service life periods. Conducting optimization and sensitivity analyses can help identify the key parameters that significantly affect the flexural capacity of geopolymer elements. Systematically investigating fundamental parameters such as different material compositions, curing conditions, and reinforcement configurations can elucidate the relative importance coefficients of these factors and ultimately facilitate the development of specific design guidelines for geopolymer-based structural systems.

REFERENCES

[1] Prasad, A. S. ve Francescutti, L. H. (2017). Natural disasters. International Encyclopedia of Public Health, 215. https://doi.org/10.1016/B978-0-12-803678-5.00519-1

[2] World Health Organization-WHO (2022). Earthquakes. https://www.who.int/healthtopics/earthquakes#tab=tab_1

[3] Mavrouli, M., Mavroulis, S., Lekkas, E., & Tsakris, A. (2023). The impact of earthquakes on public health: A narrative review of infectious diseases in the post-disaster period aiming to disaster risk reduction. Microorganisms, 11(2), 419.

[4] Imaizumi, A., Ito, K., & Okazaki, T. (2016). Impact of natural disasters on industrial agglomeration: The case of the Great Kantō Earthquake in 1923. Explorations in Economic History, 60, 52-68.

[5] UNDP. (2013). Building Resilient Communities: Lessons Learned from the 2010 Haiti Earthquake. United Nations Development Programme.

[6] Ay, Ş. (2023). Kahramanmaraş Pazarcık ve Elbistan depremleri sonrası hasarlı yapıların malzeme kalitesi ve uygulama hatalarının değerlendirilmesi. In International Conference on Engineering, Natural and Social Sciences, 1: 245-251.

[7] Türkiye Büyük Millet Meclisi. (2021). Depreme Karşı Alınacak Önlemleri ve Depremin Zararlarını En Aza İndirmek İçin Alınacak Önlemleri Belirlemek Amacıyla Kurulan Meclis Araştırma Komisyonu Raporu. Ankara.

[8] İstanbul Olası Deprem Kayıp Tahminleri Güncelleme Raporu, 2019. İstanbul Büyükşehir Belediyesi, Deprem Risk Yönetimi ve Kentsel İyileştirme Daire Başkanlığı, Deprem ve Zemin İnceleme Müdürlüğü, Ekim 2019

[9] People in Harm's Way: Flood Exposure and Poverty in 189 Countries http://hdl.handle.net/10986/34655

[10] Kent Selleri Yönetim ve Kontrol Rehberi https://marmara.gov.tr/uploads/old-site/2020/10/KENT-SELLERI-kucuk.pdf

[11] AFAD(2023).https://www.afad.gov.tr/kurumlar/afad.gov.tr/e_Kutuphane/Istatistikler/2022-YiliDoga-Kaynakli-Olay-Istatistikleri.pdf. (15.09.2023).

[12] Santana, R., J. S. Sousa, P. Soares, S. Lopes, P. Boto, and J. V. Rocha. 2020. "The demand for hospital emergency services: Trends during the first month of COVID-19 response." Portuguese J. Public Health 38 (1): 30–36. https://doi.org/10.1159/000507764.

[13] Lu, H., Wang, H., Yu, D., & Ye, J. (2023). Sharp schedule compression in urgent emergency construction projects via activity crashing, substitution and overlapping: a case study of Huoshengshan and Leishenshan Hospital projects in Wuhan. Engineering, Construction and Architectural Management, 30(8), 3696-3712.

[14] Rapid Damage and Needs Assessment 2 UKRAINE Rapid Damage and Needs Assessment February 2022 – February 2023 March 2023, the World Bank, the Government of Ukraine, the European Union, the United Nations

[15] Mülteciler Derneği, 2022; UNHCR Birleşmiş Milletler Mülteci Örgütü, 143 Topkapı Jour of Soc Sci, Vol. 2, No. 1, 2023, pp. 133–158 2022

[16] Betts, A.; Loescher, G.; Milner, J. The United Nations High Commissioner for Refugees (UNHCR): The Politics and Practice of Refugee Protection; Routledge: London, UK, 2013. Available online: https://www.unhcr.org/refugee-statistics/ (accessed on 2 July 2022)

[17] European Commission. Humanitarian Shelter and Settlements Guidelines; DG ECHO Thematic Policy Document n◦ 9 (June); European Commission: Brussels, Belgium, 2017

[18] Chen C. (2010). Environmental impact of cement production: detail of the different processes and cement plant variability evaluation. J. Clean Prod. 18(5), 478-485.

[19] Wei J, Cen K. (2019). Empirical assessing cement CO2 emissions based on China's economic and social development during 2001–2030. Sci. Total Environ. 653, 200-211.

[20] Kul, A., Ozcelikci, E., Ozel, B. F., Ilcan, H., Sahin, O., Gunal, M. F., ... & Sahmaran, M. (2024). Optimizing mechanical performance of geopolymers produced from construction and demolition waste: A comparative study of materials from different origins. Construction and Building Materials, 426, 136171.

[21] UN-Habitat. SDG Indicator 11.1.1 Training Module: Adequate Housing and Slum Upgrading; United Nations Human Settlement Programme (UN-Habitat): Nairobi, Kenya, 2018

[22] United Nations. (2019). World Population Prospects 2019: Highlights. https://population.un.org/wpp/Publications/Files/WPP2019_Highlights.pdf

[23] UN-Habitat. (2016). Housing at the Center: Supporting Slum Upgrading Strategies. https://unhabitat.org/sites/default/files/download-manager-files/Urban%20SDG6_2-4_web.pdf

[24] Drever, A. I. (2020). Housing and Economic Development: Empirical Evidence on the Causal Relationships. Housing Studies, 35(7), 1327-1349.

[25] World Bank. (2018). Affordable Housing: A Cornerstone for Sustainable Cities. https://openknowledge.worldbank.org/bitstream/handle/10986/28427/9781464811010.pdf

[26] United Nations. (2021). Sustainable Development Goals: Goal 11 - Sustainable Cities and Communities. https://sdgs.un.org/goals/goal11

[27] Turkey Circular Economy Platform. Available at: https://donguselekonomiplatformu.com/en/knowledge-hub/article_1-what-is-the-definition-of-a-circular-economy_11.html?page=3

[28] OECD (2021) Material Resources, Productivity, and the Environment: Key Findings. Available at:https://www.oecd.org/greengrowth/MATERIAL%20RESOURCES,%20PRODUCTIVITY%20AND%20THE%20ENVIRONMENT_key%20findings.pdf

[29] OECD (2021) Global Material Resources Outlook to 2060: Economic Drivers and Environmental Consequences. Available at: https://www.oecd.org/environment/waste/highlights-global-material-resources-outlook-to-2060.pdf

[30] UNEP, U. (2020). 2020 Global status report for buildings and construction: Towards a zero-emission, efficient and resilient buildings and construction sector. Renewables global status report.

[31] Kaza, S., Yao, L., Bhada-Tata, P., & Van Woerden, F. (2018). What a waste 2.0: a global snapshot of solid waste management to 2050. World Bank Publications.

[32] Chau, C.K., Leung, T.M., Ng, W.Y., 2015. A review on life cycle assessment, life cycle energy assessment and life cycle carbon emissions assessment on buildings. Appl. Energy 143 (1), 395–413, Available at: http://dx.doi.org/10.1016/j.apenergy.2015. 01.023.

[33] Ossio, F., Salinas, C., & Hernández, H. (2023). Circular economy in the built environment: A systematic literature review and definition of the circular construction concept. Journal of Cleaner Production, 137738.

[34] Kabirifar, K., Mojtahedi, M., Wang, C., & Tam, V. W. (2020). Construction and demolition waste management contributing factors coupled with reduce, reuse, and recycle strategies for effective waste management: A review. Journal of cleaner production, 263, 121265.

[35] Zhang, C., Hu, M., Di Maio, F., Sprecher, B., Yang, X., & Tukker, A. (2022). An overview of the waste hierarchy framework for analyzing the circularity in construction and demolition waste management in Europe. Science of the Total Environment, 803, 149892.

[36] Menegaki, M., & Damigos, D. (2018). A review on current situation and challenges of construction and demolition waste management. Current Opinion in Green and Sustainable Chemistry, 13, 8–15. https://doi.org/10.1016/j.cogsc.2018.02.010

[37] Maalouf, A., & El-Fadel, M. (2019). Life cycle assessment for solid waste management in Lebanon: Economic implications of carbon credit. Waste Management & Research, 37(1), 14–26.

[38] Hao, J., Di Maria, F., Chen, Z., Yu, S., Yu, W., & Di Sarno, L. (2020). Comparative study of construction and demolition waste management in China and the European Union. Detritus, 13(13), 114-121.

[39] Duan, H., Miller, T. R., Liu, G., & Tam, V. W. (2019). Construction debris becomes growing concern of growing cities. Waste Management, 83, 1-5.

[40] Purchase, C. K., Al Zulayq, D. M., O'Brien, B. T., Kowalewski, M. J., Berenjian, A., Tarighaleslami, A. H., & Seifan, M. (2021). Circular economy of construction and demolition waste: A literature review on lessons, challenges, and benefits. Materials, 15(1), 76.

[41] Hossain, M. U., Ng, S. T., Antwi-Afari, P., & Amor, B. (2020). Circular economy and the construction industry: Existing trends, challenges and prospective framework for sustainable construction. Renewable and Sustainable Energy Reviews, 130, 109948.

[42] Akanbi, L. A., Oyedele, L. O., Omoteso, K., Bilal, M., Akinade, O. O., Ajayi, A. O., ... & Owolabi, H. A. (2019). Disassembly and deconstruction analytics system (D-DAS) for construction in a circular economy. Journal of cleaner production, 223, 386-396.

[43] Coelho, A. (2016). Preliminary study for self-sufficiency of construction materials in a Portuguese region–Évora. Journal of cleaner production, 112, 771-786.

[44] Deutz, P., Baxter, H., Gibbs, D., Mayes, W. M., & Gomes, H. I. (2017). Resource recovery and remediation of highly alkaline residues: A political-industrial ecology approach to building a circular economy. Geoforum, 85, 336-344.

[45] European Comission. (2019). The European Green Deal Sets out How to Make Europe the First Climate-Neutral Continent by 2050, Boosting the Economy, Improving People's Health and Quality of Life, Caring for Nature, and Leaving No One Behind.

[46] Directive, C. (2010). Directive 2010/75/EU of the European Parliament and of the Council. Off. J. Eur. Union L, 334, 17-119.

[47] European Commission. (2020). A renovation wave for Europe—greening our buildings, creating jobs, improving lives. Communication from the European Commission to the European Parliament, the Council, the European Economic and Social Committee and the Committee of the Regions.

[48] Blackmore, P. (2012). Construction Products Regulation and CE Marking. Great Britain Building Research Establishment.

[49] Directive, E. C. (2008). Directive 2008/98/EC of the European Parliament and of the Council of 19 November 2008 on waste and repealing certain Directives. Official Journal of the European Union L, 312(3), 22.

[50] European Commission. (2020). A new circular economy action plan for a cleaner and more competitive Europe. Communication from the Commission to the European

Parliament, the Council, the European Economic and Social Committee and the Committee of the Regions.

[51] Adi, T.J.W.; Wibowo, P. Application of circular economy in the Indonesia construction industry. IOP Conf. Ser. Mater. Sci. Eng. 2020, 849, 012049.

[52] Ruiz, L.A.L., Ramón, X.R. and Domingo, S.G. (2020), "The circular economy in the construction and demolition waste sector–a review and an integrative model approach", Journal of Cleaner Production, Vol. 248, pp. 119-238, doi: 10.1016/j.jclepro.2019.119238.

[53] Siddika, A., Mamun, M.A.A., Ferdous, W., Saha, A.K. and Alyousef, R. (2020), "3D-printed concrete: applications, performance, and challenges", Journal of Sustainable Cement-Based Materials, Vol. 9 No. 3, pp. 127-164, doi: 10.1080/21650373.2019.1705199.

[54] Roxas, C. L. C., Bautista, C. R., Dela Cruz, O. G., Dela Cruz, R. L. C., De Pedro, J. P. Q., Dungca, J. R., ... & Ongpeng, J. M. C. (2023). Design for manufacturing and assembly (DfMA) and design for deconstruction (DfD) in the construction industry: Challenges, trends and developments. Buildings, 13(5), 1164.

[55] Razak, M.I.A.; Khoiry, M.A.; Badaruzzaman, W.H.W.; Hussain, A.H. DfMA for a Better Industrialised Building System. Buildings 2022, 12, 794. [CrossRef]

[56] Mesa, J., Maury, H., Arrieta, R., Corredor, L., Bris, J. (2018). A novel approach to include sustainability concepts in classical DFMA methodology for sheet metal enclosure devices. Res. Eng. Des., 29, 227–244.

[57] Boothroyd, G. (1994) Product design for manufacture and assembly. Comput. Des., 26, 505–520.

[58] Tan, T.; Lu, W.S.; Tan, G.Y.; Xue, F.; Chen, K.; Xu, J.Y.; Wang, J.; Gao, S. Construction-Oriented Design for Manufacture and Assembly Guidelines. J. Constr. Eng. Manag. 2020, 146, 12. [CrossRef]

[59] Bogue, R. (2012). Design for manufacture and assembly: background, capabilities and 556 applications. Assembly Automation, 32(2), 112-118.

[60] Lu, W., Tan, T., Xu, J., Wang, J., Chen, K., Gao, S., & Xue, F. (2021). Design for manufacture and assembly (DfMA) in construction: The old and the new. Architectural Engineering and Design Management, 17(1-2), 77-91.

[61] Emmatty, F. J., & Sarmah, S. P. (2012). Modular product development through platform-based 582 design and DfMA. Journal of Engineering Design, 23(9), 696-714.

[62] Swift, K. G, & Brown, N. J. (2013). Implementation strategies for design for manufacture 694 methodologies, Proceedings of the Institution of Mechanical Engineers. Part B: Journal 695 of Engineering Manufacture, 217(6), 827–833.

[63] Garusinghe, G. D. A. U., Perera, B. A. K. S., & Weerapperuma, U. S. (2023). Integrating circular economy principles in modular construction to enhance sustainability. Sustainability, 15(15), 11730.

[64] Kanters, J. (2018). Design for deconstruction in the design process: State of the art. Buildings, 8(11), 150.

[65] Ahn, N., Dodoo, A., Riggio, M., Muszynski, L., Schimleck, L., Puettmann M. (2022) Circular economy in mass timber construction: State-of-the-art, gaps and pressing research needs. J. Build. Eng., 53, 104562.

[66] Bertino, G.; Kisser, J.; Zeilinger, J.; Langergraber, G.; Fischer, T.; Österreicher, D. Fundamentals of Building Deconstruction as a Circular Economy Strategy for the Reuse of Construction Materials. Appl. Sci. 2021, 11, 939.

[67] Crowther, P. Design for Disassembly—Themes and Principles. In RAIA/BDP Environment Design Guide; Royal Australian Institute of Architects: Queenstown, Australia, 2005.

[68] Akinade, O.O.; Oyedele, L.O.; Ajayi, S.O.; Bilal, M.; Alaka, H.A.; Owolabi, H.A.; Bello, S.A.; Jaiyeoba, B.E.; Kadiri, K.O. Design for Deconstruction (DfD): Critical success factors for diverting end-of-life waste from landfills. Waste Manag. 2017, 60, 3–13.

[69] Machado, R.C.; de Souza, H.A.; Veríssimo, G.D.S. Analysis of Guidelines and Identification of Characteristics Influencing the Deconstruction Potential of Buildings. Sustainability 2018, 10, 2604.

[70] Lu, W. Sustainable Applications of Cold-Formed Steel Structures: Connections and Joints. In Recent Trends in Cold-Formed Steel Construction; Elsevier: Amsterdam, The Netherlands, 2016.

[71] Oluleye, B.I.; Chan, D.W.; Saka, A.B.; Olawumi, T.O. Circular economy research on building construction and demolition waste: A review of current trends and future research directions. J. Clean. Prod. 2022, 357, 131927.

[72] Iacovidou, E.; Purnell, P. Mining the physical infrastructure: Opportunities, barriers and interventions in promoting structural components reuse. Sci. Total Environ. 2016, 557–558, 791–807.

[73] Kuehlen, A.; Thompson, N.; Schultmann, F.; Nakajima, S.; Russell, M. Barriers for deconstruction and reuse/recycling of construction materials in Germany. In Barriers for Deconstruction and Reuse/Recycling of Construction Materials; CIB Publications, CIB General Secretariat Publisher: Rotterdam, The Netherlands, 2014; pp. 38–52.

[74] Nurhendi, R.N.; Khoiry, M.A.; Hamzah, N. Conceptual Framework Factors Affecting Construction Labour Productivity. J. Kejuruter. 2022, 34, 89–99.

[75] Zhao, N.; Kam, C.; TY Lo, J.; Kim, J.I.; Fischer, M. Construction Parts in Building Projects: Definition and Case Study. J. Manag. Eng. 2018, 34, 11. [CrossRef]

[76] Boothroyd G, Dewhurst P, Knight W (2002) Product design for manufacture and assembly, 2nd edn. Marcel Dekker Inc., New York

[77] Ong, K. C. G., Lin, Z. S., Chandra, L. R., Tam, C. T., & Dai Pang, S. (2013). Experimental investigation of a DfD moment-resisting beam–column connection. Engineering structures, 56, 1676-1683.

[78] Gibb A. G. F. (1999). Off-site Fabrication: Prefabrication, Pre-assembly and Modularisation, Whittles Pub., Latheronwheel.

[79] Boothroyd, G. (2005). Assembly automation and product design. CRC Press.

[80] Tan, T.; Mills, G.; Papadonikolaki, E.; Lu, W.; Chen, K. BIM-enabled design for manufacture and assembly. In Proceedings of the EG-ICE 2020Workshop on Intelligent Computing in Engineering, Proceedings, Online, 1–4 July 2020; pp. 314–323.

[81] Gao, S.; Low, S.P.; Nair, K. Design for manufacturing and assembly (DfMA): A preliminary study of factors influencing its adoption in Singapore. Arch. Eng. Des. Manag. 2018, 14, 440–456.

[82] Gao, S.; Low, S.P.; Nair, K. Design for manufacturing and assembly (DfMA): A preliminary study of factors influencing its adoption in Singapore. Arch. Eng. Des. Manag. 2018, 14, 440-456.

[83] Lu,W.; Chen, K.; Xue, F.; Pan,W. Searching for an optimal level of prefabrication in construction: An analytical framework. J. Clean. Prod. 2018, 201, 236–245.

[84] Hyun, H.; Kim, H.G.; Kim, J.S. Integrated Off-Site Construction Design Process including DfMA Considerations. Sustainability. 2022, 14, 20.

[85] Wuni, I.Y.; Shen, G.Q. Fuzzy modelling of the critical failure factors for modular integrated construction projects. J. Clean. Prod. 2020, 264, 121595.

[86] Kim, M. K., McGovern, S., Belsky, M., Middleton, C., & Brilakis, I. (2016). A suitability analysis of precast components for standardized bridge construction in the United Kingdom. Procedia Engineering, 164, 188-195.

[87] Ramaji, I. J., Memari, A. M., & Messner, J. I. (2017). Product-oriented information delivery framework for multistory modular building projects. Journal of Computing in Civil Engineering, 31(4), 04017001.

[88] Gerth, R., Boqvist, A., Bjelkemyr, M., & Lindberg, B. (2013). Design for construction: utilizing production experiences in development. Construction Management and Economics, 31(2), 135-150.

[89] Chen, K.; Lu, W. Design for Manufacture and Assembly Oriented Design Approach to a Curtain Wall System: A Case Study of a Commercial Building in Wuhan, China. Sustainability 2018, 10, 2211.

[90] Banks, C.; Kotecha, R.; Curtis, J.; Dee, C.; Pitt, N.; Papworth, R. Enhancing high-rise residential construction through design for manufacture and assembly—A UK case study. Proc. Inst. Civ. Eng.—Manag. Procure. Law 2018, 171, 164–175.

[91] Wasim, M.; Han, T.M.; Huang, H.; Madiyev, M.; Ngo, T.D. An approach for sustainable, cost-effective and optimised material design for the prefabricated non-structural components of residential buildings. J. Build. Eng. 2020, 32, 13.

[92] Trinder, L. Design for manufacture and assembly: Its benefits and risks in the UK water industry. Proc. Inst. Civ. Eng. Manag. Procure. Law 2018, 171, 152–163.

[93] Tafesse S., Girma Y.E., Dessalegn E. (2022). Analysis of the socio-economic and environmental impacts of construction waste and management practices. Heliyon, 8, e09169.

[94] Deniz, Ş., & Doğan, E. (2013). Yapıbozumuna Uygun Bina Tasarımı. Çevre Tasarım Kongresi. Uludağ Üniversitesi. Bursa. Türkiye.

[95] Webster, C., 2013. The Art of Design for Disassembly. Eng. Circ. Econ. Field Man. Re-Des. Regen. Econ. 5.

[96] International Standarts Organization [ISO], 2020

[97] Ong, K. C. G., Z. S. Lin, L. R. Chandra, C. T. Tam, and S. Dai Pang. 2013. "Experimental investigation of a DfD moment-resisting beam–column connection." Eng. Struct. 56 (Nov): 1676–1683. https://doi.org/10.1016 /j.engstruct.2013.08.006.

[98] Xiao, J., T. Ding, and Q. Zhang. 2017. "Structural behavior of a new moment-resisting DfD concrete connection." Eng. Struct. 132 (Feb): 1–13. https://doi.org/10.1016/j.engstruct.2016.11.019.

[99] Ding, T., J. Xiao, Q. Zhang, and A. Akbarnezhad. 2018. "Experimental and numerical studies on design for deconstruction concrete connections: An overview." Adv. Struct. Eng. 21 (14): 2198–2214.

[100] Broniewicz, F.; Broniewicz, M. Sustainability of Steel Office Buildings. Energies 2020, 13, 3723.

[101] Densley Tingley, D. Design for Deconstruction: An Appraisal; University of Sheffield: Sheffield, UK, 2012.

[102] Wang, L.; Webster, M.D.; Hajjar, J.F. Design for Deconstruction Using Sustainable Composite Beams with Precast Concrete Planks and Clamping Connectors. J. Struct. Eng. 2020, 146, 04020158.

[103] Ding, T.; Xiao, J.; Chen, E.; Khan, A.-U. Experimental Study of the Seismic Performance of Concrete Beam-Column Frame Joints with DfD Connections. J. Struct. Eng. 2020, 146, 04020036. [

[104] Xiao, J.; Chen, Z.; Ding, T.; Xia, B. Effect of recycled aggregate concrete on the seismic behavior of DfD beam-column joints under cyclic loading. Adv. Struct. Eng. 2020, 24, 1709–1723.

[105] Korkmaz, H. H., and T. Tankut. 2005. "Performance of a precast concrete beam-to-beam connection subject to reversed cyclic loading." Eng. Struct. 27 (9): 1392–1407. https://doi.org/10.1016/j.engstruct.2005.04 .004.

[106] Leso, L.; Conti, L.; Rossi, G.; Barbari, M. Criteria of design for deconstruction applied to dairy cows housing: A case study in Italy. Agron. Res. 2018, 16, 794–805.

[107] Basta, A.; Serror, M.H.; Marzouk, M. A BIM-based framework for quantitative assessment of steel structure deconstructability. Autom. Constr. 2019, 111, 103064.

[108] Akbarnezhad, A.; Ong, K.C.G.; Chandra, L.R. Economic and environmental assessment of deconstruction strategies using building information modeling. Autom. Constr. 2014, 37, 131–144.

[109] Swift, J., Ness, D., Kim, K.P., Gelder, J., 2017. Towards adaptable and reusable building elements: harnessing the versatility of the construction database through RFID and BIM towards adaptable and reusable building elements: harnessing the versatility of the construction database through RFID and BIM. In: Proceedings for the UAI 2017 Seoul World Architects Congress, pp. 1e7

[110] Marzouk, M.; Elmaraghy, A. Design for Deconstruction Using Integrated Lean Principles and BIM Approach. Sustainability 2021, 13, 7856.

[111] Schultmann, F.; Sunke, N. Closed-loop oriented project management in construction: An approach for sustainable construction management. In Proceedings of the Conference Rethinking Sustainable Construction 2006, Sarasota, FL, USA, 19–22 September 2006.

[112] Xia, B.; Ding, T.; Xiao, J. Life cycle assessment of concrete structures with reuse and recycling strategies: A novel framework and case study. Waste Manag. 2020, 105, 268–278.

[113] E. Leising, J. Quist, N. Bocken, Circular Economy in the building sector: three cases and a collaboration tool, J. Clean. Prod. 176 (2018) 976–989.

[114] Ortlepp, S.; Masou, R.; Ortlepp, R. Green construction methods of buildings capable for disassembly to support circular economy. In Challenges for Technology Innovation: An Agenda for the Future—Proceedings of the International Conference on Sustainable Smart Manufacturing, S2M 2016, Lisbon, Portugal, 20–22 October 2016; CRC Press: Boca Raton, FL, USA, 2017; pp. 21–26.

[115] Eckelman, M.J.; Brown, C.; Troup, L.N.; Wang, L.; Webster, M.D.; Hajjar, J.F. Life cycle energy and environmental benefits of novel design-for-deconstruction structural systems in steel buildings. Build. Environ. 2018, 143, 421–430.

[116] Densley Tingley, D., Davison, B., 2012. Developing an LCA methodology to account for the environmental benefits of design for deconstruction. Build. Environ. 57, 387–395. http://dx.doi.org/10.1016/j.buildenv.2012.06.005.

[117] Ruiz, L.A.L., Ramón, X.R., & Domingo, S.G., 2020. The circular economy in the construction and demolition waste sector–A review and an integrative model approach. J. Clean. Prod., 248, 119238. https://doi.org/10.1016/j.jclepro.2019.119238

[118] Erol, I. (2018). Financial transformation and housing finance in Turkey. In The political economy of financial transformation in Turkey (pp. 243-268). Routledge.

[119] Europea, C. (2005). Communication from the Commission to the European Parliament, the Council, the European Economic and Social Committee. Nanosciences and nanotechnologies: An action plan for Europe, 2009.

[120] Emre, Ö., Duman, T. Y., Özalp, S., Şaroğlu, F., Olgun, Ş., Elmacı, H., & Çan, T. (2018). Active fault database of Turkey. Bulletin of Earthquake Engineering, 16(8), 3229-3275.

[121] Yıldırım, G., Kul, A., Özçelikci, E., Şahmaran, M., Aldemir, A., Figueira, D., & Ashour, A. (2021). Development of alkali-activated binders from recycled mixed masonry-originated waste. Journal of Building Engineering, 33, 101690.

[122] Ozcelikci, E., Kul, A., Gunal, M. F., Ozel, B. F., Yildirim, G., Ashour, A., & Sahmaran, M. (2023). A comprehensive study on the compressive strength, durability-related parameters and microstructure of geopolymer mortars based on mixed construction and demolition waste. Journal of Cleaner Production, 396, 136522.

[123] Aktepe, R., Akduman, S., Aldemir, A., Ozcelikci, E., Yildirim, G., Sahmaran, M., & Ashour, A. (2023). Fully demountable column base connections for reinforced CDW-based geopolymer concrete members. Engineering Structures, 290, 116366.

[124] Ş. Akduman, O. Kocaer, A. Aldemir, M. Şahmaran, G. Yıldırım, H. Almahmood, A. Ashour, Experimental investigations on the structural behaviour of reinforced geopolymer beams produced from recycled construction materials, Journal of Building Engineering 41 (2021).

[125] A. Aldemir, S. Akduman, O. Kocaer, R. Aktepe, M. Sahmaran, G. Yildirim, H. Almahmood, A. Ashour, Shear behaviour of reinforced construction and demolition waste-based geopolymer concrete beams, Journal of Building Engineering 47 (2022).

[126] Akduman, S., Aktepe, R., Aldemir, A., Ozcelikci, E., Yildirim, G., Sahmaran, M., & Ashour, A. (2023). Structural performance of construction and demolition waste-based

geopolymer concrete columns under combined axial and lateral cyclic loading. Engineering Structures, 297, 116973.

[127] European Commission. Joint Research Centre. Institute for Environment and Sustainability. Supporting Environmentally Sound Decisions for Construction and Demolition (C&D) Waste Management: "A Practical Guide to Life Cycle Thinking (LCT) and Life Cycle Assessment (LCA)". (2011). https://data.europa.eu/doi/10.2788/54618.

[128] Eurostat regional yearbook. Luxembourg: Eurostat, 2019.

[129] Kotan, S., "Draft Regulation on the Control of Demolition and Excavated Soil and Construction and Demolition Wastes, Livable Environments and Brand Cities, Target 2023". (2016): Demolition Conference Istanbul, Turkey (in Turkish).

[130] Buzkan, C., and Erman, O. "Recycling Problem of Structural Wastes and Evaluation of the Situation in Turkey in Terms of Legislation". Journal of Natural Disasters and Environment, 14 December 2019, 1-12. https://doi.org/10.21324/dacd.570141.

[131] Wei, C., Sun, X., Yu, Z. and Zhang, P., "Experimental study and mechanism analysis on basic mechanical properties of basalt fiber reinforced concrete", Structural Concrete, https://doi.org/10.1002/suco.202200046.

[132] Amario, M., Pepe, M., Rangel, C.S., Filho, R.D.T., "Autogenous and drying shrinkage of structural concretes incorporating recycled concrete aggregates from different sources", Structural Concrete, https://doi.org/10.1002/suco.202200729.

[133] Li, J. and Deng, Z., "Tensile behavior of ultra-high performance concrete reinforced with different hybrid fibers", Structural Concrete, https://doi.org/10.1002/suco.202200353.

[134] Qian, Y., Sheikh, M.N., Feng, H. and Hadi, M.N.S., "Use of waste glass as fine aggregate in ambient cured alkali-activated mortars", Structural Concrete, https://doi.org/10.1002/suco.202200760.

[135] Wang, J., Li Z., and Tam, V. W. Y., "Critical Factors in Effective Construction Waste Minimization at the Design Stage: A Shenzhen Case Study, China". Resources, Conservation and Recycling 82 (January 2014): 1-7. https://doi.org/10.1016/j.resconrec.2013.11.003.

[136] Zhang, Z., Provis, J. L., Reid, A., and Wang H. "Geopolymer Foam Concrete: An Emerging Material for Sustainable Construction". Construction and Building Materials 56 (April 2014): 113-27. https://doi.org/10.1016/j.conbuildmat.2014.01.081.

[137] Kumar, S., and Kumar R. "Geopolymer: Cement for Low Carbon Economy", Indian Concrete Journal (July 2014): 10.

[138] Duxson, P., A. Fernández-Jiménez, J. L. Provis, G. C. Lukey, A. Palomo, ve J. S. J. van Deventer. "Geopolymer Technology: The Current State of the Art". Journal of Materials Science 42, pp 9 (May 2007): 2917-33. https://doi.org/10.1007/s10853-006-0637-z.

[139] Pham, D. Q., Nguyen, T. N., Le, S. T., Pham, T. T. and Ngo, T. D. "The Structural Behaviours of Steel Reinforced Geopolymer Concrete Beams: An Experimental and Numerical Investigation". Structures 33 (Oct 2021): 567-80. https://doi.org/10.1016/j.istruc.2021.04.077.

[140] Parthiban, B., and Thirugnanasambandam, S. "Flexural Behaviour of Geopolymer Concrete Beams Using Waste Glass as Coarse Aggregate". International Journal of Engineering and Advanced Technology 9 (Oct 2019): 4479-85. https://doi.org/10.35940/ijeat.A1759.109119.

[141] Nixon, P J. "Recycled Concrete as an Aggregate for Concrete-a review". Material Structure., 11 (5) (1978), pp. 371-378.

[142] Figiela, B., Šimonová, H., Korniejenko, K., "State of the art, challenges, and emerging trends: Geopolymer composite reinforced by dispersed steel fibers" Reviews on Advanced Materials Science 61(1) (2022):pp. 1-15. https://doi.org/10.1515/rams-2021-0067.

[143] Ziejewska, C., Marczyk, J., Korniejenko, K., Bednarz, S., Sroczyk, P., Łach, M., Mikuła, J., Figiela, B., Szechynska-Hebda, M., Hebda, M., "3D Printing of Concrete-Geopolymer Hybrids" Materials 2022, 15, 2819. https://doi.org/10.3390/ma15082819.

[144] Upshaw, M., and Cai, C.S., "Feasibility study of MK-based geopolymer binder for RAC applications: Effects of silica fume and added CaO on compressive strength of mortar samples" Case Studies in Construction Materials, 14, 2214-5095 (2021) https://doi.org/10.1016/j.cscm.2021.e00500.

[145] Abdollahnejad, Z., Mastali, M., Falah, M., Luukkonen, T., Mazari, M., Illikainen, M., "Construction and Demolition Waste as Recycled Aggregates in Alkali-Activated Concretes". Materials (2019), 12, 4016. https://doi.org/10.3390/ma12234016

[146] Xu, K., Shen, G.Q., Liu, G., and Martek, I., "Demolition of Existing Buildings in Urban Renewal Projects: A Decision Support System in the China Context" Sustainablity (Jan 2019) 11(2), 491, https://doi.org/10.3390/su11020491

[147] Katarzyna, B., Le, CH., Louda, P., Michał, S., Bakalova, T., Tadeusz, P., Prałat, K.. "The Fabrication of Geopolymer Foam Composites Incorporating Coke Dust Waste". Processes. 8(9):1052 (2020). https://doi.org/10.3390/pr8091052.

[148] Ganesan, N., Abraham, R., Raj, S. D., Sasi, D., "Stress–strain behaviour of confined Geopolymer concrete" Construction and Building Materials (2014) 73 pp. 326-331. https://doi.org/10.1016/j.conbuildmat.2014.09.092

[149] Noushini, A., Aslani, F., Castel, A., Gilbert, R.I., Uy, B., Foster, S., "Compressive stress-strain model for low-calcium fly ash-based geopolymer and heat-cured Portland cement concrete". Cement and Concrete Composites, (2016) 73-0958-9465 pp. 136-146.

[150] Ulugöl, H., Kul, A., Yıldırım, G., Sahmaran, M., Aldemir, A., Figueira, D., and Ashour A. "Mechanical and Microstructural Characterization of Geopolymers from Assorted Construction and Demolition Waste-Based Masonry and Glass". Journal of Cleaner Production 280 (Jan 2021): 124358. https://doi.org/10.1016/j.jclepro.2020.124358.

[151] Ma, C. K., Awang, A.Z., Omar, W. "Structural and material performance of geopolymer concrete: A review". Construction and Building Materials (Oct 2018): 186, pp 90–102.

[152] Hadi, M. N.S., Al-Azzawi, M., and Yu T. "Effects of Fly Ash Characteristics and Alkaline Activator Components on Compressive Strength of Fly Ash-Based Geopolymer Mortar". Construction and Building Materials 175 (June 2018): pp 41-54. https://doi.org/10.1016/j.conbuildmat.2018.04.092.

[153] Nikoloutsopoulos N, Sotiropoulou A, Kakali G. and Tsivilis S. "Physical and Mechanical Properties of Fly Ash Based Geopolymer Concrete Compared to Conventional Concrete". Buildings 11, pp 5 (21 April 2021): 178. https://doi.org/10.3390/buildings11050178.

[154] Sruthi, S., and Priya, A.K. "A review on eco-green geopolymer concrete". International Journal of Science and Research (IJSR) (Sep 2017): pp. 1169-1172.

[155] Irfanita, R., Ansar, A., Armayani, M. and Subaer S. "The Use of Fermipan in the Production of Lightweight Geopolymer as an Environmentally Friendly and Fire-Resistant Concrete". Materials Science Forum 841 (Jan 2016): pp 72-78. https://doi.org/10.4028/www.scientific.net/MSF.841.72.

[156] Krishnan, L., Karthikeyan, S., Nathiya, K., Suganya, K. "Geopolymer Concrete an Eco-Friendly Construction Material". International Journal of Research in Engineering and Technology 03, pp 23 (June 2014): 164-67.

[157] Zain, H., Abdullah, M.M.A., Hussin, K., Ariffin, N. and Bayuaji R. "Review on Various Types of Geopolymer Materials with the Environmental Impact Assessment". MATEC Web of Conferences 97 (2017): 01021. https://doi.org/10.1051/matecconf/20179701021.

[158] Davidovits, J. "Geopolymers Based on Natural and Synthetic Metakaolin a Critical Review". Içinde Ceramic Engineering and Science Proceedings, 201-14. Hoboken, NJ, USA: John Wiley & Sons, Inc., (2018): https://doi.org/10.1002/9781119474746.ch19.

[159] Sheikh, S. A. "A Comprative Study of Confinement Models". ACI Journal (1982): 79-30.

[160] Mertol, H. C. "Behavıor of Hıgh-Strength Concrete Members Subjected to Combıned Flexure and Axıal Compressıon Loadıngs". (2006) PhD Thesis, North Carolina State University, North Carolina.

[161] Oztekin, E., Pul, S., Husem, M. "Determination of Rectangular Stress Block Parameters for High Performance Concrete". Engineering Structures (2003): 25, 371– 376.

[162] Uzbaş, B. "Beton İçin Geliştirilen Gerilme-Şekil Değiştirme Modellerinin Karşılaştırılması". Journal of Polytechnic (2014): 115-126.

[163] Kent, D. C., Park, R., "Flexural Members with Confined Concrete". Journal of Structural Division, ASCE (July 1971): 97.

[164] Hognestad, E., Hanson, N. W., McHenry, D. "Concrete Stress Distribution in Ultimate Strength Design". ACI Journal, Proceedings (1955): 52(12), pp 455–480.

[165] Sheikh, S. A., Uzumeri, S. M. "Analytical Model for Concrete Confinement in Tied Columns". Journal of the Structural Division (Dec. 1982): 108-12.

[166] Roy, H. E. H., Sozen, M. "Ductility of concrete, Proceedings of the International Symposium on Flexural Mechanics of Reinforced Concrete". ASCE ACI Joint Symposium (Nov. 1964).

[167] Saatcioglu, M, Razvi. "Strength And Ductility Of Confined Concrete". Journal of Structural Engineering ASCE (1992): 118(6) 1590. https://doi.org/10.1061/(ASCE)0733-9445(1992)118:6(1590).

[168] American Concrete Institute (ACI) Building code requirements, structural concrete and Commentary 318, ACI Committee (2011).

[169] Yacob, N. S., ElGawady, M. A., Sneed, L. H., Said, A. "Shear strength of fly ash-based geopolymer reinforced concrete beams". Engineering Structures (Oct 2019): 196-109298.

[170] Wu, C., Hwang, H., Shi, C., Li, N., and Du Y. "Shear Tests on Reinforced Slag-Based Geopolymer Concrete Beams with Transverse Reinforcement". Engineering Structures 219 (Sep 2020): 110966. https://doi.org/10.1016/j.engstruct.2020.110966.

[171] Dattatreya, J. K., Rajamane, N. P., Sabitha, D., Ambily, P. S., Nataraja, M. C. "Flexural behaviour of reinforced Geopolymer concrete beams". International Journal of Civil and Structural Engineering (2011): 0976 – 4399.

[172] Lisantono, A. "Flexural Behavior of Fly Ash-Based Geopolymer R/C Beam with Bauxite Material as Coarse Aggregates". International Journal of GEOMATE (Jan 2020):18 pp 80-85. https://doi.org/10.21660/2020.65.43211.

[173] Kumaravel, S., Thirugnanasambandam S., Jeyaseha, C. A., Salahuddin M. "Flexural behaviour of geopolymer concrete beams" International Journal of Advanced Engineering Research and Studies (July 2012).

[174] Hassan, A., Arif, M. and Shariq, M. "Structural Performance of Ambient-cured Reinforced Geopolymer Concrete Beams with Steel Fibres". Structural Concrete 22, (Feb 2021): 457-75. https://doi.org/10.1002/suco.202000191.

[175] Nithya, S., Gunasekaran, K., and Sankar G. "A Study on the Flexural Behaviour of Geopolymer Lightweight Eco-Friendly Concrete Using Coconut Shell as Coarse Aggregate". Advances in Civil Engineering 2021 (16 July 2021): 1-20. https://doi.org/10.1155/2021/5534019.

[176] Pham, D. Q., Nguyen, T. N., Le, S. T., Pham, T. T. and Ngo, T. D. "The Structural Behaviours of Steel Reinforced Geopolymer Concrete Beams: An Experimental and Numerical Investigation". Structures 33 (Oct 2021): 567-80. https://doi.org/10.1016/j.istruc.2021.04.077.

[177] ANSYS (2018). ANSYS Users Manual, ANSYS, Inc., USA.

[178] Nguyen, K. T., Le, T. A., Lee K. "Experimental Study on flexural strength of Reinforced geopolymer concrete beams". Engineering and Technology International Journal of Civil and Environmental Engineering (2016):10-4.

[179] Pelisser, F., Silva, B. V., Menger, M. H., Frasson, B. J., Keller, T. A., Torii, A. J. and Lopez R. H. "Structural Analysis of Composite Metakaolin-Based Geopolymer Concrete". Revista IBRACON de Estruturas e Materiais 11 (May 2018): 535-43. https://doi.org/10.1590/s1983-41952018000300006.

[180] Drucker, D. C., and Prager W. "Soil Mechanics and Plastic Analysis or Limit Design". Quarterly of Applied Mathematics 10, (1952): 157-65. https://doi.org/10.1090/qam/48291.

[181] William, K.J., and Warnke E.P. "Constitutive Model for the Triaxial Behaviour of Concrete". (1974). https://doi.org/10.5169/SEALS-17526.

[182] Arici, Y., Binici, B., Aldemir, A., "Comparison of the expected damage patterns from two and three-dimensional nonlinear dynamic analyses of a roller compacted concrete dam". (Jun 2012): 10-3. https://doi.org/10.1080/15732479.2012.753921

[183] Gharibdoust, A., Aldemir, A. and Binici, B. "Seismic Behaviour of Roller Compacted Concrete Dams under Different Base Treatments". Structure and Infrastructure Engineering (Feb 2020): 355-66. https://doi.org/10.1080/15732479.2019.1661500.

[184] Aldemir, A. (2021), "Prediction equation for the fundamental vibration period of concrete gravity dams with impounded water", Earthquake Spectra, 37(3), 1710-1725, DOI: 10.1177/8755293020981965.

[185] Sevim, B., Bayraktar, A., Altunisik, A.C., Finite element model calibration of Berke arch dam using operational modal testing. Journal of Vibration and Control 2009; 17(7): 1065–1079.

[186] A Gharibdoust, A Aldemir, B Binici, Seismic behaviour of roller compacted concrete dams under different base treatments. Structure and Infrastructure Engineering 16 (2), 355-366.

[187] Matsumoto, M. and Nishimura, T. (1998). "Mersenne twister: A 623-dimensionally equidistributed uniform pseudo-random number generator", ACM Transactions on Modeling and Computer Simulation, Vol. 8, No. 1, pp. 3-30, DOI:10.1145/272991.272995.

[188] A. Bisarya, R.K. Chouhan, M. Mudgal, S.S. Amritphale, Fly ash based geopolymer concrete a new technology towards the greener environment: a review, Int. J. Innov. Res. Sci. Eng. Technol. (2015) 12178–12186, http://dx.doi.org/10.15680/IJIRSET.2015.0412089.

[189] J. Davidovits, Soft Mineralogy and Geopolymers, Proceedings of the Geopolymer 88 International Conference, the Université de Technologie, Compiègne, France, 1988.

[190] N. Hamdi, I.B. Messaoud, E. Srasra, Production of geopolymer binders using clay minerals and industrial wastes, C. R. Chim. 22 (2019) 220–226.

[191] J.L. Provis, Alkali-activated materials, Cem. Concr. Res. 114 (2018) 40-48.

[192] V.M. Malhotra, Making concrete greener with fly ash, Concr. Int. 21 (1999) 61–66.

[193] E. Hognestad, A study on combined bending and axial load in reinforced concrete members. Univ. of Illinois Engineering Experiment Station, Univ. of Illinois at Urbana-Champaign, IL, 1951, 43-46.

[194] S. Popovics, A numerical approach to the complete stress-strain curves of concrete, Cem. Concr. Res. 3 (5) (1973) 583-599.

[195] M. Sargin, Stress-Strain Relationship for Concrete and the Analysis of Structural Concrete Sections, Study 4, Solid Mechanics Division; University of Waterloo, Waterloo, Canada, 1971.

[196] Z.L. Wang, H. Konietzky, R.Y. Huang, Elastic–Plastic-Hydrodynamic Analysis of Crater Blasting in Steel Fiber Reinforced Concrete, Theor. Appl. Fract. Mech. 52 (2009) 111–116.

[197] J.B. Mander, J.N. Priestley, R. Park, Theoretical stress-strain model for confined concrete, J. Struct. Eng. 114(8) (1988) 1804-1826.

[198] B.D. Scott, Stress:strain relationships for confined concrete:rectangular sections (1980).

[199] CSA. Design and construction of building structures with fibre reinforced polymers. Canadian Standards Association; 2012. (CAN/CSA S806—12).

[200] TR55. Design guidance for strengthening concrete structures using fibre composite materials. 2012. Confined concrete has stress-strain characteristics that are distinctly different than those of plain concrete.

[201] D. Hardjito, S.E. Wallah, D.M.J. Sumajouw, B.V. Rangan, Introducing fly ash-based geopolymer concrete: manufacture and engineering properties. In 30th conference on our world in concrete & structures 24 (2005, August).

[202] D. Hardjito, Studies of fly ash-based geopolymer concrete, PhD Thesis. Perth, Australia: Curtin University of Technology; 2005.

[203] M. Sofi, J.S.J. van Deventer, P.A. Mendis, G.C. Lukey, Engineering properties of inorganic polymer concretes (IPCs), Cem. Concr. Res. 37 (2007) 251-7.

[204] T.T. Tung, M.P. Thong, H. Hong, Rectangular Stress-block Parameters for Fly-ash and Slag Based Geopolymer Concrete, Struct. 19 (2019) 143-155.

[205] Z. Pan, J.G. Sanjayan, B.V. Rangan, Fracture properties of geopolymer paste and concrete, Mag. Concr. Res. 63(10) (2011) 763-771. doi: 10.1680/macr.2011.63.10.7, 763-771.

[206] W. Prachasaree, S. Limkatanyu, A. Hawa, A. Samakrattakit, Development of Equivalent Stress Block Parameters for Fly-Ash-Based Geopolymer Concrete, Arab. J. Sci. Eng. 39 (2014) 8549-58.

[207] E. Thorenfeldt, A. Tomaszewicz, J.J. Jensen, Mechanical properties of high strength concrete and application in design. In: Proceedings of the Symposium Utilization of High Strength Concrete, Tapir, Trondheim, pp. 149–159 (1987).

[208] O. Kocaer, A. Aldemir, Compressive stress–strain model for the estimation of the flexural capacity of reinforced geopolymer concrete members. Struct. Conc. (2022)

[209] B. Zhang, T. Yu, J.G. Teng, Behavior of concrete-filled FRP tubes under cyclic axial compression, J. Compos. Constr. 19 (2015) 04014060.

[210] Y. Idris, T. Ozbakkaloglu, Seismic behavior of high-strength concrete-filled FRP tube columns, J. Compos. Constr. 17 (2013) 04013013.

[211] P. Velu, D. Kothandaraman, B. Ashok Kumar, Comparative study of confined concrete models, Int. J. Sci. Eng. 11 (12) (2020) 2229-5518.

[212] A.N. Talbot, Tests of Concrete and Reinforced Concrete Columns, Bulletin No. 10, 1906, and Bulletin No. 20, 1907, University of Illinois, Urbana.

[213] M.O. Withey, Tests on Reinforced Concrete Columns, Bulletin No. 300, 1910, and Bulletin No. 466, 1911, University of Wisconsin, Madison.

[214] P. Desayi, S. Krishnan, Equation for the Stress-Strain Curve of Concrete. (1964).

[215] D.M.J. Sumajouw, D. Hardjito, S.E. Wallah, B.V. Rangan, Fly ash-based geopolymer concrete: study of slender reinforced columns, J. Mater. Sci. 42 (2007) 3124–3130.

[216] U.K. Danda, Y.H. Kumar, B.S.C. Kumar, Experimental study on reinforced geopolymer concrete columns using GGBS, Materials Today: Proceedings, Volume 33, Part 1, 2020, Pages 632-636, ISSN 2214-7853, https://doi.org/10.1016/j.matpr.2020.05.607.

[217] M. Elchalakani, A. Karrech, M. Dong, M.S.M. Ali, B. Yang, Experiments and Finite Element Analysis of GFRP Reinforced Geopolymer Concrete Rectangular Columns Subjected to Concentric and Eccentric Axial Loading, Struct. 4 (2018) 273-289. doi:10.1016/j.istruc.2018.04.001

[218] P. Saranya, P. Nagarajan, A.P. Shashikala, Behaviour of GGBS - dolomite geopolymer concrete short column under axial loading. J. Build. Eng. 30 (2020) 101232.

[219] M. Albitar, S.M. Ali, P. Visintin, Experimental study on fly ash and lead smelter slag-based geopolymer concrete columns, Constr. Build. Mater. 141 (2017) 104–112.

[220] S.K.K.V. Kumar, M. Prakash, K. Satyanarayanan, J. Ind. Pollut. Control. 33 (2017) 1341-1344.

APPENDIX

Appendix 1- Publications Derived From Thesis

Kocaer, O., & Aldemir, A. (2023). Compressive stress–strain model for the estimation of the flexural capacity of reinforced geopolymer concrete members. *Structural Concrete*, *24*(4), 5102-5121.